2009

Bench-Scale Conversion of Carbon Dioxide to a Hydrocarbon Fuel

Melissa L. Kennedy
Wright State University

BENCH-SCALE CONVERSION OF CARBON DIOXIDE

TO A HYDROCARBON FUEL

A thesis submitted in partial fulfillment
of the requirements for the degree of
Master of Science

By

MELISSA LAUREN KENNEDY
B.S., Denison University, 2007

2009
Wright State University

WRIGHT STATE UNIVERSITY

SCHOOL OF GRADUATE STUDIES

August 4, 2009

I HEREBY RECOMMEND THAT THE THESIS PREPARED UNDER MY SUPERVISION BY Melissa Lauren Kennedy ENTITLED Bench-Scale Conversion of Carbon Dioxide to a Hydrocarbon Fuel BE ACCEPTED IN PARTIAL FULFILLMENT OF THE REQUIREMENTS FOR THE DEGREE OF Master of Science

Abinash Agrawal, Ph.D.
Thesis Director

David Dominic, Ph.D.
Department Chair

Committee on
Final Examination

Abinash Agrawal, Ph.D.

Chad Hammerschmidt, Ph.D.

Charles Bleckmann, Ph.D.

Joseph F. Thomas, Jr., Ph.D.
Dean, School of Graduate Studies

ABSTRACT

Kennedy, Melissa Lauren. M.S., Department of Earth and Environmental Science, Wright State University, 2009. Bench-Scale Conversion of Carbon Dioxide to a Hydrocarbon Fuel.

There is a growing concern about the effects of global warming that many believe is anthropogenically caused. As such, scientists are trying to uncover a viable alternative fuel source and establish a way to reduce atmospheric carbon dioxide levels. A potential solution that addresses both of these aspects would be to capture atmospheric carbon dioxide and convert it into a natural gas, in particular methane, which could be used as an energy source. A laboratory-scale experiment using 6 160 mL microcosms (3 with anaerobic wetland soil and 3 relatively soil free) and 2 7.2 L bioreactors was conducted to learn more about the efficiency of the naturally occurring process called methanogenesis. The 6 microcosms and 2 reactors were analyzed regularly for methane, hydrogen and carbon dioxide in gaseous samples and pH in aqueous samples. The microcosms with soil were more productive and therefore produced more methane than the soil-free microcosms, presumably because the soil offered a higher surface area for the microbes to attach to and obtain micronutrient from. It was found that hydrogen utilization was in stoichiometric proportion to methane production indicating, hydrogenotrophic methanogenesis was the dominant process occurring in the microcosms. This study proved that hydrogen utilizing methanogens can be grown in a microcosm setting relatively easily and that the kinetics of methanogenesis is pseudo-first order. However, the hydrogen utilization was not in stoichiometric proportion to the methane production in the larger volume bioreactors. The hydrogen uptake in the reactors was greater than expected if hydrogenotrophic methanogenesis was the sole process occurring. This study

indicates that some other microbial pathway is occurring in addition to hydrogenotrophic methanogenesis. As such, the trends observed in the microcosms differed from the trends that evolved in the bioreactors. Further research is needed in order to determine if carbon dioxide conversion to methane could be feasible on an industrial scale.

Table of Contents

List of Figures

Page No.

List of Tables

Page No.

Appendices: Tables, Graphs and Standard Operating Procedures

Page No.

Acknowledgements

In these acknowledgements I would like to thank all of the people who supported me throughout the duration of this project. First and foremost, I would like to thank my advisor, Dr. Abinash Agrawal for his support, expertise and helpfulness in this research project. In addition, I would like to thank the other members of my committee, Dr. Chad Hammerschmidt and Dr. Charles Bleckmann, for their assistance and efforts.

My sincere thanks go to my fellow colleagues in the lab: Sarah Tritschler, Christina Powell, Brian Congiu and David Kelly. Without their support and friendship I would not have been able to make it through this. I truly appreciate their advice and their willingness to listen to me complain on a regular basis. I would also like to thank my friends Jason Esselburn, Jim Ferreira, and Larry Mastera for their support outside of the lab and their continued efforts to keep me motivated when I felt like I had hit a dead end.

Finally, I would like to thank my family for always sticking by me. My parents, brother and sister always have confidence in me even when I do not have confidence in myself. The everlasting love of my family has made me who I am today and for that I am truly grateful.

I. Introduction

There is a growing concern over the detrimental effects of global warming. One way to protect against the catastrophic impacts of global warming is to diminish greenhouse gas concentrations, specifically carbon dioxide. Finding a way to reduce carbon dioxide levels in the atmosphere is vital to the health of the environment.

Several ideas have been proposed using alternative energies to reduce carbon dioxide levels in the atmosphere such as using hydrogen, wind, solar or ethanol as a new fuel source (Bossel et al., 2003; Fairley, 2002; Hoekman, 2008). Unfortunately, there are negative aspects with all of these ideas. For instance, large scale ethanol production would put a demand on agricultural land and would compete with land used for food production (Bossel et al., 2003), wind or solar energy is geographically limited (Fairley, 2002), and the unique physical properties of hydrogen make it difficult to utilize as an energy source (Bossel et al., 2003). However, there is another possible idea that is more feasible than the aforementioned with fewer unfavorable aspects. Production of methane, a natural gas, presents an attractive option to the current controversy over finding a viable alternative fuel source while still remaining carbon neutral. To do this, atmospheric carbon dioxide would be captured and converted into methane using naturally occurring microorganisms called methanogens. Using methane is a good alternative to other proposed fuels sources because it does not require new infrastructure and it is easily stored and transported. However, there are uncertainties on how to fully optimize methane production at both bench and large-scale levels.

This study sought to contribute to current knowledge by examining the rate of carbon dioxide conversion to methane at a bench-scale level. No studies in the literature have directly explored the efficiency of this conversion. As such, the main goal of this research project is to evaluate the efficiency of microbial reduction of carbon dioxide to methane (methanogenesis) at a bench-scale using gaseous hydrogen as electron donor and to identify various factors that can potentially affect this conversion. Investigations will focus on common methanogenic bacteria isolated from a nearby wetland. This preliminary study will explore if carbon dioxide conversion to methane can be feasible/practical in engineered systems (bench-scale bioreactors). If the experiment yields promising results, a larger pilot-scale could be implemented.

Batch reactors (160 mL serum bottles) and bioreactor (7 Liter Plexiglas reactors) experiments attempted to address the following topics:

- The ideal conditions for growing methanogenic bacteria (appropriate nutrient solution, pH, partial pressure of hydrogen and carbon dioxide)
- The following factors were studied in order to determine the efficiency of hydrogen utilizing methanogens:
    - Total mass of methane produced
    - Rate of methane production
    - Rate of carbon dioxide conversion to methane
    - Rate of hydrogen consumption as a result of methane production
- Comparison of carbon dioxide, hydrogen, and methane trends in batch reactors and larger bioreactors

II. Background

2.1 Motivation for finding an alternative fuel

The idea of finding an alternative fuel has been a popular topic of discussion for awhile. The ideal solution would be a fuel source that could end the United States' dependence on foreign fossil fuel supplies and reduce the uncertainty of energy security. There also are concerns over resource availability; it is well-known that worldwide sources of oil are limited. Combustion of the current non-renewable fuel sources of oil and coal release carbon dioxide emissions into the atmosphere, which raises the potential for global warming. Because of these issues, wind power, solar power, biofuels and hydrogen have been extensively examined as new energy technologies. Still, limitations to these new fuel sources have slowed the development of these technologies. As a result, biotically derived methane is being considered as a potential option.

2.2 Limitations of various alternative fuels

2.2.1 Hydrogen

The prospect of using hydrogen as a fuel source is a burgeoning field; when utilized as an energy source hydrogen does not release any pollutants or greenhouse gases into the atmosphere only pure water. The use of hydrogen could reduce concerns over global warming. However, there are many limitations from its unique physical properties to the difficulty of storage and transport that make technologic advancements necessary.

Hydrogen is very light, with a density of 0.0887 kg/m^3, compared to methane, which has a density of 0.707 kg/m^3 (Bossel et al., 2003). As a result, more energy can be derived from methane than hydrogen per unit volume. With respect to storage and transport, more energy would be required to compress hydrogen into a container as compared to an equivalent amount of methane (Bossel et al., 2003). Hydrogen also must be stored at a high pressure, otherwise it will disperse out of the storage container (Bossel et al., 2003). New technologies would need to be created to effectively store hydrogen and separate hydrogen from the other molecules to which it naturally attaches. This must be done in an economically feasible way.

2.2.2. Wind and Solar Energy

Similar to hydrogen, wind and solar energy do not release greenhouse gases into the atmosphere; however in depth investigations that have shown numerous limitations. Wind and solar energy are renewable energy sources and do not add to global warming concerns. The main restrictions for wind and solar energy are geographical, dictated by the weather conditions of any area making this energy source not totally reliable. Wind mills or solar panels should be located where there is an ample amount of wind speed and sunlight (Fairley, 2002). In addition to geographical restrictions, public support of wind technologies may be difficult to achieve (Pimental, 2002).

2.2.3. Biofuels

Other forms of alternative fuels that have been investigated extensively are biofuels, such as biomass and ethanol. Carbon from the atmosphere is used to create the plants that would be used in biofuels, so there is no net increase in atmospheric carbon

when biofuels are utilized. Biofuels are greatly limited due to geography of the area and land availability. Ethanol is traditionally derived from corn or sugar cane, which needs a large amount of land to be cultivated and it is limited since corn cannot be grown in all climates. Using the agricultural land to produce energy may put a strain on food production and increase the amount of fertilizer and/or water needed to effectively grow an ample amount of corn (Hoekman, 2008).

2.3 Conversion of atmospheric carbon dioxide to methane

Because of the numerous limitations that still exist with the aforementioned technologies and the continually growing energy demands, a new idea has emerged. That idea includes an attempt to reduce the level of carbon dioxide in the atmosphere by application of methane producing microbes. Concentrations of atmospheric carbon dioxide are rising, due to the increased combustion of fossil fuels. Carbon dioxide is emitted into the atmosphere from the combustion of fossil fuels. A large amount of fossil fuels are produced and used worldwide; for instance, in 2007, 1,146.6 million short tons of coal were produced and used for energy needs (Hutchison, 2009), and worldwide consumption of petroleum was 25 billion barrels per year (Herron, 2000). It is estimated that of the 30 billion tons of carbon dioxide emitted globally per year, about 50% is from coal combustion (Ecoworld, 2009) and 40% is from petroleum combustion (gasoline, diesel, and jet fuel) (CleanPower.org, 2009).

It is proposed here to capture the atmospheric carbon dioxide and redirect it into a bioreactor facility where it would be converted to methane by naturally occurring microbes. There are currently no official regulations dealing with the capturing of carbon

dioxide, but they are likely to arise in the near future as there is on-going, active research to develop capture technologies.

There are three capturing approaches that are available and several experimental plants are testing the technologies (Johnson, 2007). One approach that is being experimented with to capture point source carbon dioxide is to use ammonium carbonate or other amines which will react with and capture carbon dioxide in solution from flue gas that would be vented from an industrial site (Johnson, 2007). Another method called oxy-fuel combustion works to modify combustion in a way that the output product is pure carbon dioxide (Johnson, 2007). . The third method is called *precombustion* and in this approach coal is processed with steam and oxygen so that a syngas is produced. Carbon dioxide is easily removed from the syngas produced in precombustion (Johnson, 2007).

The methane that could be produced from the captured carbon dioxide could be utilized as energy. Methane is a hydrocarbon fuel consisting of one carbon and four hydrogen atoms. Methane is a natural gas that can easily be stored and transported through the infrastructure that has already been established for fossil fuels, particularly natural gas. In fact, methane even has been used by NASA to fuel rockets due to its characteristics, such as the ability to be stored at warm temperatures and in smaller fuel tanks (Barry, 2007). Methane is one of the largest contributing factors to the greenhouse effect due to the amount of infrared radiation that it absorbs. However, if methane was a result of atmospheric carbon dioxide conversion and methanogenesis, then the methane would be renewable and effectively carbon neutral (Chong, 2008). Atmospheric carbon will show no net increase through this process (Figure 2.1).

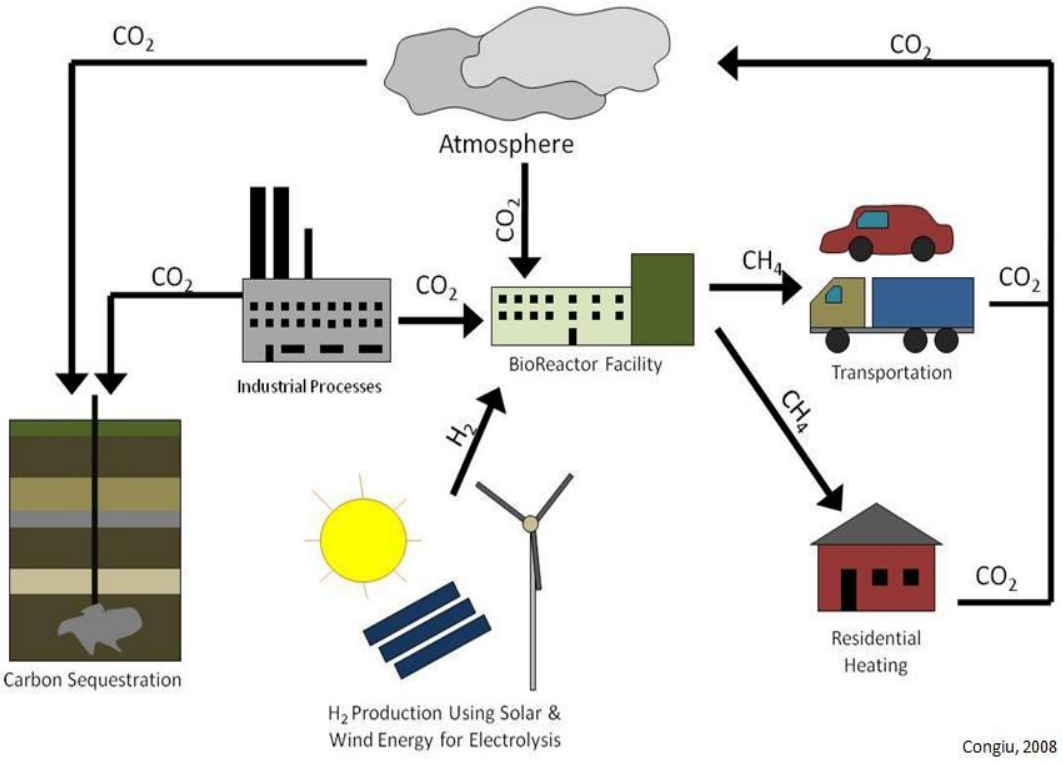

Figure 2.1: Schematic of the carbon neutral process of capturing atmospheric carbon dioxide and converting it to a methane fuel source (Congiu, personal communication)

2.4 Sources of hydrogen

In order to convert atmospheric carbon dioxide to methane, the naturally occurring bacteria that do the conversion use hydrogen as a substrate. For this process to be effective, an ample amount of hydrogen must be supplied to the bioreactor facility as shown in Figure 2.1. The hydrogen required for this reaction will be produced from the breakdown of water through electrolysis, for example by carbon neutral solar or nuclear energy. The energy needed to break apart water must be a green method of energy

production such as electricity generated from a wind turbine that does not yield any greenhouse gases (Figure 2.1). Given that the energy used to separate hydrogen from water molecules is a clean source then the idea of capturing atmospheric carbon dioxide and converting to methane remains a carbon neutral process.

2.5 Introduction to methanogenesis

Methanogenesis is the formation of methane from hydrogen and carbon dioxide (Equation 1). This process is done by a group of naturally occurring microbes called methanogenic bacteria, or methanogens that are common to anoxic subsurface environments (Boone, et al. 1993). Methanogens have been found in all anaerobic environments investigated (Chong, 2008).

$$4H_2 + CO_2 \rightarrow CH_4 + 2H_2O \qquad \text{(Eq. 1)}$$

Methanogenesis is the last step in the degradation of organic material. A more detailed description of methanogenesis is displayed in Figure 2.2. Fermenting bacteria excrete enzymes to degrade the organic matter and break it down to simpler monomers. There are numerous pathways that can result from the primary fermentation that occurs. One such pathway is the production of carbon dioxide and hydrogen that can be utilized by hydrogenotrophic methanogens, and ultimately produce methane. Another path is for the carbon dioxide and hydrogen to be utilized by acetotrophic bacteria that will produce acetate through a process called acetogenesis. The acetotrophic bacteria will cleave the acetate to produce methane and carbon dioxide. In addition, primary fermentation can directly produce acetate or other organic acids and alcohols which undergo acetogenesis. (Megonigal, 2004).

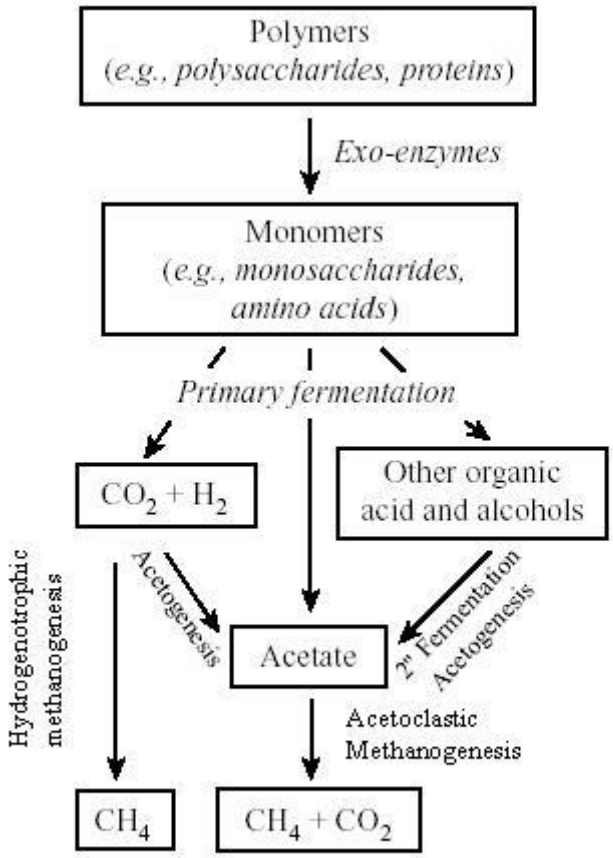

Figure 2.2: A graphical representation of organic matter degradation pathway, and its eventual transformation to methane (Megonigal, 2004).

Methanogenesis is a part of many complex reactions that take place as the terminal step in the degradation of organic matter and oxidation-reduction sequence or terminal electron acceptor processes (TEAPs) (Figure 2.3). Ideally, these reactions should follow a thermodynamic order of reduction; going from the highest redox potential to the lowest (Achtnich et al., 1995). In anaerobic environments, the following species or electron acceptors follow a sequential order of reduction: O_2, NO_3^-, Mn (IV), Fe (III), SO_4^{2-}, and CO_2 (Figure 2.3) (Achtnich et al., 1995). The microorganisms that catalyze

the reactions are active at different redox potentials and cause the order of reduction (Achtnich et al., 1995). The competition for the substrate of hydrogen could dictate which electron acceptor is reduced first. Methanogens utilize hydrogen at a lower threshold than other microorganisms. In a natural environment, once the ideal hydrogen threshold is reached, methane production will dominate. If hydrogen levels increase or decrease other processes will take precedence over methanogenesis.

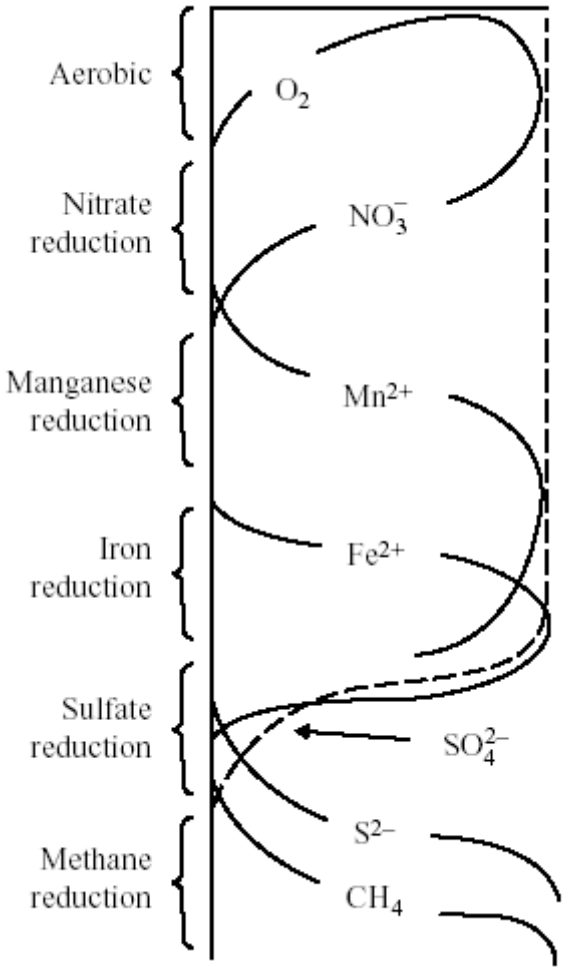

Figure 2.3: Sequence of redox reactions or terminal electron accepting processes (TEAPs) from oxygen reduction to methanogenesis (Megonigal, 2004).

In addition to the formation of methane by microbes, methane can be produced through a chemical process called *methanation*. Similarly to methanogenesis, methanation requires hydrogen and carbon dioxide to produce methane, but methanation also needs a catalyst which can consist of a single crystal nickel, Ru/RuO_x or TiO (Peebles and Goodman, 1983 and Thampi, Kiwi, and Gratzel, 1987). Peebles and Goodman (1983) studied methanation at temperatures between 450 and 750 k and they found methane formation from carbon dioxide to have an activation energy of 21.2 kcal mol^{-1}. The equation for methanation is described in equation 2.The reaction is thermodynamically favorable and has a Gibbs Free energy of -27 kcal mol^{-1}. However, this reaction is hard to achieve because it requires high temperatures, produces a lot of intermediates such as CO, and has large kinetic barriers (Thampi, Kiwi, and Gratzel, 1987).

$$CO_2+4H_2 \rightarrow CH_4 + 2H_2O(g) \qquad \text{(Eq. 2)}$$

2.6 Factors affecting methanogenesis

2.6.1 Effect of hydrogen thresholds on methanogenesis

In anaerobic environments where microbes have depleted all other electron acceptors, methanogenesis is the last process to occur, thus reducing carbon dioxide. At this phase, hydrogen, an important precursor for methane production, can only be consumed by methanogenic and homacetogenic bacteria (Conrad 1999). The process of H_2/CO_2 utilization by methanogens is the main pathway of methane production in peatlands (Galand, et al. 2005) and on washed rice roots (Conrad and Klose, 1999). The

formation of methane from carbon dioxide and hydrogen gas is called hydrogenotrophic methanogenesis (Equation 1). Hydrogen acts as the electron donor for the reduction of carbon dioxide to methane and is one of the most important substrates used by methanogens (Zinder, 1993). The amount of hydrogen in the environment can effect which group of these bacteria are active. Leybo, Netrusov, and Conrad (2006) found that the bacterial community structure changes as a result of hydrogen concentration. At high hydrogen concentrations there is less diversity in the community than there is in low hydrogen conditions (Leybo et al., 2006).

Hydrogen concentrations are usually low in anaerobic environments, where methanogenesis occurs, and is quickly turned over (Conrad, 1999). In natural environments, hydrogen concentrations are between 10-300 ppm when methanogenesis is at steady state, and, upon flooding, the hydrogen levels may increase to thousands of ppm (Chidthaisong et al., 2002). As a result, hydrogen is utilized by the most thermodynamic processes first. For methanogenesis to take place it needs a hydrogen threshold that is equivalent to Gibb's Free Energy of -23 kJ mol^{-1} CH_4. If the hydrogen threshold goes below this level then methane production is inhibited. The only way for a lower threshold to be reached is if another reaction with a lower hydrogen threshold is working faster and more efficiently than methanogenesis (Conrad, 1999). Hydrogen is not consumed by methanogens below a certain threshold, which is dependent on the strain of bacteria. For example, a study found that in nongastrointestinal methanogenic conditions, a partial pressure between 1 and 7 Pa is maintained by hydrogen-utilizing methanogens (Lovley and Ferry, 1985). However, *Methanobacterium formicicum* was observed to only metabolize hydrogen down to 7 Pa and showed no further decline upon increased

incubation (Lovley, 1985). *Methanobacterium byrantii* and *Methanospirillum hungatei* had a hydrogen threshold that varied from *M. formicicum* (6.9 ± 1.5 Pa and 9.5±1.3 Pa, respectively) (Lovley, 1985).

The stoichiometric proportions of hydrogenotrophic methanogenesis indicate that for every 4 moles of hydrogen that are utilized, 1 mole of methane is produced. However, there are cases in the environment that have more or less than the 4:1 hydrogen to methane ratio (Conrad, 1999). Figure 2.2 shows that hydrogen can be coupled with carbon dioxide and directly converted to methane or it can be used to create acetate, by acetogenesis (Megonigal, 2004). As a result, the lower hydrogen contributions can be explained by the contribution of acetogenesis, where methane is produced from acetate and therefore the hydrogen to methane ratio is less than the 4:1 ratio shown in Equation 1. Seeing a greater than 4:1 hydrogen to methane ratio can be explained by other processes utilizing hydrogen besides just hydrogenotrophic methanogenesis.

2.6.2 Effect of acetogenesis on methanogenesis

Hydrogen is not the only substrate that can be used to produce methane; in fact acetate is another important substrate (equation 3). It is estimated that about 70% of methane in freshwater systems is a result of acetate breakdown (Ogrinc et al., 2008). The acetate can be cleaved through acetoclastic methanogenesis to produce methane and carbon dioxide (Equation 3). Acetate is formed through a process called homoacetogenesis, which like hydrogenotrophic methanogenesis, is a product of the coupling of hydrogen and carbon dioxide (Equation 4).

$$CH_3COOH \rightarrow CO_2 + CH_4 \qquad \text{(Eq. 3)}$$

$$2CO_2 + 4H_2 \rightarrow CH_3COOH + 2H_2O \quad \text{(Eq. 4)}$$

The process of homoacetogenesis uses the same substrates as hydrogenotrophic methanogenesis and therefore the two reactions may compete (Florencio, et al., 1995; Strapoc et al., 2008; Jones and Simon 1985). Hydrogenotrophic methanogens are not the only microbes that reduce carbon dioxide to methane. In fact, acetogenesis can be implemented to degrade carbon dioxide as well (Achtnich et al., 1995). Acetogenesis, like methanogenesis, may consume hydrogen as a precursor to reducing carbon dioxide (Conrad et al., 1985). The consumption of hydrogen by acetogens keeps the partial pressure of hydrogen low enough that other thermodynamically favorable reactions, such as hydrogenotrophic methanogenesis, cannot occur (Conrad et al., 1985). The reason why acetogens can outcompete hydrogenotrophic methanogens is not fully understood, but it is predicted that the competition occurs because acetogens can consume hydrogen at lower thresholds than those useful to hydrogenotrophic methanogens (Conrad and Klose, 1999). If acetogens are consuming all of the available hydrogen, the production of methane by hydrogenotropic methanogens may be inhibited. As such, it can disrupt the 4:1 stoichiometric ratio of hydrogen utilization to methane production that is seen in hydrogenotrophic methanogenesis (Equation 1) because hydrogen is used in acetogenesis instead of hydrogenotrophic methanogenesis. The competition between the two processes has been observed in natural environments; it is estimated that only 20-50% of methane in rice paddies is produced by the reduction of CO_2 (Equation 1), and the remaining methane is produced by the reduction of CH_3COOH, or acetic acid (Chin and Conrad, 1995).

2.6.3 Effect of competition with other TEAPs on methanogenesis

Reactions occur as a result of the thermodynamic theory; the highest energy producing reactions occur first with the lowest energy producing reactions occurring last: O_2, NO_3^-, Mn (IV), Fe (III), SO_4^{2-}, and CO_2 (Figure 2.3) (Achtnich et al., 1995). Many studies have been conducted to determine the effects of different terminal electron accepting processes (TEAPs) on carbon dioxide reduction to methane.

A study by Achtnich et al. (1995) focused on the interactions and competition between the reduction of NO_3^-, Fe (III), and SO_4^{2-} in anoxic soils. They also investigated how the production of methane was altered with respect to the availability of various electron donors in the same soil. They found that reduction processes were a result of competition and resulted in depletion of common electron donor thresholds. Adding electron acceptors such as NO_3^- inhibited Fe (III), and SO_4^{2-} reduction since nitrate has a higher redox potential than ferric iron and sulfate. However, when additional hydrogen was made available, Fe (III) and SO_4^{2-} were able to become reduced as a result of a higher availability of electron donors. Upon adding any of the electron acceptors Gibb's free energy increased and the production of methane was inhibited. In support of these results, another investigation was conducted to study the competition between sulfate reducing bacteria and methanogenic bacteria for hydrogen. This study determined that sulfate reducing bacteria have the ability to lower the partial pressure of hydrogen to a point where methanogenesis in no longer energetically favorable (Lovely et al., 1982). Overall, the results show that methanogenic activity was outcompeted by the other, more oxidizing TEAPs (Achtnich et al., 1995).

Methane production can be inhibited because of thermodynamics of the TEAPs and competition for hydrogen, but some microbes are affected differently under these TEAPs. Under iron reducing conditions, ferric iron is responsible for the direct inhibition of methanogenesis (van Bodegom, Scholten & Stams, 2004). The inhibition is thought to be caused partly by substrate competition and increased redox potential, but methane suppression is variable among different species of methanogens. Bodegom et al. (2004) found that some methanogens were more sensitive to ferric iron than others. Upon further investigation, they found that, in particular, *Methanosarcina barkeri* has the capacity to efficiently reduce ferric iron and make conditions more methanogenically favorable. As a result, Fe (III) had less of an inhibitory effect on *M. barkeri* than on other strains of methanogens.

In addition to the inhibition of methanogenesis due to unfavorable redox conditions and competition for substrates, it has been found that some products of TEAPs have a toxic effect on methanogens; specifically, nitrate and other denitrification products such as nitrite, NO and N_2O. Kluber and Conrad (1998) added nitrate to previously methanogenic soils and observed that methane production was stopped immediately. When methanogenic conditions were resumed, methane production in the nitrate treated systems remained lower than methane production in systems that were never amended with nitrate. This implies that there are toxic effects associated with nitrate (Kluber and Conrad, 1998). A study by Roy and Conrad (1999) found supporting evidence that intermediates such as NO and N_2O have toxic effects of methanogenesis.

2.6.4 Effect of temperature on methanogenesis

Methanogens can survive at various temperatures and have been found in environments ranging from 5 to 110^{o}C (Zinder, 1993). The most common environment for methanogenesis to occur is in flooded rice fields which range in temperature from 15-30^{o}C (Chin and Conrad, 1995). Temperature, among other things, can ultimately affect the methane yield from hydrogenotrophic methanogens in a specific environment (Chin and Conrad, 1995). The temperature can affect the way organic matter is decomposed and therefore change the rate of methane emission. An experiment by Chin and Conrad (1995) identified the effects of temperature on methanogenesis by analyzing anoxic soil samples from 15^{o}C and 30^{o}C. In order to gain a clear understanding of temperature effects on methanogenesis, they also examined the different contributing fermentation products as well. It was found that methane and hydrogen formation decreased at 15^{o}C, in comparison to 30^{o}C. Numerous intermediates (hydrogen, and volatile fatty acids (VFAs), such as acetate, propionate, and lactate) were found in the degradation of organic matter to methane and accumulated when methanogenesis was inhibited by chloroform. There was a larger degree of VFA accumulation at higher temperatures than lower temperatures. Adding hydrogen to the soils at both temperatures increased the rate of methane production, but the hydrogen had a lesser affect at 15^{o}C.

The effects of temperature on methane production were studied by Schulz and Conrad (1996). Acetoclastic production of methane was the focus of this experiment, whereas the previous experiment looked solely at hydrogenotrophic methanogens. They showed that lake sediments, which are dominated by acetate dependent methanogenesis, can increase methane production upon an increase in temperature. There are large

seasonal changes in temperatures that occur at this lake; as such, Schulz and Conrad (1996) compared methane production between winter and summer months. Profundal sediments, found in the deep zone of a body of water, produce more methane in the summer months because of the decomposition of algal biomass deposited at this depth. The activity of methanogenic bacteria was minimal at 6^{o}C since methanogenesis was typically limited at colder temperatures: (a) methane was produced by cleavage of acetate only (acetoclastic methanogenesis), and the growth of bacteria was slow, and (b) hydrogen turnover did not increase methane production, as the activity of hydrogenotrophic methanogens was nearly absent at 6^{o}C. At higher temperatures, however, methane was produced by acetate and CO_2 reduction in the presence of greater hydrogen and VFA availability. Degradation processes are dominated by homoacetogens ($CO_2 + H_2$=acetate) and acetoclastic methanogens (Acetate =CH_4+CO_2) at low temperatures, and fermentation and hydrogen dependent methanogenesis at higher temperatures.

2.6.5 Effect of oxygen exposure on methanogenesis

It is well known that methanogenesis occurs in anaerobic environments, but the methane producing microbes also can persevere in environments where oxygen exposure is common. Some scientists previously believed that aerobic upland soils could not support methanogenesis. As such, Peters and Conrad (1995) wanted to explore this concept and determine if anaerobic bacteria were frequently, if ever, found in oxic habitats. They collected soil from five aerobic sites and provided the soil with anaerobic conditions. They found strictly anaerobic bacteria to be in all five soil samples. This

indicates that methanogens are present in oxic soils, but remain dormant until the proper conditions are provided. A later study by Peters and Conrad (1996) confirmed that methanogenic bacteria are present in oxic upland soils. They flooded upland soil and studied the sequential reduction processes to examine what factors initiate methane production. Peters and Conrad (1996) monitored the methanogenic bacteria population, electron donors and electron acceptors. They found that the bacteria can in fact survive in oxic conditions and that redox-active substances such as hydrogen thresholds were the signal for methanogens to become active.

Some methanogenic bacteria have the ability to lower the redox potential caused by the presence of oxidants to provide a favorable condition for methanogenesis. In particular, *Methanosarcina barkeri* was found to be able to reduce ferric iron under certain conditions (Fetzer and Conrad, 1993). The ability of methanogens to reduce oxidants may explain why the anaerobic bacteria are able to survive in dry, oxic soils.

A study conducted by Liu, Miyaki and Aono (2008) isolated methanogenic bacteria and subjected them to a period of desiccation in order to determine their tolerance to prolonged periods of air exposure. They found that methanogens that were clustered had a higher survival rate than single strands of bacteria because in the aggregation a barrier of dead cells formed that acted as protection from the oxygen for the inner most bacteria. Similarly, methanogens that were desiccated with soil present were also more successful because the soil acted as an oxygen scavenger, retained moisture and provided shelter for the bacteria (Liu et. al, 2008).

Thus, minimal exposure to oxygen in the batch reactors or bioreactor should not have a toxic impact on the methanogens seeing as they have been found to be oxygen-tolerant and robust bacteria.

2.6.6 Effect of pH on methanogenesis

The pH can alter the overall productivity and the microbial community structure in a system. A study by Oh, Van Ginkel and Logan (2003) was conducted to learn more aboure how pH affects methanogenesis. They found that lowering the pH in the system from 7.5 to 6.2 dramatically reduced methanogenesis, but did not completely inhibit it. Similarly, Dunfield et al. (1993) found that processes that allow for methane production were not well adapted to low pH values. Furthermore, methanogenesis in a landfill was found to optimally occur at a pH between 6.8 and 7.2 (Kasali et al., 1988) and samples that fall out of that pH range produced little or no methane (Gurijala and Suflita, 1993).

In addition, pH not only affects the rate of methane production, but also the pathway of methane production. Kotsyurbenko et al., 2007, found that there was a shift from acetoclastic to hydrogen-dependent methanogenesis at a pH between 4.7 and 3.8. The pathway shift is attributed to acetic acid persisting in a free form at a pH values less than 4.7 (Kotsyurbenko et al., 2007). At a lower pH acetate was able to inhibit methanogenesis, but at a higher pH around 4.5 acetate did not inhibit methanogenesis (Horn, et al. 2003). However, the pH at which the shift between pathways is debatable. For instance, Oh et al. (2003) found the shift between acetoclastic and hydrogen-utilizing methanogenesis to occur around a pH of 6.

These studies show that at a higher pH more methane is likely to be produced and the dominant pathway will be hydrogenotrophic methanogenesis. Therefore my experimental systems must remain at a pH greater than 6, if pH drops lower than 6 methane production may still occur, but perhaps through another microbial process.

2.6.7 Effect of carbon (DOC/DIC) on methanogenesis

Carbon dioxide is a required ingredient in hydrogenotrophic methanogenesis (equation 1), if DIC in the system is decreased, then methane production will likely slow down, and hydrogen will accumulate. A study addressing the relationship between DIC and hydrogen found that decreasing the concentration of carbon dioxide in the headspace of a system from 24.5% to 5.2% caused an increase in hydrogen by 43%. It is thought that the reduced level of carbon dioxide suppressed the hydrogen consumption by acetogenesis and methanogenesis, therefore increasing the total concentration of hydrogen in the system (Park et al., 2005). Reducing carbon in the system diminishes methane production, in the same way that increasing the amount of carbon will stimulate methane production (Amaral and Knowles, 1994). The implications of this experiment show that the bioreactors in this experiment must remain at a high concentration of carbon dioxide to support methanogenesis.

If methanogenesis is occurring, it is expected that dissolved inorganic carbon (DIC) will be converted to dissolved organic carbon (DOC) throughout the duration of a sampling period. DIC is equal to the amount of carbonic acid, bicarbonate and carbonate in the system (equation 5) (Florencio et al., 1995). In systems near neutral pH, the amount of carbonate is negligible. DOC exists as a variety of organic carbons such as

volatile fatty acids like acetic and propionic acids (Mohammadzadeh and Clark, 2008; Conrad and Klose 1999). Carbon dioxide may also go to other organic carbons, such as propionate or acetate, or it may go towards forming biomass (equation 6) (Botz et al., 1996).

$$DIC = H_2CO_3^* + HCO_3 + CO_3^{2-} \quad \text{(Eq. 5)}$$

$$CO_2 = CH_4 + DOC + \text{biomass} \quad \text{(Eq. 6)}$$

2.6.8 Effect of various support materials on methanogenesis

There are many types of support material that can be used to promote anaerobic processes. Adding support materials can jumpstart a failing system if the properties are correct. Smaller particle sizes, hydrophobic properties and a rough, positively charged surface makes a support material more effective (Chauhan and Ogram, 2005 and Kida et al., 1990). Smaller particle sizes have more surface area and therefore more area for microbes to attach. The hydrophobic nature of a media would allow for more hydrophobic aggregates and methanogenic bacteria to attach (Chauhan and Ogram, 2005). In general, microbes have a negative charge and for that reason have a larger affinity for positively charged support medias (Kida et al., 1990).

One study was done to compare the effectiveness of perlite (volcanic rock) versus sepiolite (clay mineral) and their ability to serve as an anaerobic support media (Arnaiz, Gutierrez, and Lebrato, 2006). The physical properties of perlite and sepiolite are compared in the table below:

Table 2.1: Physical properties of perlite and sepiolite (Arnaiz et al., 2006)

	Density (kg/m^3)	Specific Surface Area (m^2/m^3)	Particle Diameter (μm)
Perlite	213	6199	968
Sepiolite	2300	5.5×10^8	250-600

The amount of biomass that was attached to the two mediums was the determining factor on which was a more effective support material. Arnaiz et al., (2006) found that there was more biomass on the sepiolite than the perlite. The sepiolite had a much larger specific surface area than perlite and was therefore a better support media. Sepiolite was also compared to other support mediums, pumice and sand, in a study by Balaguer, Vincent, and Paris (1997). They found there to be no strong initial difference in biomass growth between sepiolite, sand and pumice. However, towards the end of their experimental run time, sepiolite again proved to be able to support more biomass growth than the other two substrates (Balaguer et al., 1997)

Sepiolite was not available for purchase for my experiment whereas perlite was, so the effectiveness of perlite was investigated further. Sowmeyan and Swaminathan (2008) used perlite as a support medium in their anaerobic fluidized bed reactor. They found perlite to have similar physical properties as described by Arnaiz et al. (2006). Perlite was found to be an excellent substance to support biomass growth, so it was added to one of the two large bioreactors. It was hypothesized that the reactor with perlite would be more effective at carbon dioxide reduction and methane production than the reactor without support media.

2.7 Kinetics (Alexander, 1999)

The microorganisms within the microcosms and bioreactors use hydrogen as a source of energy and, as such, kinetics investigations can offer insight to the rate of hydrogen utilization with the systems. Varying amounts of hydrogen availability can change the population of the microbial community. If the substrate concentration increased, then the growth rate will increase as well, up to a certain point. At high concentrations of substrate, the population will no longer increase proportionally to substrate availability. This relationship is described mathematically by Monod (1949):

$$\mu = \frac{\mu_{max} S}{K_S + S} \qquad \text{(Eq. 7)}$$

Where μ= specific growth rate of the microorganism, μ_{max} = maximum specific growth rate, S= substrate concentration and K_S = constant, equivalent to a chemical concentration at which growth rate is half the maximum. The same equation can be expressed in alternative form:

$$\mu = \frac{\mu_{max}[B]}{K_M + [B]} \qquad \text{(Eq. 8)}$$

Where μ= specific growth rate of the microorganism, μ_{max} = maximum specific growth rate, [B] = cell abundance and $K_M = K_S$ constant, equivalent to a chemical concentration at which growth rate is half the maximum. The rate of change of substrate with respect to time can be modeled as:

$$-\frac{dS}{dt} = \frac{v_{max}[S]}{K_M + [S]} \qquad \text{(Eq. 9)}$$

Where dS/dt= change in substrate concentration [S] with time (t), S= substrate concentration, t= time, V_{max}=maximum rate and $K_M = K_S$ constant, equivalent to a chemical concentration at which growth rate is half the maximum. If V_{max} is substituted for by an equivalency factor of:

$$V_{max} = \frac{\mu_{max}[B]}{Y} \quad \text{(Eq. 10)}$$

Where V_{max} = maximum rate, [B] = cell abundance and Y= yield coefficient (Number of bacteria/mg of substrate); then the new equation becomes:

$$-\frac{dS}{dt} = \frac{\mu_{max}[B][S]}{Y(K_M+[S])} \quad \text{(Eq. 11)}$$

Where dS/dt= reaction rate, μ_{max} = maximum specific growth rate, B= cell abundance (cells/liter), S= substrate concentration Y= yield coefficient (Number of bacteria/mg of substrate) K_M= constant, equivalent to a chemical concentration at which growth rate is half the maximum. An exponential form of the equation can be written as:

$$[C] = [C]_o e^{\mu t} \quad \text{(Eq. 12)}$$

Where C=substrate concentration at a given time, C_o = Initial substrate concentration, μ= rate constant, t= time

All of the above equations have a component of cell density (B) or biomass because it is assumed that there is cell growth in the microcosms. Cell density (B) is changing due to of periods of potential starvation or periods of ample substrate availability.

2.8 Motivation of study

There is rising concern over the affects of increasing carbon dioxide concentrations in the atmosphere while at the same time there is an incentive to find a renewable fuel source. It is proposed here that atmospheric carbon dioxide be captured and used in a bioreactor that has the proper conditions to produce methane. Methane, a natural gas, could then be used as a fuel source. This process is carbon neutral meaning no 'new' carbon would be emitted into the atmosphere, but instead atmospheric carbon would be transferred into a hydrocarbon fuel. A more in depth study of the interactions that occur under methanogenic conditions is needed to see if this approach is feasible. Many studies have been done on methanogenic systems that focus of various parameters that ultimately affect the amount of methane produced. However, there is no research that specifically examines the microbial conversion rate of carbon dioxide to methane and the corresponding hydrogen that is consumed in the process. As such, that is the primary focus that this thesis will take. Investigating these factors is more manageable and less costly in a bench-scale study than implementing a large-scale experiment. A small scale lab study allows for more freedom in altering factors within the system and ease of sampling. It also allows for optimizing good sampling techniques of a system under methanogenic conditions before applying it to a large-scale operation.

2.9 Objectives

This research experiment investigates the bench-scale conversion of carbon dioxide to methane, a hydrocarbon fuel. Six small microcosms as well as two larger bioreactors were prepared with anaerobic wetland soil nutrient solution and high purity

H_2/CO_2 gas mix. Parameters such as, but not limited to gaseous methane, carbon dioxide, and hydrogen will be measured by gas chromatography and analyzed; further details are explained in the methods section. From these measurements, it will be determined if a successful microbial community can be established and to gain insight into hydrogen/carbon dioxide consumption and methane production. Investigating the process will determine the efficiency of carbon dioxide reduction and methane production by hydrogen utilizing methanogenic bacteria.

Batch reactors (160 mL serum bottles) and bioreactor (7 Liter Plexiglas reactors) experiments attempted to address the following factors:

- The ideal conditions for growing methanogenic bacteria (pH, temperature, TEAPs)
- Total mass of methane produced
- Rate of methane production
- Rate of carbon dioxide conversion to methane
- Rate of hydrogen consumption as a result of methane production
- Comparison of trends in batch reactors and larger bioreactors

Results from this work are applicable to understanding if capturing atmospheric carbon dioxide and using it as a substrate in a large-scale reactor would be feasible to produce considerable amounts of methane, a fuel source.

III. Materials and Methods

3.1 Culture and growth medium

A soil sample was collected from a wetland near Wright State University (located at the Wright Patterson Air Force Base, OH), and used as source for growing methanogenic cultures at a bench scale. The soil was amended with basal medium to ensure appropriate growth conditions for methanogenic cultures. The basal medium (modified after Yang and McCarty, 1998) used for methanogenic enrichment was prepared by dissolving the following in 1 liter of deionized or DI water : 0.5 g of K_2HPO_4, 1.5 g of Na_2CO_3, 5 mg of Na_2S as a sulfur source and reductant, 200 mL of Mineral Solution (4 g of NaCl, 5 g of NH_4Cl, 0.5 g of KCl, 0.5 g of KH_2PO_4, 0.5 g of $MgCl_2.6H_2O$, 0.2 mg of $CaCl_2.2H_2O$ in 1 liter of DI water), 25 mL of Trace Metal solution (0.2 g of $MnCl_2.4H_2O$, 0.04 g of $CoCl_2.6H_2O$, 0.024 g of H_3BO_3, 0.004 g of $ZnCl_2$, 0.004 g of $CuCl_2.2H_2O$, 0.004 g of $NiCl_2.6H_2O$, 0.004 g of $Na_2MoO_4.2H_2O$, 0.004 g of Na_2SeO_4, 0.004 g of $Na_2WO_4.2H_2O$, 0.008 g of $Al_2(SO_4)_3.18H_2O$, and 20 mL of 1 N HCl in 1 liter of DI water), and 1 mL of vitamin solution (0.02 g of biotin, 0.02 g of folic acid, 0.1 g of pyridoxine, 0.05 g of riboflavin, 0.05 g of thiamine, 0.05 g of nicotinic acid, 0.05 g of pantothenic acid, 0.05 g of p-aminobenzoic acid (PABA), 0.05 g of cyanocobalamine, and 0.05 g of thioctic acid in 1 liter of DI water).

3.2 Batch reactor experimental design

Bench-scale experiments to study microbial methanogenesis with wetland soil were conducted in 160 mL serum bottles (in triplicate, identified as MS-1, MS-2, and MS-3). Each bottle was filled with 80 mL liquid volume: 20 mL of wetland slurry and 60 ml of anaerobic basal medium, and the remaining 80 mL of headspace was filled with an anaerobic gas mixture (80% H_2, 20% CO_2). After 3 weeks, new soil-free microcosms were established in 160 mL serum bottles (in triplicate, identified as TMS-1, TMS-2 and TMS-3) with 60 mL of deoxygenated basal medium and 20 mL of supernatant fluid from MS microcosms, and the remaining 80 mL of headspace was filled with an anaerobic gas mixture (80% H_2, 20% CO_2). The original serum bottles were replenished with 20 mL of deoxygenated basal medium.

All 6 batch reactor bottles were prepared by sealing them with 20 mm Teflon-lined, grey butyl rubber stoppers (catalog #224100-175; Wheaton, Millville, NJ) and aluminum crimps to maintain anaerobic conditions, wrapped in aluminum foil to inhibit light penetration and photosynthesis, and were continuously mixed on a rotator shaker (catalog # 099A RD4512, Glas-Col Terre Haute, IN) at a gentle speed (22 rpm).

All bottles were purged with an anaerobic, high purity gas mix to initiate a new cycle which typically lasted one week in duration. In order to replenish and restart the microcosms they were purged with 50:50% H_2:CO_2 gas-mix for 1 hour each to rid the bottles of the methane from the previous cycle. At the beginning of alternating cycles (Appendix J), 20 mL of supernatant fluid was removed from each bottle and replaced with 20 ml of anaerobic basal medium. There were 24 total cycles for MS bottles and 23 total cycles for TMS bottles (cycle details are described in Appendix J). Cycles 1-20 for

MS bottles and 1-19 for TMS bottles were injected with 50:50% H_2:N_2 before sampling and cycles 21-24 for MS and 20-23 for TMS were injected with high purity N_2 before sampling to obtain a partial pressure near 1 atm in the microcosms.

Three control reactors (identified as CR-1, CR-2, and CR-3) were set-up in clean 160 ml serum bottles similar to the procedure described above. One of the control reactors (CR-1) was set-up to assess if methane production would occur without adding an external microbial culture; this reactor contained 80 ml of deoxygenated basal medium. The second control reactor (CR-2) was set-up to assess the effect of known microbial inhibitors (3 mg L^{-1} sodium azide, 5 mg L^{-1} bromoethanesulfonic acid or BES) on methanogenic activity or methane production; this reactor was set-up with 60 mL of deoxygenated basal medium amended with 20 mL of inoculum from an active methanogenic microcosm (MS-1). CR-2 was maintained for 3 cycles in order to show copious methane production, following which anaerobic solutions of microbial inhibitors were added (3 mg L^{-1} sodium azide was added twice, followed by a single addition of bromoethanesulfonic acid or BES at 5 mg L^{-1}) The third control reactor (CR-3) was set-up to confirm that methane production in the microcosms was solely due to microbial activity; CR-3 was set- up with 70 ml of deoxygenated basal medium and 5 mg L^{-1} of BES solution (a methanogenesis inhibitor) (after Gurijala and Suflita, 1993) and 10 ml of inoculum from an MS microcosm. All 3 control bottles were purged with the same gas mix as the experimental bottles.

The affect of various support media (kaolinite and calcite) on methane production was examined. Two batch reactors (identified as TMS-4 and TMS-5) were set-up to assess the effect of increased particle surface area on methane production by adding

powdered minerals, kaolinite (1 g) and calcite (1 g), separately. These microcosms were maintained for several cycles and evaluated for methane production in the same manner as other microcosms.

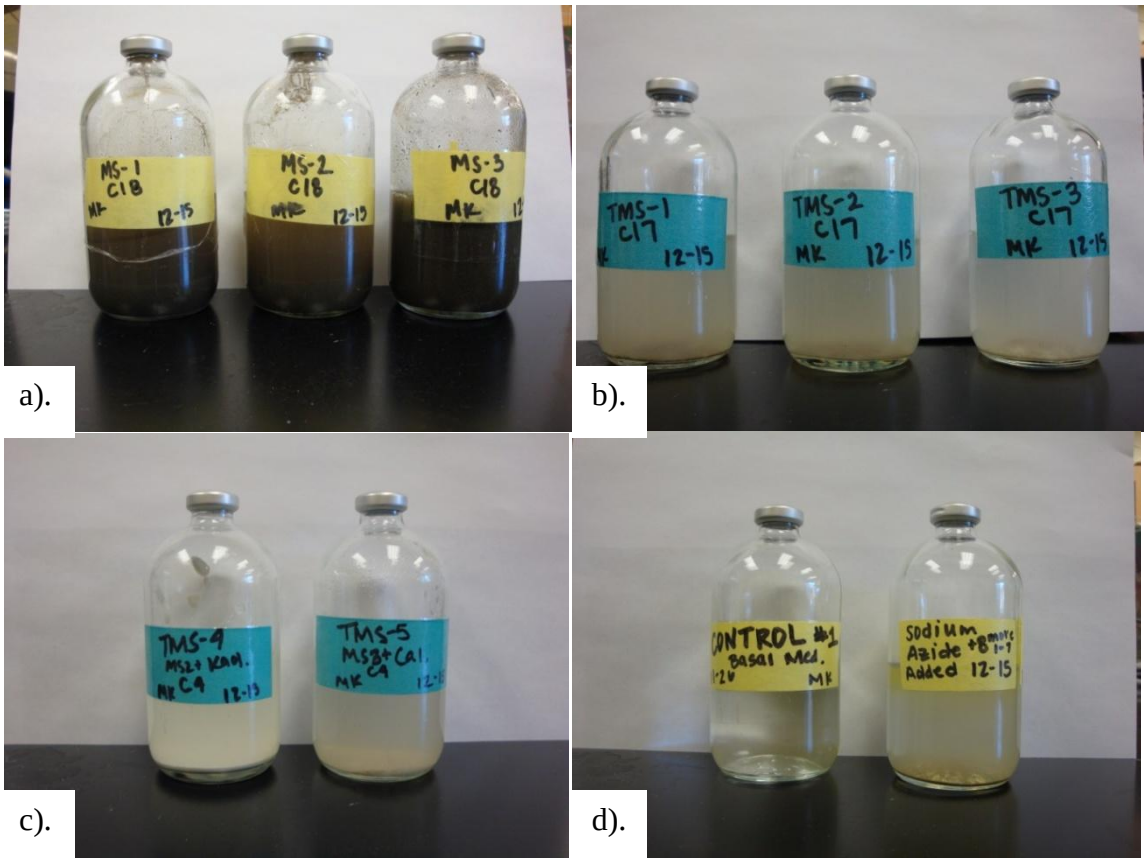

Figure 3.1: Photograph of various microcosms:(a). Original microcosms containing wetland soil (MS-1, MS-2, MS-3); (b). Soil free microcosms (TMS-1, TMS-2, TMS-3); (c). Microcosm with kaolinite (left) and microcosm with calcite (right) (TMS-4 and TMS-5); (d). Control (CR-1) with only basal medium; (left) Control (CR-2) with sodium azide (right); CR-3 not pictured

3.3 Bioreactors

3.3.1 Bioreactor experimental design

Bioreactor experiments set-up in two 7.2 liter Plexiglas cylindrical reactors (17.5 cm diameter x 30 cm tall; internal volume: 7215.85 mL; Figure 3.2) with a screw-on,

customized Plexiglas lid complete with an o-ring. The lid of the reactor is custom fitted with 3 ports, two of which were fitted with male pipe-adapters for connection with ¼" Teflon tubing that were connected with a two-way stop valves with a luer lock (Figure 3.2). The first port was for gas injection and it had a frit/sparger at the end to disperse the gas in the aqueous phase. The other was a liquid injection port that was open ended and also served as a release valve for when the reactor was purged with gases. In addition to these two injection ports, there was another port adapted to fit a Teflon-lined grey butyl rubber stopper with an aluminum cap that could be sealed with an aluminum crimp and was used for headspace sampling.

3.3.2 Bioreactor set-up and experimental conditions

The reactors were rinsed with DI water followed by ethanol to ensure it was sterilized. One reactor was filled with 15% aqueous phase (~1L) (MR#1) and the other reactor with 30% aqueous phase (~2.1 L) (MR#2) which included inoculum from the original batch experiment microcosms and basal medium. A stir bar and resazurin (final concentration 1g/L), a color indicator of anoxic conditions, were added to each reactor. The system showed a blue color when oxygen was present and pink or clear color in reduced conditions (Neumann et al., 1996; Guerlin et al., 2001). One reactor had 50 g of perlite added to it as a substrate for microbes to grow on (MR#2). The reactors were closed by screwing each lid on securely. The reactors were then purged with nitrogen gas for one hour to remove the majority of the oxygen present. To make the reactor completely anaerobic, sodium thioglycolate, an oxygen scavenger, was added. Two grams of sodium thioglycolate were dissolved in 50 ml of DI water in a 72 ml serum bottle and then purged with nitrogen gas for 15 minutes to make in anaerobic. A syringe

with an attached luer lock tip was used to transfer the sodium thioglycolate directly into the reactor. Once this was added the reactor was assumed to be completely reduced, as indicated by the clear color and the reactors were inoculated by the original microcosm bottles. Both reactors were placed on a stir plate and covered with aluminum foil to produce dark conditions to prevent photosynthesis.

The bioreactors were purged with a high purity gas mix to initiate a new cycle which typically lasted two weeks in duration. In order to replenish and restart the bioreactors, they were purged with 50:50% H_2:CO_2 gas-mix for 1 hour each to rid them of the methane from the previous cycle. There were 9 total cycles for MR#1 and 5 total cycles for MR#2.

a). MR#1  b). MR#2 

Figure 3.2: Photograph of bioreactors. Photograph on the left does not contain perlite and has 15% aqueous phase (a) the one on the right has perlite with 30% aqueous phase (b).

3.4 Analysis

The microcosms were analyzed regularly for methane, hydrogen and carbon dioxide in gaseous samples, and for alkalinity, pH, Fe (II), DON, DIC and DOC in aqueous samples. The bioreactors were analyzed regularly for methane, hydrogen and carbon dioxide in gaseous samples and pH in aqueous samples. Methane was analyzed by a HP 6890 series GC System equipped with an FID detector, and a capillary column (GS GasPro, 30m x 0.32mm; J&W Scientific) with helium as the carrier gas at constant flow of 2.1 mL min^{-1}. The GC inlet and detector temperatures were kept at 200 ^{o}C and 250 ^{o}C, respectively. The oven temperature was programmed at 50 ºC for 2 minutes, 10 ºC from 50 to 160 ºC, and no hold at 160 ºC (total 13 minutes). Hydrogen and carbon dioxide analysis were analyzed by a HP 5890 series GC System equipped with a TCD detector, and a packed column (Shin Carbon 100/120, 2m x 1mm, Restek). The carrier gases for hydrogen and carbon dioxide analysis were helium and nitrogen, respectively. The GC method settings for carbon dioxide analysis were as follows: inlet and detector temperatures at 100 ºC and 160 ºC, respectively, and oven temperature program was 30 ºC for 1.5 minutes, 25 ºC min from 30 to 155 ºC, and no hold at 155 ºC (total 7.5 minutes). The GC method setting for hydrogen analysis was as follows: inlet and detector temperatures at 100 ºC and 150 ºC, respectively, and oven temperature program was 30 ºC for 3.0 minutes, and no hold at 30 ºC (total 3.0 minute). Carbon dioxide gas chromatograph data was used to calculate the total, headspace, and aqueous phase inorganic carbon in the systems. Hydrogen gas chromatograph data was used to calculate total, headspace and aqueous hydrogen concentrations in the systems. Further details on

how gases were quantified are shown in Appendix G, H, and I (after Burris et al., 1996). The hydrogen gas chromatograph data was also used to determine the reaction kinetics occurring the microcosm and bioreactor systems. Both the hydrogen concentration and the natural log of hydrogen were plotted versus time for every cycle.

Alkalinity was measured by UV-VIS Spectrophotometry (modified after Sarazin, et al., 1998). A TOCN Analyzer (model: Apollo 9000, Teledyne Tekmar, Cincinnati, OH) was used to analyze DOC, DON, and DIC of the filtered microcosm samples. Dissolved Fe (II) was quantified by 1, 10- phenanthroline method (Fortune and Mellon 1938). The same data was collected at the beginning as it was at the end of each cycle. Duplicates or triplicates were used when measuring each parameter (See Appendix J for more details).

IV. Results and Discussion

4.1 Stoichiometry

4.1.1 Methane, hydrogen, and inorganic carbon variations in methanogenic microcosms

Rapid methane production was observed in the microcosms as a result of carbon dioxide reduction in the presence of hydrogen. The typical trends in methane production and the corresponding utilization of hydrogen and IC in soil (MS) and soil free (TMS) microcosm over a 24 week study period are shown in Figures 4.1 and 4.2. In general, given an equivalent amount of time after reset, the microcosms with soil (MS) have more methane produced than the soil-free microcosms (TMS). Methane mass in MS-1 Cycle 22 and Cycle 24 increased from 0 to 410 micromoles and 0 to 415 micromoles, respectively, and methane accumulated during the cycles. The methane mass accumulated in soil free microcosms was somewhat less than soil microcosms; in TMS-1 in Cycle 23, methane increased from 0 to 294 micromoles and TMS-2 Cycle 23 increased from 0 to 303 micromoles. Methane production was the highest immediately after reset and leveled off towards the end of the cycle probably a result of an initial phase of cell growth followed by a phase of no further cell growth (Figure 4.1 and 4.2) (Botz et al., 1996).

With regard to variation in measured hydrogen mass in the soil and soil free microcosms investigated in several cycles, it is evident that hydrogen decreased during

each cycle (e.g., Figure 4.1 and 4.2). This is to be expected since hydrogen is used as a substrate in the conversion of carbon dioxide to methane (Wu et al., 2002). However, rate of hydrogen utilization in these closed, laboratory systems is often greater than what be expected in natural environments (Chidthaisong et al., 2002). Regardless, it was typically observed that the microcosms with soil (MS) had greater hydrogen uptake during the cycle causing less remaining hydrogen at the end of the cycle than the soil-free microcosms (TMS). For example, hydrogen mass in MS-1 in cycles 22 and 24 decreased from 879 to 20 micromoles and 1644 to 0 micromoles, respectively, throughout the cycle, whereas hydrogen mass in TMS-1 and TMS-2 in cycle 23 went from 1512 to 234 micromoles and 1561 to 459 micromoles, respectively during the same period.

Further, a net decline in total inorganic carbon or IC in the microcosms was expected due to its conversion to methane (Figure 4.1 and 4.2). All microcosms show an initial decline in IC followed by stabilization, but IC utilization is slightly greater in the soil microcosms than the soil-free microcosms. IC mass in MS-1 in cycles 22 and 24 went from 5707 to 3214 micromoles and 6194 to 3323 micromoles, respectively, whereas in TMS-1 and TMS-2 in cycle 23 IC was much less, i.e., from 5533 to 4107 micromoles and 5675 to 3953, respectively. The IC values described above and in Figure 4.1 and 4.2 are quite consistent with the DIC data obtained from the TOCN Analyzer; both sets of data show IC utilization during a cycle (see Appendix K for IC data by TOCN analyzer). Further evidence of IC decrease in the microcosms is also from decrease in alkalinity values (spectrophotometrically determined alkalinity data shown in Appendix K). All of the above data support the hypothesis that hydrogen and IC mass in the systems would decrease while methane mass would increase.

4.1.2 Stoichiometry of hydrogen utilization and methane production

In systems where hydrogenotrophic methanogenesis is dominant, methane production in stoichiometric proportion to hydrogen utilization is indicated (Sakai, et al., 2007). If methanogenesis is sole process for hydrogen uptake, every 4 moles of hydrogen utilized would be converted to 1 mole of methane (see equation 1 below). In order to determine if this was the only responsible process, the measured hydrogen mass were utilized as a proxy to calculate the mass of theoretical or ideal methane mass to be produced. The actual methane mass formed matched closely with the theoretical methane mass for both the soil and soil-free microcosms (Figures 4.1 - 4.2). For example, in MS-1 Cycle 24, the actual methane observed reached 415 micromoles and the theoretical methane mass based on hydrogen data was 406 micromoles. Further in TMS-1 Cycle 23, the actual methane increased up to 294 micromoles, which is closely comparable to the theoretical methane mass of 319 micromoles. Based on the results presented above, it can be argued that methane production is in stoichiometric proportion to hydrogen utilization in these microcosms, which indicates that hydrogenotrophic methanogenesis is a dominant microbial process for hydrogen uptake in these microcosms.

$$4H_2 + CO_2 \rightarrow CH_4 + 2H_2O \qquad \text{(Eq. 1)}$$

4.1.3 Stoichiometry of inorganic carbon utilization and methane production

In the same way that methane production is in stoichiometric proportion to hydrogen utilization, inorganic carbon should be in stoichiometric proportion to methane (equation 1) in systems if hydrogenotrophic methanogenesis is a sole microbial process

for hydrogen uptake. However, the stoichiometric ratio between IC uptake and methane produced maybe somewhat different; every 1 mole of inorganic carbon should be converted to 1 mole of methane in hydrogenotrophic methanogenesis (see equation 1 above). In order to determine if this was the only responsible process, the measured cumulative methane mass in the microcosms was were used to calculate a theoretical IC depletion curve. However, unlike with hydrogen data, the actual IC curve did not match closely with the theoretical IC curve for soil as well as soil-free microcosms (Figure 4.3). In both systems, the actual amount of inorganic carbon depleted was much greater than the theoretical IC depletion expected if hydrogenotrophic methanogenesis was the dominant process occurring. For example, in MS-1 Cycle 22, the theoretical inorganic curve was expected to only decrease from 5707 to 5309 micromoles, but in reality it decreased from 5707 to 3214 micromoles. The same trend was observed in TMS-1 Cycle 24; the theoretical inorganic curve was expected to only decrease from 5533 to 5239 micromoles, but in reality it decreased from 5533 to 4107 micromoles. Based on the examples presented above, it is evident that the methane production was not in stoichiometric proportion to IC uptake like it was for hydrogen; instead there was a significantly larger decrease in IC than expected. It can be argued that the difference in expected and observed inorganic carbon mass can be attributed to IC being used through other pathways. One potential pathway could be the conversion of IC to biomass (uation 5) (Botz et al., 1996); around 90% of carbon dioxide utilized goes to methane production and less than 10% is converted to biomass or cell production (Fuchs et al., 1979). One other possible pathway is the conversion of carbon to organic carbons, such as acetate and propionate (equation 6) (Conrad and Klose 1999). Both of these processes would

result in carbon being utilized in other ways than only through hydrogenotrophic methanogenesis and could account for the difference in theoretical and measured inorganic carbon shown in Figure 4.3.

$$CO_2 = CH_4 + DOC + biomass \quad \text{(Eq. 6)}$$

4.2 Methane data

Immediately after microcosm set-up, methane production was very limited (0.1 micromoles hr^{-1}, but in the following cycles, subsequent to achieving active methanogenic conditions, methane production increased (between 3 and 5 micromoles hr^{-1}). In the first cycle, iron reduction was occurring as evident by the increase in Fe (II) mass (Appendix K). However, in the second cycle Fe (II) production was no longer active and methane production took over thereafter (Krylova et al., 1997). The initial lag in methane production has been observed in other studies as well (Yavitt, et al., 2006; Wu et al., 2002).

4.2.1 Average methane

The average amount of methane produced in all six experimental microcosms is shown in Figure 4.4. The average methane production in the microcosms with soil was lowest in MS-1, followed by MS-2 and MS-3, which had the highest average methane production (220, 303 and 311 micromoles, respectively) (Figure 4.4). Of the soil-free microcosms, TMS-2 had the lowest average methane production, followed by TMS-3 and finally TMS-1 was the highest (173, 185, and 214 respectively) (Figure 4.4). The pattern seen for methane production directly correlates with the pattern of average rate of

methane production (micromoles/hour) in the soil and soil-free microcosms (Figure 4.5). MS-1 had the lowest rate of methane production (3.5 micromoles/hour), MS-2 (5.1 micromoles/hour) was in the middle and MS-3 (5.28 micromoles/hour) was the highest. Similarly to methane mass, the rate of methane production ranged from TMS-2 being the lowest, then TMS-3 and then TMS-1 (2.9, 3.11 and 3.4 micromoles/hour respectively). The microcosms with soil, on average, displayed higher rates and higher amounts of total methane production than the soil-free microcosms. It was speculated that this trend would emerge because the microcosms with soil offer greater surface area for the microbes to attach to, and therefore the microbes becoming more efficient and productive. However, the rate of methane production observed in TMS and MS microcosms were both much higher than what was found in a methanogenic study by Leybo et al., (2006). They reported a normalized rate of only 5 micromoles L^{-1} hr^{-1} whereas the normalized rates of methane production in MS and TMS were often near 50 micromoles L^{-1} hr^{-1}. Furthermore, it is likely that both this study and Leybo's study had indicated higher rates of methanogenesis than what would be found in natural systems (Franklin et al., 1988).

To further investigate the affect of surface area on methane production, two additional microcosms were created to analyze other support mediums, in particular powdered kaolinite and calcite minerals. There were similar trends in methane mass and rate of production in the microcosm with kaolinite (TMS-4) and calcite (TMS-5). On average, TMS-4 produced 163 micromoles of methane and TMS-5 produced 184 micromoles. The average rate of methane production was 2.2 and 2.5 micromoles $hour^{-1}$ for TMS-4 and TMS-5, respectively. The amount of methane mass produced in TMS-4 and TMS-5, however, is less to that produced in the other soil-free (TMS) microcosms.

These results suggest that perhaps the MS bottles were more successful for other reasons than solely due to availability of mineral surface area as sites for microbes to attach and grow. Another possibility is that TMS-4 and TMS-5 potentially had unintentional differences in experimental set-up that negatively affected the methane production.

4.2.2 Comparison of methane data across cycles

The average mass of methane produced in each cycle is compared for all MS and TMS microcosms in Figure 4.6 and 4.7. The average mass of methane produced varied in microcosms for each cycle. The first cycle produced very low or no methane (data not shown). The initial lag in methane production has been observed in other studies as well (Yavitt, et al., 2006; Wu et al., 2002). Varying methane production could also be due to the fact that some cycles had a longer duration than others or some experimental parameters were drastically changed from cycle to cycle. With these things considered, the methane data was truncated to show the most common rates and amounts of methane production that occurred over the first 96 hours.

Even with the truncated data, methane production averages varied. The average mass of methane produced in MS-1 ranged from 143 to 346 micromoles (Figure 4.6). Most commonly, the mass of methane produced was near 200 micromoles in 96 hours. MS-2 ranged from 69 to 523 micromoles of methane; MS-3 varied between 138 and 571 micromoles of methane (Figure 4.6). In most cycles, in MS-2 and MS-3, about 300 micromoles of methane were produced on average. Like the soil microcosms, the soil-free microcosms also varied in average methane produced per cycle. TMS-1 ranged from 47 to 482 micromoles of methane, TMS-2 from 15 to 445 micromoles and TMS-3 from

32 to 294 micromoles of methane (Figure 4.7). In all microcosms there was a sharp initial increase in methane mass that leveled off usually in 24-48 hours which may have been a result of low concentrations of hydrogen (Roy et al., 1997).

The average rate of methane production for MS and TMS per cycle is shown in Figure 4.8 and 4.9. Soil-free microcosms had a lower rate of methane production than the soil microcosms. The soil-free microcosms ranged from 0.18 to 8.9 micromoles of methane per hour whereas the microcosms with soil ranged for 0.6 to 12 micromoles of methane per hour. These variations could be attributed to varying amounts of biomass or difference in active microbial species and biogeochemical processes in the two systems during the specific cycles as it has been found that changes in methanogenic communities can occur quickly (Leybo et al., 2006).

Figure 4.10 shows the typical amount of methane production that was achieved. Figure 4.10 shows all of the methane data that was obtained for MS-1 throughout all cycles, but it is comparable to the other microcosms as well. Methane production shows a consistent linear trend in the first several hours after cycle reset in Figure 4.10 and all the other microcosms.

4.3 Kinetics

Understanding kinetics in a system is important to knowing how fast a substrate is being depleted and determining the metabolism of given chemicals (Alexander, 1999). In order to gain knowledge on the kinetics of substrate degradation in the microcosm systems, hydrogen concentrations were measured at varying time intervals during several cycles. It is evident from hydrogen concentrations profiles as a function of time that the

majority of the microcosms display pseudo first order reactions (Figure 4.11). The hydrogen concentration over time plot showed to have an exponential relationship, and with strong correlation coefficients (Table 4.1). The rate constant (K_{obs}) for hydrogen depletion in MS microcosms is slightly higher (-0.03 Hr^{-1}) than the rate constant in TMS microcosms (-0.02 Hr^{-1}). In support, Figures 4.1 and 4.2 showed that methane production was higher and hydrogen was depleted faster (around 50-100 hours after reset) in MS microcosms than in TMS microcosms that still had hydrogen present after 200 hours. The MS microcosms were able to utilize hydrogen faster and therefore produced more methane than the TMS bottles in a similar amount of time. As such, the rate constants were slightly higher in MS than TMS microcosms (Table 4.1).

As shown in Table 4.1, there were strong patterns in some bottles for some cycles indicating pseudo-first order kinetics, but there were also some cycles that did not display strong trends. In a few instances, the microcosm kinetics was not strictly pseudo first order, and appeared to show mixed order kinetic behavior (data not shown). Due to very limited dataset, further discussion of hydrogen uptake kinetics may be difficult to accomplish.

The microorganisms in the batch systems were growing, so in order to determine kinetics, a measurement of cell density (B) or biomass was needed (eq. 7). Cell density (B) was changing due to of periods of potential starvation or periods of ample substrate availability. As a result of the biomass changing and possibly different microorganisms dominating at different periods during the cycle, the parameters involved in hydrogen kinetics (μ_{max}, V_{max}, and K_M) were constantly changing (Conrad, 1999). In addition to

not being able to measure biomass, kinetics were hard to determine in these systems due to mass transfer limitations across the gas-liquid interface.

$$-\frac{dS}{dt} = \frac{\mu_{max}[B][S]}{Y(K_M + [S])}$$

(Eq. 11)

Where dS/dt= reaction rate, μ_{max} = maximum specific growth rate, B= cell abundance (cells/liter), S= substrate concentration Y= yield coefficient (Number of bacteria/mg of substrate) K_M= constant, equivalent to a chemical concentration at which growth rate is half the maximum.

4.4 Controls and inhibitors

Control experiments were conducted in order to verify if methane production was an artifact of the experimental set-up or if it was a result of microorganisms present in the wetland soil. CR-1 that contained only basal medium was monitored for 4 cycles showed no methane production. The lack of methane production with basal medium alone may indicate directly that the methanogenic reactions occurring in the MS and TMS microcosms are not artifacts of the basal medium utilized.

A second control batch reactor, CR-2, with 20 ml of methanogenic inoculum and 60 ml basal medium showed methane production in initial 3 cycles of incubation (data not shown). During cycle 4, the microcosm was amended with 3 mg L^{-1} sodium azide. The methane production did not stop completely, but did seem to slow by the end of the cycle (Figure 4.12). In cycle 5, additional mg L^{-1} sodium azide was added to the

microcosm, and methane production was not completely inhibited yet again (Figure 4.12). In cycle 6, methane production ceased immediately after amending the microcosm with was 5 mg L^{-1} of BES, and methane production leveled off (Figure 4.12).

Another control batch microcosm, CR-3, with 10 ml of inoculum, 70 ml of basal medium, and 5 mg L^{-1} of BES,(data not shown) did not show any evidence of methane production. BES as a methanogenic inhibitor has been used and proven effective in other studies as well (Horn, et al., 2003; van Bodegom et al., 2004). These results suggest that methane production in the microcosms could be facilitated by addition of a live microbial culture to the basal medium, which became totally inhibited by amending the system with a known methanogenic inhibitor, BES.

4.5 Bioreactors

It was expected that the reaction rates observed in the microcosms would be similar to what would occur in a larger bioreactor; however, it was found that large Plexiglas reactors behaved differently in some aspects. In order to compare the two systems, the methane production rates were normalized to the fluid volume present in the microcosm (0.08L) and of the bioreactors (MR#1= 1L and MR#2= 2.1L) (Appendix K-methane raw data). The trends observed in the Plexiglas reactors were somewhat different than those of the 160 mL microcosms. The reactor without perlite (MR#1) had normalized rates that ranged from 1.8 to 56.2 micromoles L^{-1} of aqueous phase Hr^{-1} and the reactor with perlite (MR#2) ranged from 0 to 44.5 micromoles L^{-1} of aqueous phase Hr^{-1}. These rates are comparable to the MS and TMS bottles that were consistently around 40 micromoles L^{-1} of aqueous phase Hr^{-1}, but during some cycles the microcosms

reached much higher normalized rates. For example, MS-3 Cycle 3 reached a high of 124 micromoles L^{-1} of aqueous phase Hr^{-1}.

As a result of carbon dioxide conversion and hydrogen utilization, methane was produced in the bioreactors. The typical trends in methane production and hydrogen and DIC utilization through 10 cycles for MR#1 and 6 cycles for MR#2 are shown in Figure 4.13. Methane mass in MR#1 Cycle 9 increased from 0 to 3581 micromoles (Figure 4.13). The methane mass in MR#2 Cycle 5 increased from 0 to 9187 micromoles (Figure 4.13). It was expected that the reactor with perlite would produce more methane since perlite has been found to be an excellent material for biomass growth (Sowmeyan and Swaminathan, 2008; Arnaiz et al., 2006). It is evident in this figure that in MR#1 and MR#2 hydrogen is diminishing. This is to be expected since hydrogen is used as a substrate in the conversion of carbon dioxide to methane. Hydrogen mass in MR#1 Cycle 9 and decreased from 116521 to 93647 micromoles throughout the duration of the sampling period whereas hydrogen mass in MR#2 Cycle 5 went from 105041 to 39297 micromoles in a similar amount of time. There was more hydrogen depletion in MR#2 because there was more methane produced than in MR#1. In addition to hydrogen depletion, it was predicted that there would be a net decline in the amount of total inorganic carbon due to its conversion to methane. The pattern of total inorganic carbon in the systems is shown in Figure 4.13. There is not much inorganic carbon utilization occurring. Inorganic carbon mass in MR#1 Cycle 9 stayed around 160194 micromoles and MR#2 Cycle 5 stayed near 200053 micromoles through the entire cycle.

In systems where hydrogenotrophic methanogenesis is dominant, methane production is shown to be in stoichiometric proportion to hydrogen utilization (Sakai, et

al., 2007). For this process to be the dominant or sole process for hydrogen uptake, every 4 moles of hydrogen utilized would be converted to 1 mole of methane (see equation 1 above). In order to determine if this was the only responsible process in the bioreactors, the measured hydrogen values were used to calculate a theoretical methane production curve. The actual methane formation was much lower than the theoretical methane mass for both MR#1 and MR#2 (Figure 4.13). For example, in MR#1 Cycle 9, the actual methane observed reached 3581 micromoles whereas the theoretical methane mass based on hydrogen data was 9958 micromoles. Also in MR#2 Cycle 5, the actual methane increased up to 9187 micromoles which is much lower than the theoretical methane mass of 16435 micromoles. Based on the results presented above, it can be argued that hydrogen utilization was not in stoichiometric proportion to methane production in these reactors, which indicates that hydrogenotrophic methanogenesis was not the only microbial process for hydrogen uptake in these microcosms. A study by Amaral and Knowles (1994) also found hydrogen consumption to be larger than accounted for by solely methanogenesis and therefore predicted other anaerobic metabolism processes were dominating. Since a greater uptake of hydrogen than accounted for by hydrogenotrophic methanogenesis was observed, perhaps hydrogen was being used to create other products like propionate (C_2H_5COO),a distant methanogenic precursor, or acetate (CH_3COO), an immediate methanogenic precursor (Roy and Conrad, 1998; Tsurumi et al., 2000). It has been shown in other studies that methane, propionate and acetate can be produced from the reduction of carbon dioxide (Conrad and Klose, 1999). Methanogens can tolerate an accumulation of these volatile fatty acids and still produce methane as long as the system is a neutral pH, which was true of the both the batch

experiments and bioreactors in this study (Horn et al., 2003). However, as a result of the accumulation of intermediates (acetate and propionate), there was a smaller amount of methane produced than expected by hydrogenotrophic methanogenesis (Chin and Conrad 1995).

V. Summary

This research has proved helpful to better understand the processes involved in hydrogenotrophic methanogenesis at a bench-scale, such as the utilization of hydrogen and the conversion rate of carbon dioxide to methane. The newly gained insight on methanogenesis can be applied to determine if a larger scale reactor could produce a great enough quantity of methane to act as an alternative fuel source. The following is a summary of the findings from this thesis:

- Hydrogen-utilizing methanogens can be grown in a reactor setting and maintained relatively easily. As long as methanogenic conditions were provided, methane production continued. Microcosm methane data was collected for over one year and was continuing to produce viable amounts of methane.
- The amount of methane produced and the rate of methane production was larger in the microcosms with soil (MS) than in the microcosms without soil (TMS). This is presumably caused by the fact that the microbes have greater surface area to attach to and also obtain micronutrients from in the MS microcosms which makes them more productive than TMS microcosms.
- The hydrogen utilization in the MS and TMS microcosms displayed pseudo-first order kinetics. The overall rate of reaction was fast, and near complete hydrogen utilization was accomplished in about 5 days after cycle reset.

- Based on the theoretical methane curve generated from the actual hydrogen mass remaining in the system, it can be argued that hydrogenotrophic methanogenesis is the dominant microbial process occurring. The actual methane curve matched closely with the theoretical methane curve and was in stoichiometric proportion to hydrogen loss.
- Based on the theoretical inorganic carbon curve generated from the actual methane mass produced in the system, it can be argued that the process of hydrogenotrophic methanogenesis is not the only pathway responsible for inorganic carbon depletion. It is expected that some inorganic carbon was used to produce biomass or other organic carbons, such as acetate or propionate.
- The normalized rates of methane production were similar between the microcosms and the bioreactors, but the bioreactors behaved differently in some other aspects. The hydrogen utilization and methane production were not stoichiometrically proportional in the bioreactors as they were in the microcosms. It appears that hydrogenotrophic methanogenesis may not be the only process occurring in the systems with the larger volume.
- Further work still needs to be conducted in order to gain more insight on the rate of carbon dioxide conversion to methane and the corresponding hydrogen utilization in larger reactors before it can be determined if the process can be feasible on an industrial scale.

VI. Figures

a).

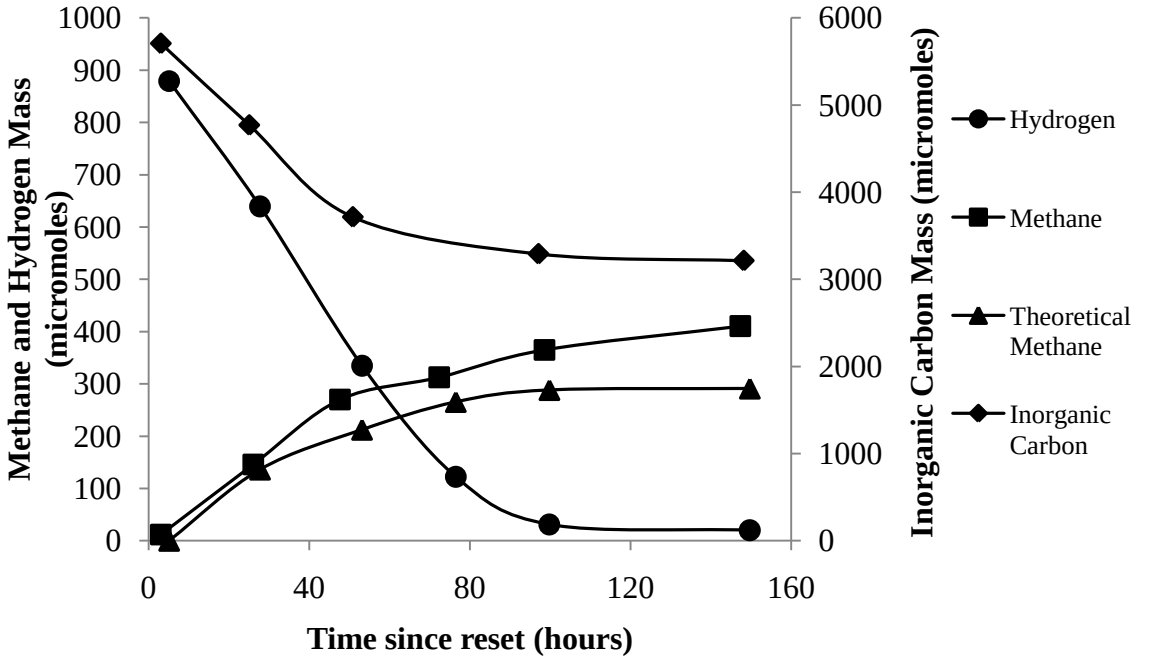

b).

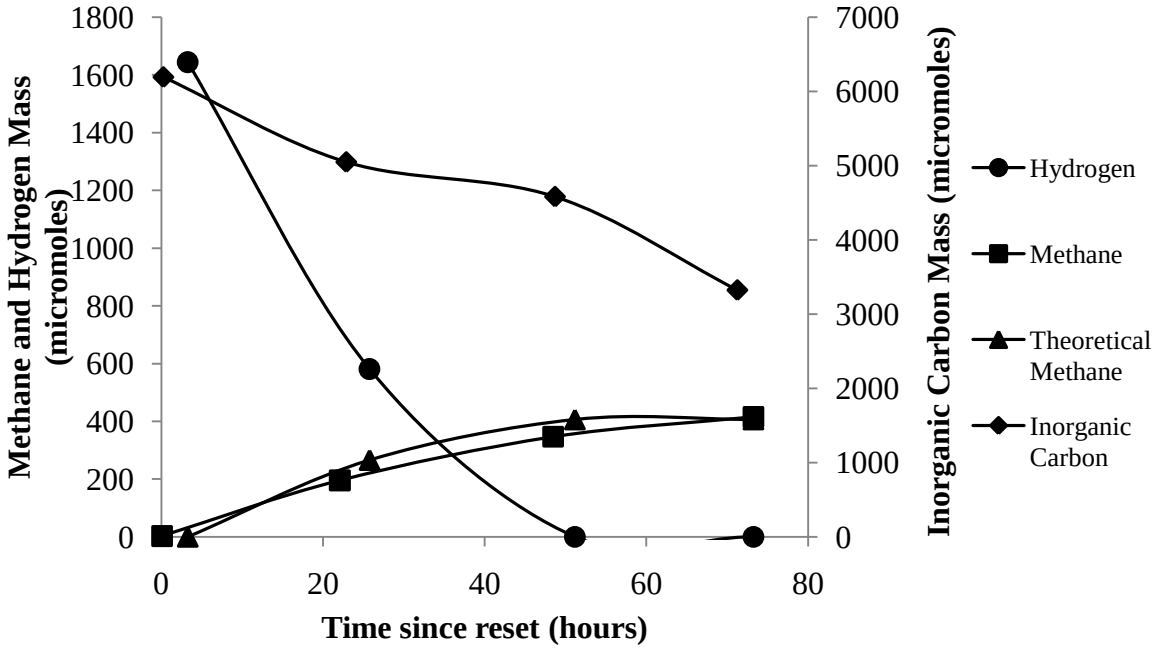

Figure 4.1: Typical mass variation of methane, hydrogen, and inorganic carbon in a microcosm with soil in two different cycles: a). MS-1, cycle #22, b). MS-1, cycle #24. Theoretical methane production calculated from measured hydrogen values compared to actual methane observed.

a).

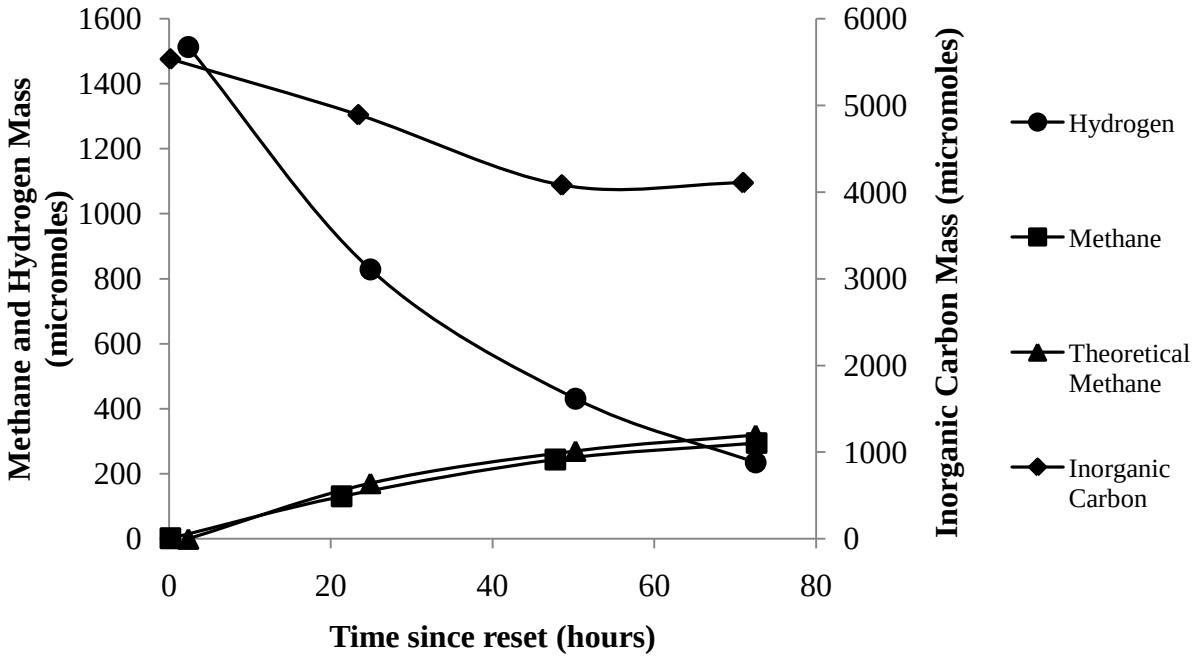

b).

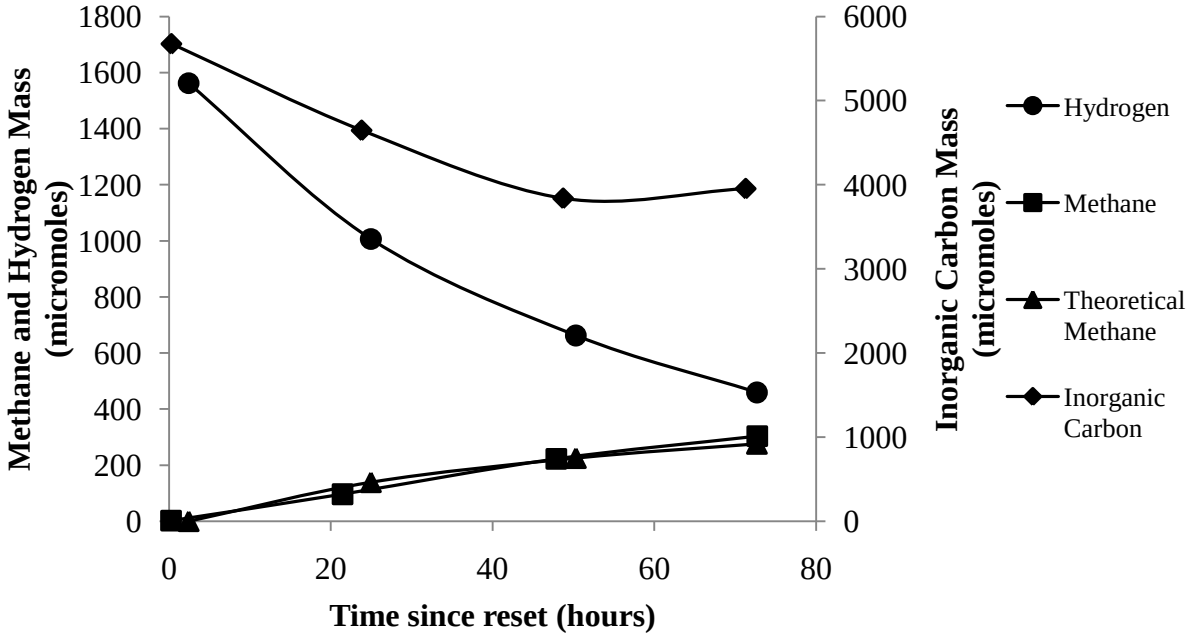

Figure 4.2: Typical mass variation of methane, hydrogen, and inorganic carbon in a microcosm without soil. Theoretical methane production calculated from measured hydrogen values compared to actual methane observed. a). TMS-1, Cycle #23 b). TMS-2, Cycle #23

a).

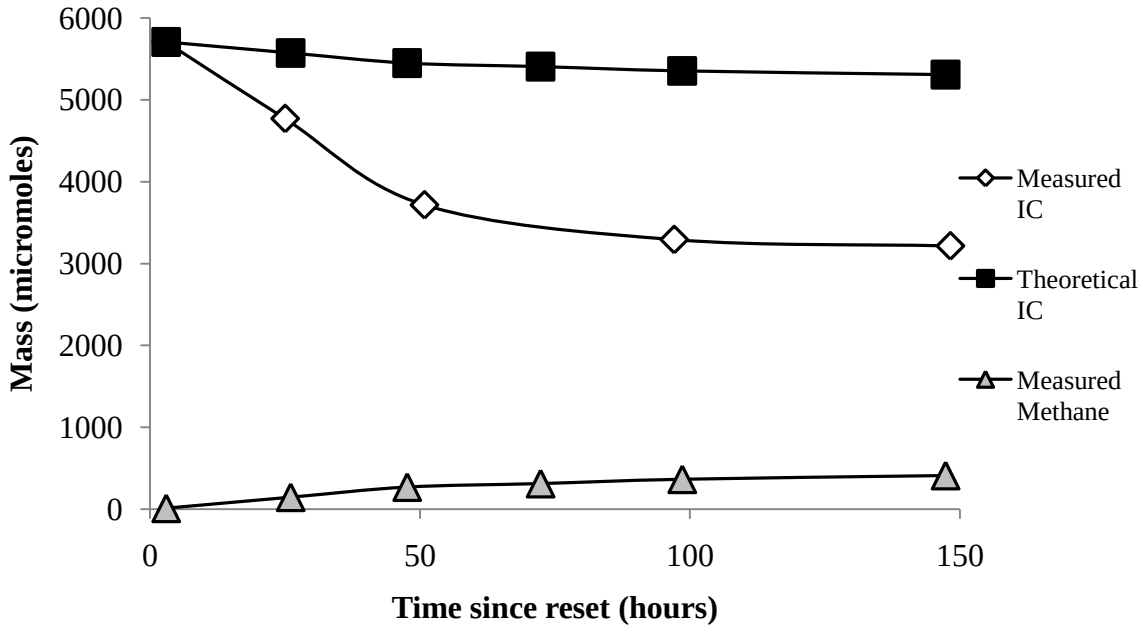

b).

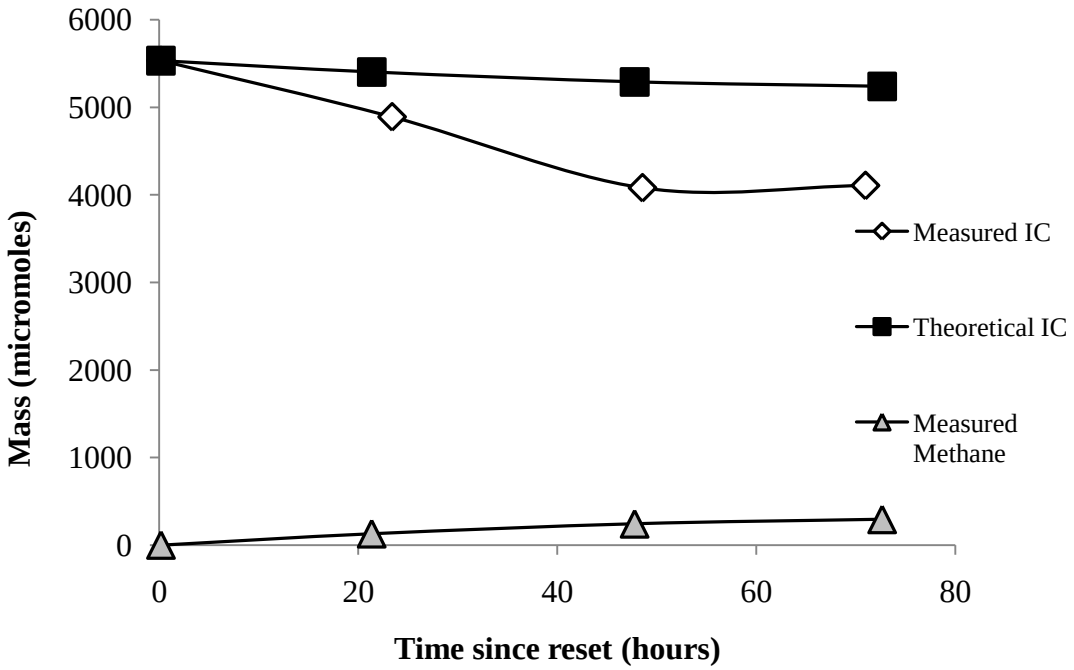

Figure 4.3: Theoretical inorganic carbon (IC) values calculated from measured methane data compared to actual measured inorganic carbon. a). MS-1, cycle #22. b). TMS-1, cycle #23

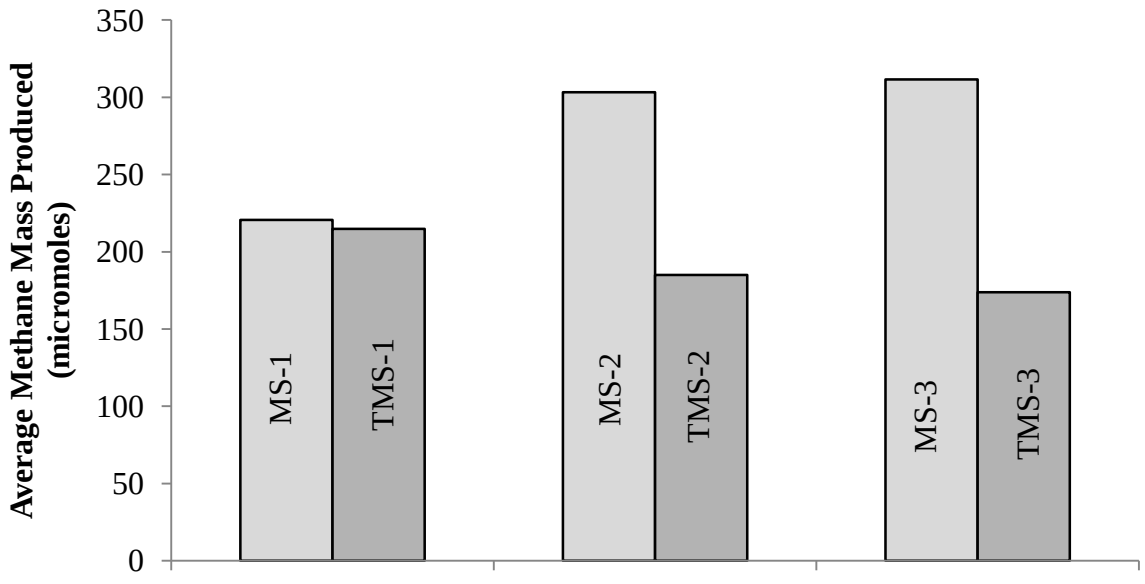

Figure 4.4: Average methane production in MS (soil) and TMS (soil-free) microcosms

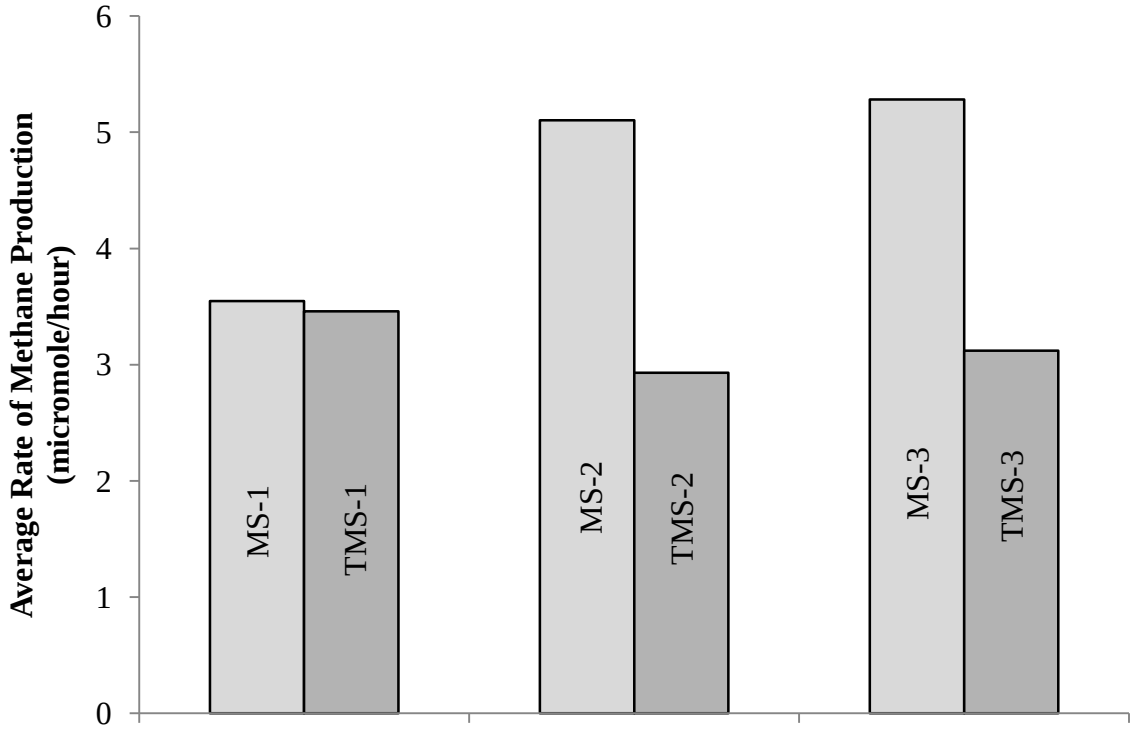

Figure 4.5: Average rate of methane production in MS (soil) and TMS (soil-free) microcosms

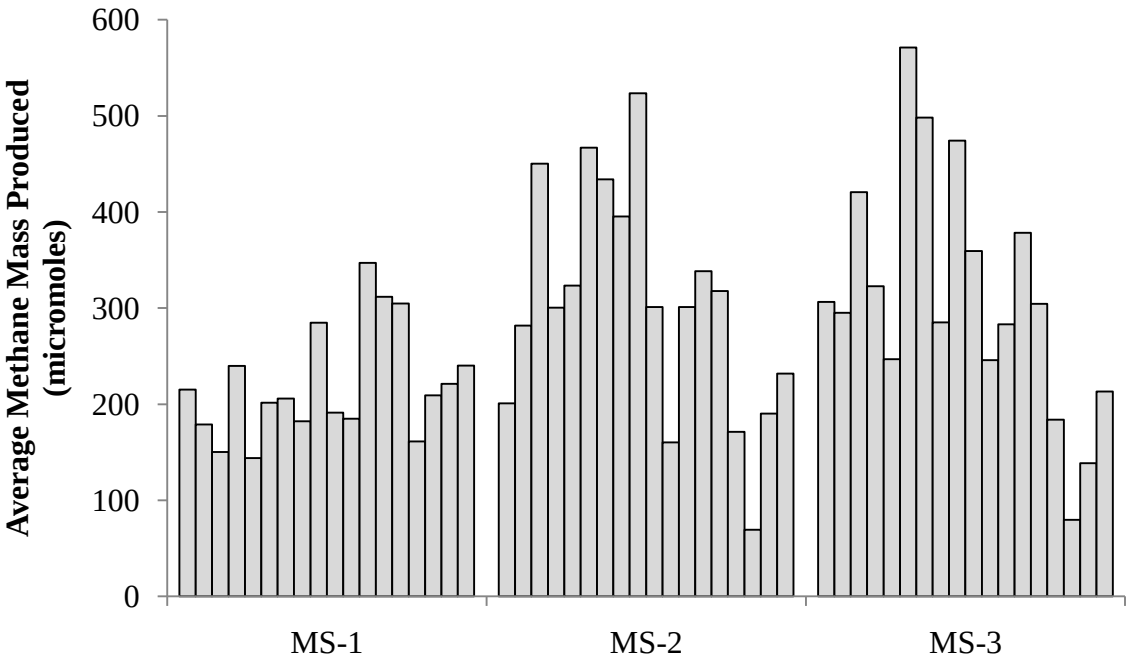

Figure 4.6: Comparison of average methane production per cycle for each MS (soil) microcosm

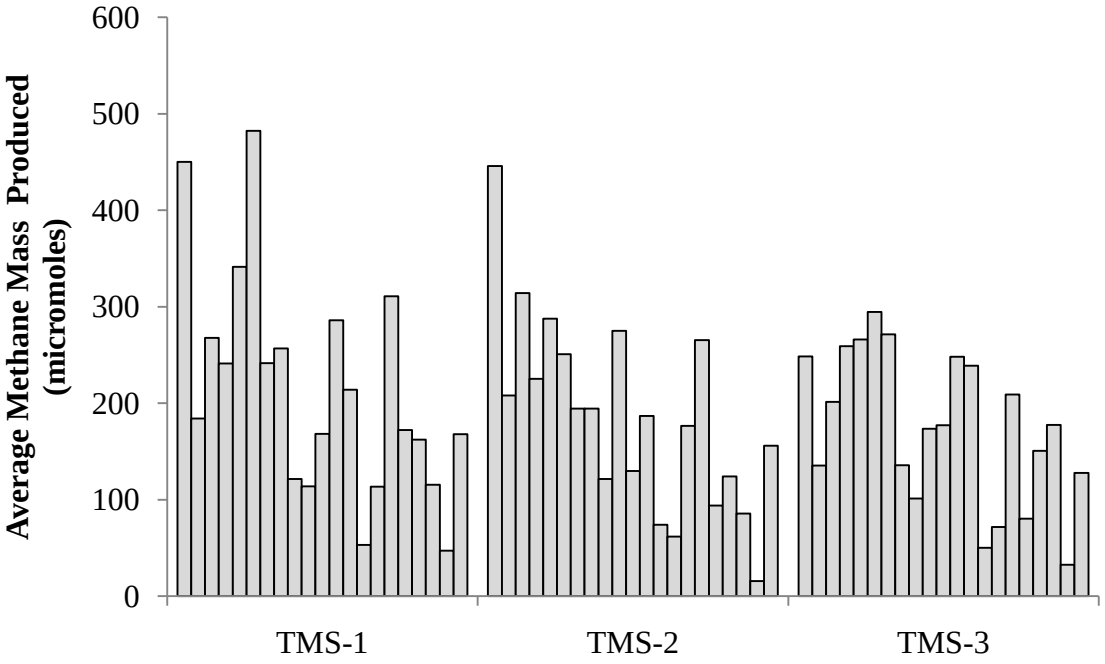

Figure 4.7: Comparison of average methane production per cycle for each TMS (soil free) microcosm

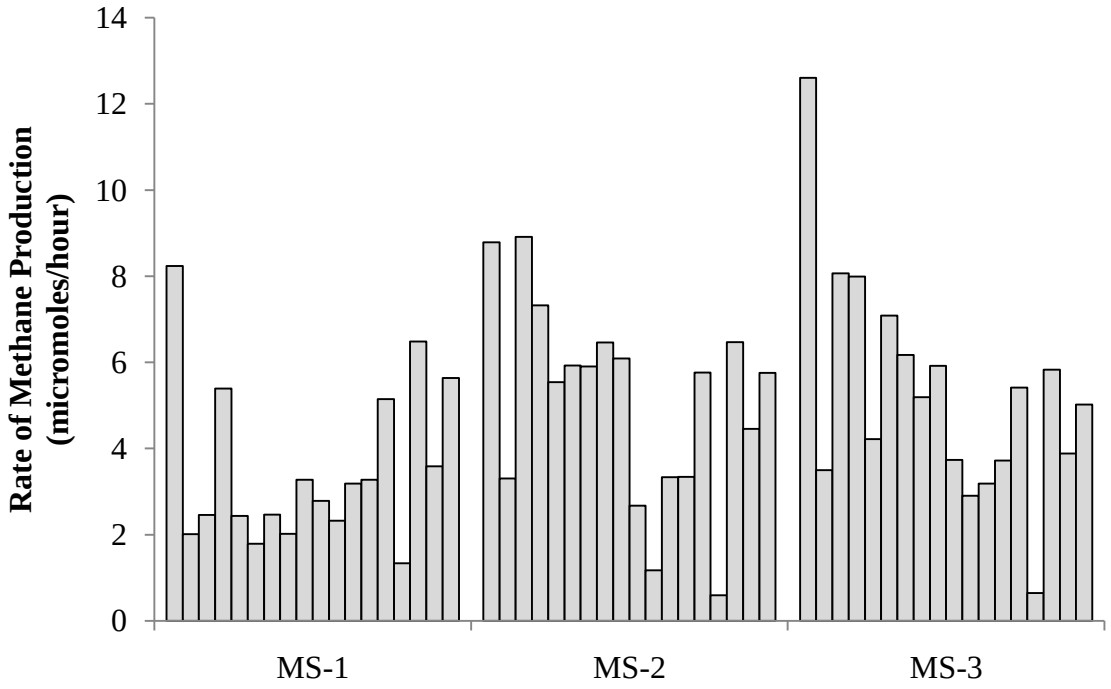

Figure 4.8: Comparison of average rate of methane production per cycle for MS (soil) microcosms

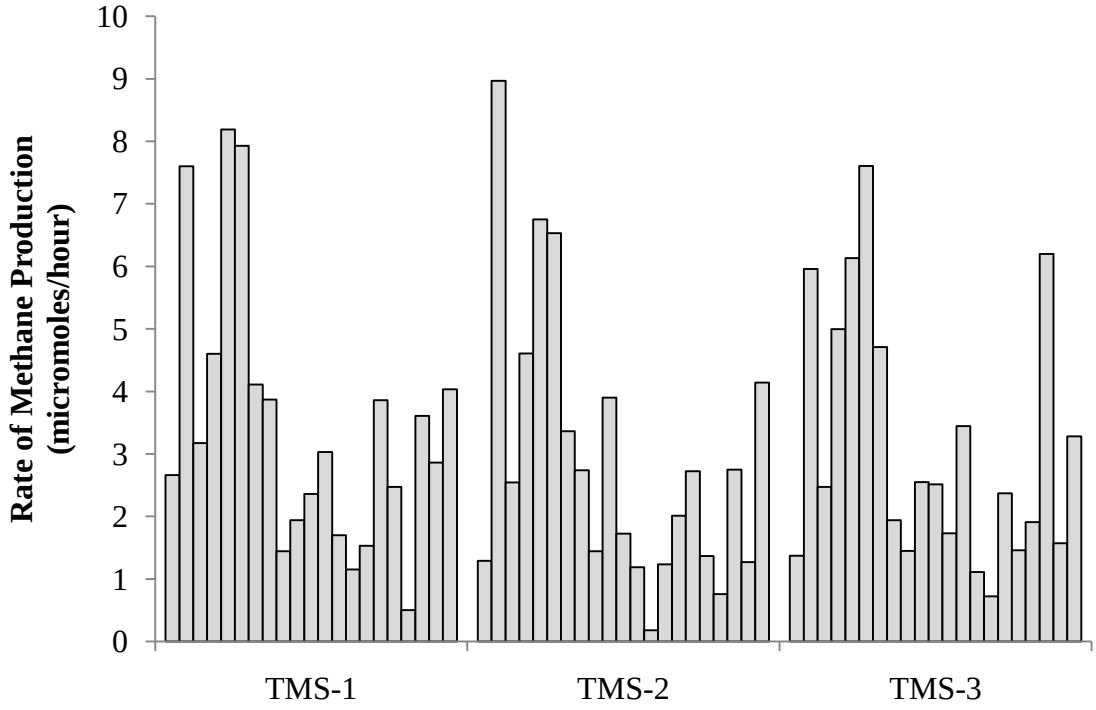

Figure 4.9: Comparison of average rate of methane production per cycle for each TMS (soil free bottle) microcosms

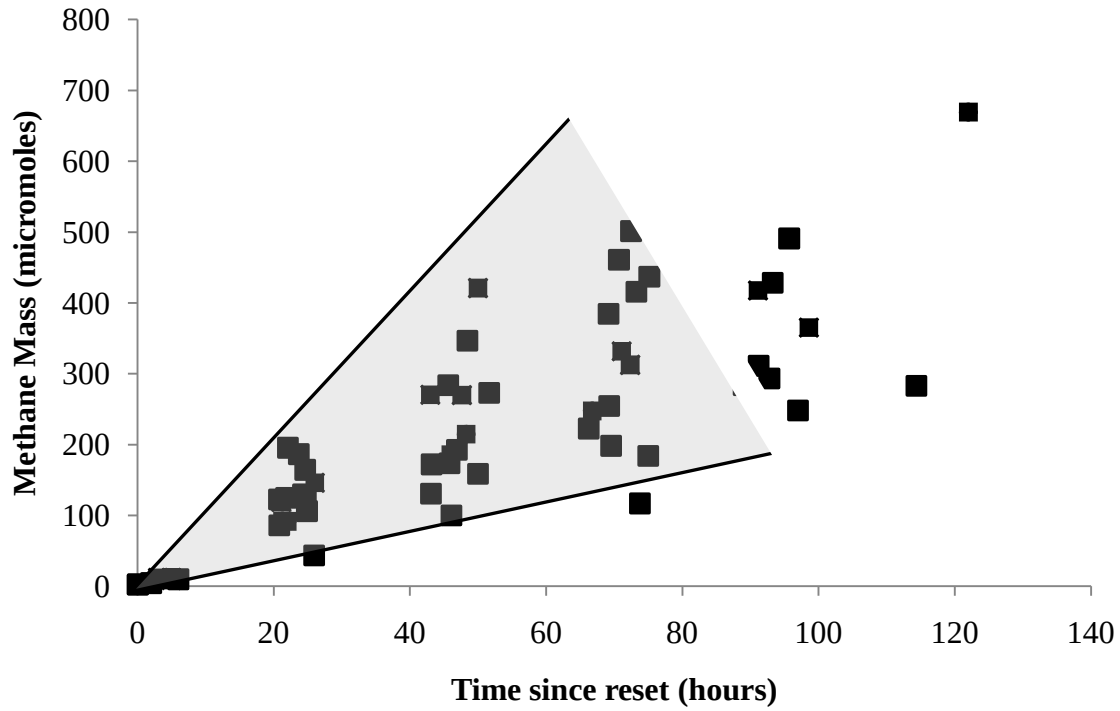

Figure 4.10: Typical trend of methane production per cycle in a microcosm (MS-1, various cycles).

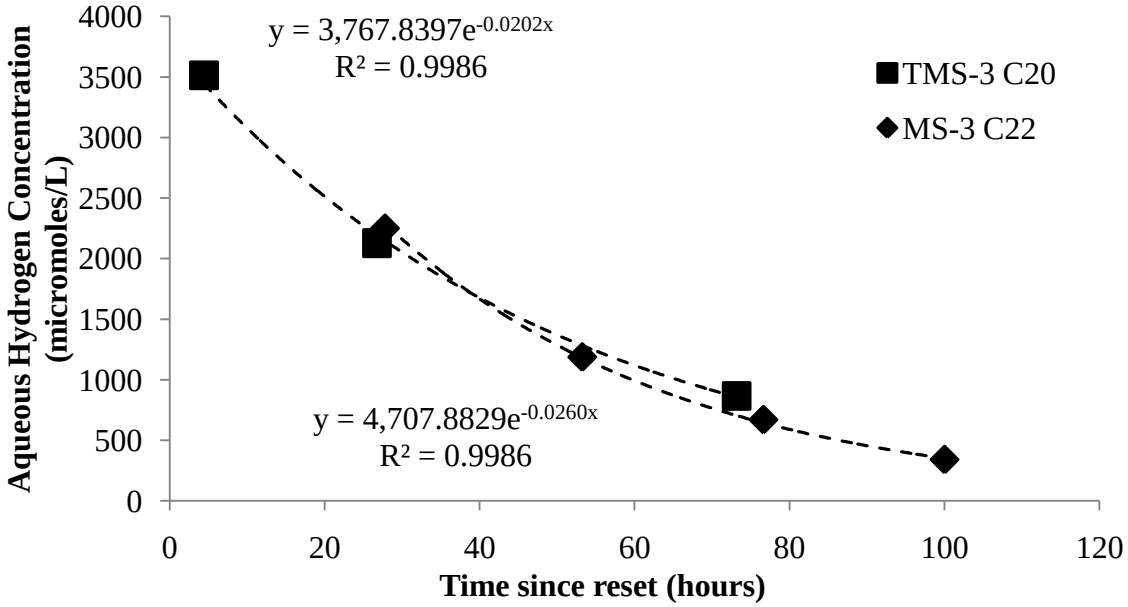

Figure 4.11: Pseudo-first order kinetics occurring in TMS-3, Cycle 20 and MS-3, Cycle 22.

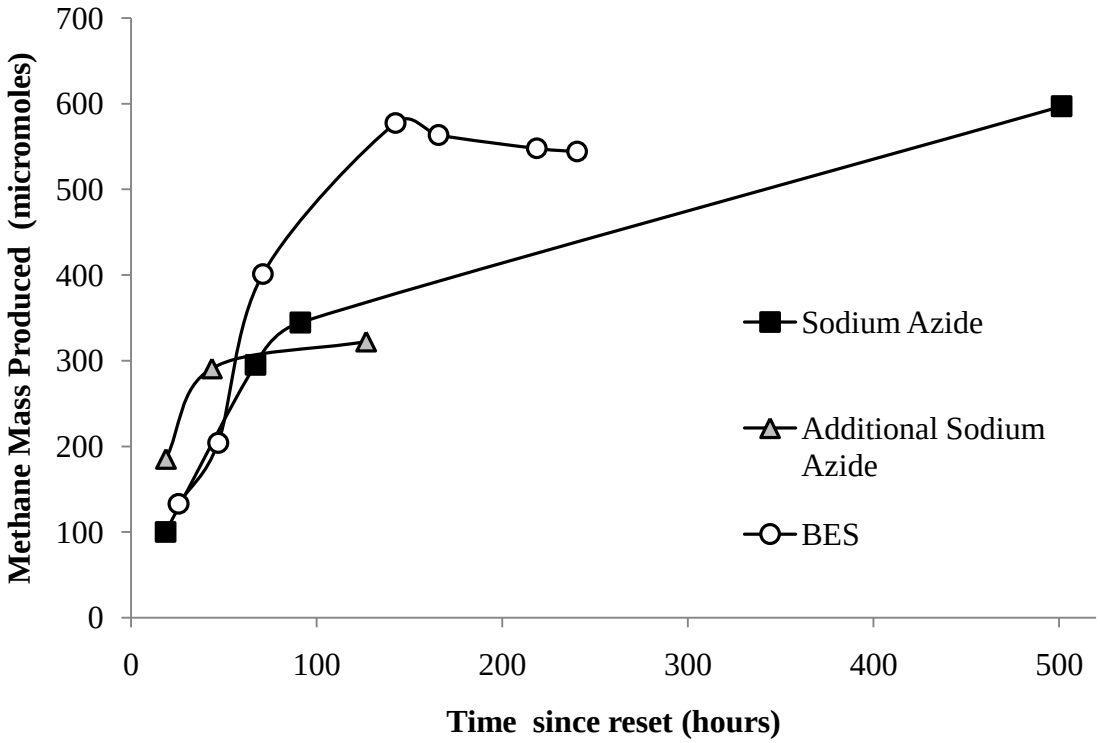

Figure 4.12: Effects on methane production as a result of sodium azide (3mg/L added twice) and BES (5 mg/L) amendments.

Table 4.1: K-values obtained from [H2] versus time plots that show pseudo-first order kinetics occurring. Predicted initial hydrogen values were obtained from C_o values in [H2] versus time plots. Only correlation coefficients (R^2) greater than 0.99 were accepted and displayed in this table.

Microcosm ID#	**Cycle ID#**	**Pseudo-First order Rate Constant k_{obs} (Hr^{-1})**	**Fitted Initial H_2 Mass, C_o (micromoles)**	**Correlation Coefficient (R^2)**
MS-2	22	-0.031	2233.4	0.999
MS-3	22	-0.026	4707.9	0.999
TMS-1	20	-0.015	3976.7	0.997
	21	-0.013	2758.5	0.993
	23	-0.026	4710.4	0.999
TMS-2	20	-0.013	3705.6	0.999
	23	-0.017	4663.1	0.998
TMS-3	20	-0.020	3767.8	0.999
	23	-0.016	44002.4	0.998

a).

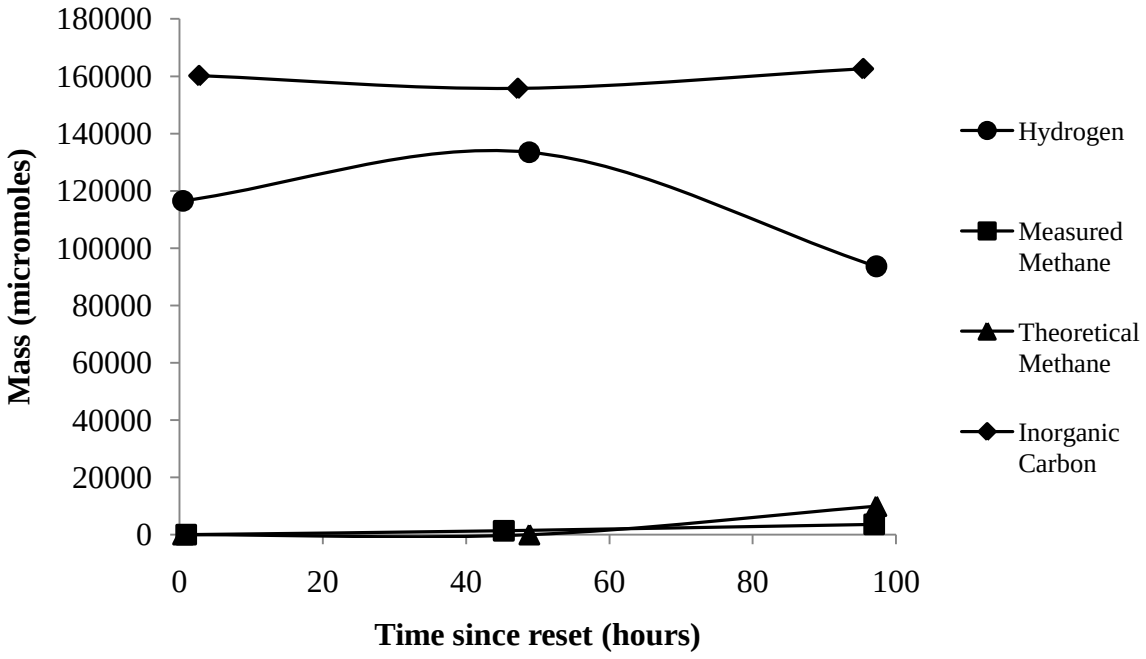

b).

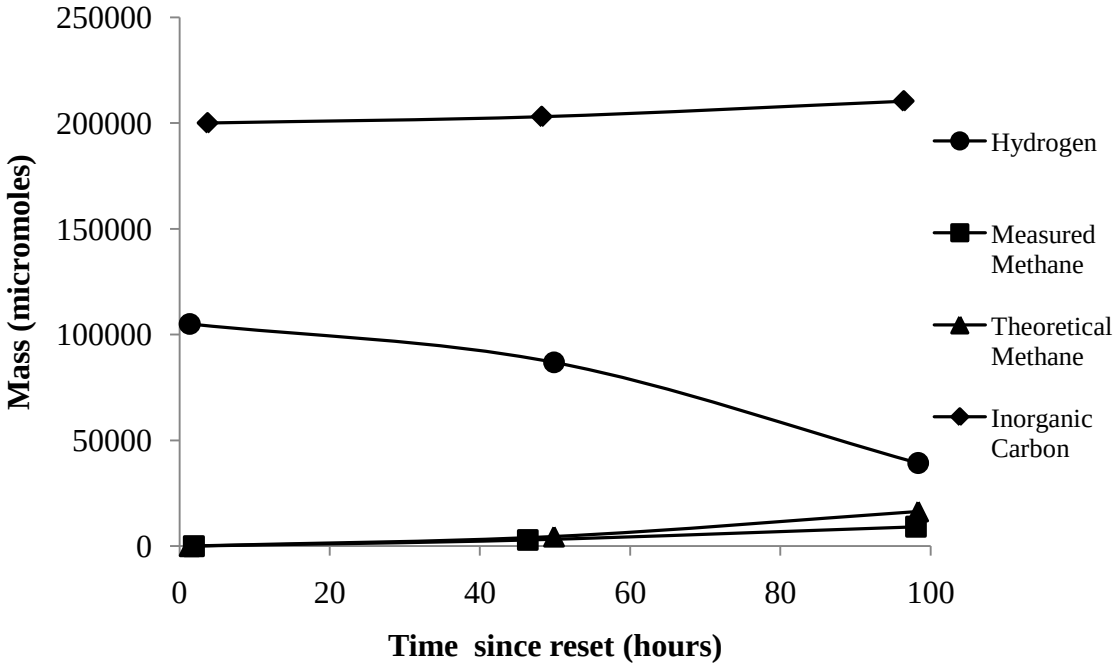

Figure 4.13: Typical mass variation of methane, hydrogen, and inorganic carbon in a bioreactor without perlite (a). and with perlite (b). a). MR#1, cycle #9, b). MR#2, cycle #5. Theoretical methane production calculated from measure hydrogen values compared to actual methane observed.

VII. References

Achtnich, C., Bak, F. and Conrad, R. (1995). Competition for electron donors among nitrate reducers, ferric iron reducers, sulfate reducers, and methanogens in anoxic paddy soil. Biol. Fertil. Soils 19, 65-72.

Alexander, M. (1999). "Kinetics." Biodegradation and bioremediation. 2nd Edition: Chapter 6.

Amaral, J.A. and R. Knowles. (1994). Methane metabolism in a temperate swamp. Applied and Environmental Microbiology. 60(11):3945-3951.

Arnaiz, C., J.C. Gutierrez and J. Lebrato. (2006). Support material selection for anaerobic fluidized bed reactors by phospholipids analysis. Biochemical Engineering Journal. 27: 240-245.

Balaguer, M.D., M.T. Vicent and J.M. Paris. (1997). A comparison of different support materials in anaerobic fluidized bed reactors for the treatment of vinasse. Environmental Technology. 18: 539-544.

Barry, P. (2007). Methane Blast. Science@NASA. Accessed on 2/23/2009.

Boone, D. R., R.L. Johnson, Y. Liu. (1989). Diffusion of the interspecies electron carriers H_2 and formate in methanogenic ecosystems and its implication in the measurement of K_m for H_2 or formate uptake. Applied and Environmental Microbiology. 55(7): 1735-1741.

Boone, D. R., W. B. Whitman, and P. Rouviere. 1993. Diversity and taxonomy of methanogens. Methanogenesis. J. G. Ferry, ed. Chapman and Hall, New York. Pg. 35-80.

Bossel, U., B. Eliasson, G. Taylor. 2003, The future of the hydrogen economy: bright or bleak? Proceedings of the European Fuel Cell Forum, Lucerne, pg.39.

Botz, R., H. Pokojski, M. Schmitt, and M. Thomm. (1996). Carbon isotope fractionation during bacterial methanogenesis by CO_2 reduction. Org. Geochem. 25(3/4): 255-262.

Chidthaisong, A., K. Chin, D. L. Valentine, and S. C. Tyler. (2002). A comparison of isotope fractionation of carbon and hydrogen from paddy field rice roots and soil bacterial enrichments during CO_2 /H_2 methanogenesis. Geochemica et Cosmochimica Acta. 66(6):983-995.

Chin, K.J. and Conrad, R. (1995). Intermediary metabolism in methanogenic paddy soil and the influence of temperature. FEMS Microbiol. Ecol. 18, 85-102.

Chauhan, C. and A. Ogram. (2005). Evaluation of support matrices for immobilization of anaerobic consortia for efficient carbon cycling in waste regeneration. Biochemical and Biophysical Research Communication. 327: 884-893.

CleanPower.org. "Petroleum" April, 7, 2009. Accessed August 10, 2009. http://www.cleanpower.org/section_03/petroleum.html

Chong S. and J. Chong. (2008). Methane: a natural gas. Microbiology Today. 124- 127.

Congiu, Brian. Personal Communication. 2009

Conrad, R., T.J. Phelps, and J.G. Zeikus. (1985). Gas metabolism evidence in support of the juxtaposition of hydrogen-producing and methanogenic bacteria in sewage sludge and lake sediments. Applied and Environmental Microbiology 50(3): 595-601.

Conrad, R. (1996). Soil microorganisms as controllers of atmospheric trace gases (H2, CO, CH4, OCS, N2O, and NO). Microbiological Review 60, 609-640.

Conrad, R. (1999). Contribution of hydrogen to methane production and control of hydrogen concentrations in methanogenic soils and sediments. FEMS Microbiol. Ecol 28, 193-202.

Conrad, R. and M. Klose. (1999). Anaerobic conversion of carbon dioxide to methane, acetate and propionate on washed rice roots. FEMS Microbiol Ecol. 30:147-155.

Dunfield, P., R. Knowles, R. Dumont and TR Moore. (1993). Methane production and consumption in temperate and sub-artic peat soils-response to temperature and pH. SOIL Biology & Biochemistry 25(3): 321-326.

Ecoworld, Inc. "Replacing coal with solar." 2009. Accessed August 10, 2009. http://www.ecoworld.com/business/cost-to-replace-coal-with-solar.html

Fairley, P. (2002). Wind power for pennies. Technology Review. July/August: 40-45.

Fetzer, S. and R. Conrad. (1993) Effect of redox potential on methanogenesis by *Methanosarcina barkeri*. Arch Microbiol. 160:108-113.

Florencio, L., J.A. Field, G. Lettinga. (1995). Substrate competition between methanogens and acetogens during the degradation of methanol in UASB reactors. Water Resources. 29 (3): 915-922.

Fortune, W.B. and M.G. Mellon. (1938) Determination of iron with o-phenanthroline: A spectrophotometric study. Ind. Eng. Chem. Anal. Ed. 10 (2): 60-64.

Franklin, M.E., W. J. Wiebe and W.B. Whitman. (1988). Populations of methanogenic bacteria in a Georgia salt marsh. Applied and Environmental Microbiology. 54: 1151-1157.

Fuchs, G.D., R. Thauer, H. Ziegler and W. Stichler. (1979). Carbon isotope fractionation by *Methanobacterium thermoautotrophicum*. Arch. Microbiol. 120: 135-139.

Galand, P.E., H. Fritze, R. Conrad, K. Yrjala. (2005). Pathways for methanogenesis and diversity of methanogenic archaea in three boreal peatland ecosystems. Applied and Environmental Microbiology. 71(4): 2195-2198.

Guerin, T.F., M. Mondido, B. McClenn, B. Peasley. (2001). Application of resazurin for estimating abundance of contaminant-degrading micro-organisms. Letter in Applied Microbiology. 32: 340-345.

Gurijala, R. and J.M. Suflita. (1993). Environmental factor influencing methanogenesis from refuse in landfill samples. Environ. Sci. Technol. 27: 1176-1181.

Herron, E.H. 2000. "The looming crisis in worldwide oil supplies." Petroleum Equities, Inc. Accessed August 10, 2009. http://www.petroleumequities.com/oilsupplyreport.htm

Hoekman, S.K. (2008). Biofuels in the U.S. – challenges and opportunities, Renewable Energy. In press: 1-9.

Horn, M.A., C. Matthies, K. Kusel, A. Schramm, and H.L. Drake. (2003). Hydrogenotrophic methanogenesis by moderately acid-tolerant methanogens of a methane-emitting acidic peat. Applied and Environmental Microbiology. 69(1): 74-83.

Hutchison, F.H. 2009. "About coal" Clean-Energy.US. Accessed August 10, 2009. http://www.clean-energy.us/facts/coal.htm

Johnson, J. (2007). Capturing carbon and saving coal. C&EN Washington. 25-28.

Jones, J.G., B.M. Simon. (1985). Interaction of acetogens and methanogens in anaerobic freshwater sediments. Applied and Environmental Microbiology. 49(4): 944-948.

Kasali, G., E. Senior, and I. Wastsoncraik. (1988). Preliminary investigation of the influence of pH on the solid-state refuse methanogenic fermentation. J. of Applied Bacteriology. 65(3): 231-239.

Kida, K., S. Morimura, Y. Sonoda, M. Obe, and T. Kondo. (1990). Support media for microbial adhesion in an anaerobic fluidized-bed reactor. Journal of Fermentation and Bioengineering. 69(6): 354-359.

Kluber, H.D. and R. Conrad. (1998). Effects of nitrate, nitrite, NO and N_2O on methanogenesis and other redox processes in anoxic rice field soil. FEMS Microbiol Ecol. 25:301-318.

Kotsyurbenko, O.R., M.W. Friedrich, M.V. Simankova, A.N. Nozhevnikova, P.N. Golyshin, K.N. Timmis, and R. Conrad. (2007). Shift from acetoclastic to H_2-dependentmethanogenesis in a west Siberian peat bog at low pH values and isolation of an acidophilic *Methanobacterium* strain. Applied and Environmental Microbiology. 73(7): 2344-2348.

Krylova, N.I., P.H. Janssen, and R. Conrad. (1997). Turnover of propionate in methanogenic paddy soil. FEMS Microbiology Ecology. 23:107-117.

Leybo, A.I., A.I. Netrusov, and R. Conrad. (2006). Effect of hydrogen concentration on the community structure of hydrogenotrophic methanogens studied by T-RELP analysis of 16S rRNA gene amplicons. Microbiology 75(6): 786-791.

Liu, C.T., T. Miyaki, T. Aono, and H. Oyaizu. (2008) Evaluation of methanogenic strains and their ability to endure aeration and water stress. Curr Microbiol. 56:214-218.

Lovley, D.R., D.F. Dwyer, M.J. Klug. (1982). Kinetic analysis of competition between sulfate reducers and methanogens for hydrogen in sediments. Applied and Environmnetal Microbiology. 43(6): 1373-1379.

Lovley, D.R. and J. G. Ferry. (1985). Production and consumption of H_2 during growth of *Methanosarcina* spp. on acetate. Applied and Environmental Microbiology. 49(1): 247-249.

Megonigal, J.P., M.E. Hines and P.T. Visscher. (2004). Anaerobic metabolism: linkages to trace gases and aerobic processes. Schlesinger, W.H. (Ed.) Biogeochemistry. Elsevier-Pergamon, Oxford, UK. Pg 317-424.

Mohammadzadeh, H. and I. Clark. (2008). Degradation pathways of dissolved carbon in landfill leachate trace with compound-specific ^{13}C analysis of DOC. Isotopes in Environmental and Health Studies. 44 (3): 267-294.

Neumann, M.G., C.C. Schmitt, C.M. Previtali, and S.G. Bertolotti. (1996). Photoreduction of resazurin in the presence of aliphatic amines. Dyes and Pigments. 32(2): 93-99.

Ogrinc, N., M. Zagar, J. Faganeli, T. Kanduc, and P. Vreca. (2008). Methane formation in a remote mountain lake (Lake Planina, NW Slovenia). Geomicrobiology Journal. 25: 346-356.

Oh, S.E., S. Van Ginkel, and B. Logan. (2003). The relative effectiveness of pH control and heat treatment for enhancing biohydrogen gas production. Environ. Sci. Technol. 37: 5186-5190.

Park, W., S. Hyun, S.E. Oh, B. Logan, and I. Kim. (2005). Removal of headspace CO_2 increases biological hydrogen production. Environ. Sci. Technol. 39: 4416-4420.

Peebles, D.E. and D.W. Goodman. 1983. Methanation of carbon dioxide on Ni(100) and the effects of surface modifiers. J Phys. Chem. 1003 (87): 4378-4387.

Peters, V. and R. Conrad. (1995). Methanogenic and other strictly anaerobic bacteria in desert soil and other oxic soils. Applied and Environmental Microbiol. 1673-1676.

Peters, V. and R. Conrad. (1996). Sequential reduction processes and initiation of CH4 production upon flooding of oxic upland soils. Soil Biol. Biochem. 28, 371-382.

Pimentel, D., M. Herz, M. Glickstein, M. Zimmerman, R. Allen, K. Becker, J. Evans, B. Hussain, R. Sarsfeld, A. Grosfeld, T. Seidel. (2002). Renewable energy: current and potential issues, BioScience. 52(12): 1111-1120.

Roy, R., H.D. Kluber and R. Conrad. (1997) Early initiation of methane production in anoxic rice soil despite the presence of oxidants. FEMS Microbiol. Ecol. 24:311-320.

Sakai, S., H. Imachi, Y. Sekiguchi, A. Ohashi, H. Harada, and Y. Kamagata. (2007). Isolation of key methanogens for global methane emission from rice paddy fields: a novel isolate affiliated with the clone cluster rich cluster I. Applied and Environmental Microbiology. 73(13): 4326-4331.

Sarazin G, Michard G and Prevot F. (1998) A rapid and accurate spectroscopic method for alkalinity measurements in sea water samples. Water Research 33: 290-294.

Schrag, D.P. (Feb 9, 2007) Preparing to capture carbon. Science 315(5813):812-813.

Schulz, S. and Conrad, R. (1996). Influence of temperature on pathways to methane production in the permanently cold profundal sediment of Lake Constance. FEMS Microbiol. Ecol. 20, 1-14.

Sowmeyan, R. and G. Swaminathan. (2008). Performance of inverse anaerobic fluidized bed reactor for treating high strength organic wastewater during start-up phase. Bioresource Technology. 99: 6280-6284.

Strapoc, D., F.W. Picardal, C. Turich, I. Schaperdoth, J. L Macaladay, J.S. Lipp, Y. Lin, T. F. Ertefai, F. Schubotz, K. Hinrichs, M. Mastalerz, A. Schimmelmann. (2008). Methane-producing microbial community in a coal bed of the Illinois basin. Applied and Environmental Microbiology. 74(8):2424-2432.

Thampi, K.R., J. Kiwi, and M. Gratzel. 1987. Methanation and photo-methation of carbon-dioxide at room-temperature and atmospheric-pressure. Nature 327(6122): 506-508.

Tsurumi, R., K. Takeda, and A. Tonouchi. (2000). Characteristics and propionate production of *Propionibacterium* isolated from a methane fermentation digester. Microbes and Environment. 15(3):151-159.

van Bodegom, P.M., J.C.M. Scholten and A.J.M. Stams. (2004). Direct inhibition of methanogenesis by ferric iron. FEMS Microbiol Ecol. 49:261-268.

Wu, X., K. Chin, and R. Conrad. (2002). Effect of temperature stress on structure and function of the methanogenic archaeal community in a rice field soil. FEMS. 39:211-218.

Yang, Y. and P.L. McCarty. (1998) Competition for hydrogen within a chlorinated solvent dehalogenating anaerobic mixed culture. Environmental Science Technology. 32: 3591-3597.

Yavitt, J.B., N. Basiliko, M.R. Turetsky, A. G. Hay. (2006). Methanogenesis and methanogen diversity in three peatland types of the discontinuous permafrost zone, boreal western continental Canada. Geomicrobiology Journal. 23: 641-651.

Zinder, S.H. (1993). Physiological ecology of methanogens. In: Methanogenesis: Ecology, Physiology, Biochemistry and Genetics (Ferry, J.G., Ed.), pp. 128-206. Chapman and Hall, New York.

Standard Operating Procedure for Preparing Deoxygenated Basal Medium

Required Reagents:

$NaCl$, NH_4Cl, KCl, KH_2PO_4 , $MgCl_2.6H_2O$, $CaCl_2.2H_2O$, $MnCl_2.4H_2O$, $CoCl_2.6H_2O$, H_3BO_3, $ZnCl_2$, $CuCl_2.2H_2O$, $NiCl_2.6H_2O$, $Na_2MoO_4.2H_2O$, Na_2SeO_4, $Na_2WO_4.2H_2O$, $Al_2(SO_4)_3.18H_2O$, 1 N HCl, Biotin, Folic acid, Pyridoxine, Riboflavin, Thiamine, Nicotinic acid, Pantothenic acid, p-Aminobenzoic acid (PABA), Cyanocobalamine, and Thioctic acid

Preparation Procedure:

1. Combine the following chemicals into a clean 1 L volumetric flask, and dissolve them in 1 liter of DI water to prepare the **mineral solution** (*solution A):*

   4 g of $NaCl$, 5 g of NH_4Cl, 0.5 g of KCl, 0.5 g of KH_2PO_4 ,0.5 g of $MgCl_2.6H_2O$, 0.2 mg of $CaCl_2.2H_2O$
2. Combine the following chemicals into a clean 1 L volumetric flask, and dissolve them in 1 liter of DI water to prepare the **trace metal solution** (*solution B):*

   0.2 g of $MnCl_2.4H_2O$, 0.04 g of $CoCl_2.6H_2O$, 0.024 g of H_3BO_3, 0.004 g of $ZnCl_2$, 0.004 g of $CuCl_2.2H_2O$, 0.004 g of $NiCl_2.6H_2O$, 0.004 g of $Na_2MoO_4.2H_2O$, 0.004 g of Na_2SeO_4, 0.004 g of $Na_2WO_4.2H_2O$, 0.008 g of $Al_2(SO_4)_3.18H_2O$, and 20 mL of 1 N HCl.
3. Combine the following chemicals into a clean 1 L volumetric flask, and dissolve them in 1 liter of DI water to prepare the **vitamin solution** (*solution C):*

0.02 g of biotin, 0.02 g of folic acid, 0.1 g of pyridoxine, 0.05 g of riboflavin, 0.05 g of thiamine, 0.05 g of nicotinic acid, 0.05 g of pantothenic acid, 0.05 g of p-aminobenzoic acid (PABA), 0.05 g of cyanocobalamine, and 0.05 g of thioctic acid

4. Prepare 'basal medium' by adding 0.5 g of K_2HPO_4, 1.5 g of Na_2CO_3, 5 mg of Na_2S, 200 mL of mineral solution (*solution A*), 25 mL of trace metal solution (*solution B*), and 1 mL of vitamin solution (*solution C*), and dissolve them in 1 liter of DI water in a clean volumetric flask
5. Pour the above basal medium from the volumetric flask into a 1L media bottle and secure a cap.
6. Refrigerate basal medium solutions when not in use.
7. Basal medium may be prepared in advance, and stored in a 1L media bottle in the refrigerator.
8. Basal medium should be thoroughly deoxygenated before each use.

Procedure for Deoxygenating the Basal Medium Solution:

1. Remove the media bottle containing the basal medium from the refrigerator
2. Remove the cap was taken off the media bottle.
3. Connect a flexible ¼" ID tygon tubing to the low pressure copper tubing of the liquid nitrogen tank by a poly propylene reducing union (to bubble the basal medium with nitrogen). Attach a glass sparge tube (Fisher, part# LG-8680-110,12 MM coarse) to the tygon tube at the other end.
4. Place the glass sparge tube inside the media bottle containing basal medium and secured in place with parafilm.

5. Once the parafilm is sealed around the top of the bottle, poke holes in the parafilm with a 23 gauge stainless steel hypodermic needle (B-D; part # 305145) to create a vent.

6. Open the gas regulator gradually (line pressure: <5 psi), and bubble nitrogen gas vigorously into the bottle containing basal medium for 1 hour.

7. After 1 hour of bubbling with nitrogen, remove the sparge tube and then the parafilm from the bottle, and quickly secure the bottle's cap.

8. Transfer the capped bottle into an anaerobic chamber glovebox (Coy Laboratory Products, Inc., MI).

9. Once inside the glove box, remove the cap from the bottle for another round of deoxygenation by bubbling (described below).

10. Employ an electric-powered fish tank bubbler to sparge the basal medium once again inside the glovebox with the gas filled in the chamber (high purity 95% nitrogen and 5% hydrogen gas mix), attached with sparge tube and the procedure described earlier (steps 4 and 5 above).

11. After 1 hour of bubbling, the basal medium is considered to be nearly deoxygenated and is ready to be added to methanogenic microcosms.

Appendix B

Standard Operating Procedure for Microcosm Alkalinity Determination by Spectrophotometric Technique (adapted from Sarazin, 1998)

Required Materials:

10 ml Pyrex beakers, 23 gauge needles (B-D; part # 305145), 5 ml syringes (B-D; part # 309603), 12 15 mL centrifuge tubes with caps, 200 μL Fisher brand Finnpipette, pipettetips (MBP; cat. # 3550)

Preparation of Alkalinity Reagents:

1. Add 260 μL of formic acid (88% or 19.12 M) stock concentration into a clean 500 mL volumetric flask.

   $$V_1 = C_2 * V_2 / C_1$$

   Where C_2 is the final concentration of formic acid which is 10 mM

   V_2 is the final volume of 500 mL

   C_1 is the formic acid stock concentration of 19120 mM

   Then V_1= 0.26 mL of formic acid
2. Weigh out 25 mg of bromophenyl and add it to above 500 mL volumetric flask.
3. Fill the rest of the volumetric flask with DI water.

Preparation of Sodium Bicarbonate Standards Solution:

1. Prepare a 20 mM or 1680 mg L^{-1} sodium bicarbonate (formula weight: 84.01) stock solution, by weighing out 840 mg of $NaHCO_3$ powder and transfer it to a 500 mL volumetric flask. Fill the rest of the flask with DI water.

2. To prepare alkalinity standards of variable concentrations ranging from 0-20 mM of $NaHCO_3$ (as shown in italics in the table below), dilutions of the 20 mM stock will be needed as follows:

$$V_1 = C_2 * V_2 / C_1$$

C_1 $NaHCO_3$ Stock Concentration (mM)	*V_1* Volume of $NaHCO_3$ required (mL)	*C_2* Final (Desired) $NaHCO_3$ Concentration (mM)	*V_2* Final Volume (mL)	*C_2 values expressed in mg L^{-1}*
20	0	0	50	*0*
20	2.5	1	50	*84.0*
20	5	2	50	*168.0*
20	12.5	5	50	*420.0*
20	25	10	50	*840.0*
20	50	20	50	*1680.0*

3. To begin reagent mixing for preparing a calibration curve for alkalinity measurement in unknown samples, label 6- 15 mL centrifuge tubes for the varying concentrations of standards, and label them appropriately (such as 0, 1, 2, 5, 10 and 20 mM of $NaHCO_3$ in the table above).

4. Transfer 200 µL of each of the $NaHCO_3$ standards into individual pre-labeled centrifuge tubes.

5. Add 2 mL of alkalinity reagent (identified above) to each individual centrifuge tube.

6. Cap the centrifuge tubes, and mix the sample thoroughly on a vortex mixer.

7. Wait 30 min for the reaction to be complete before running the samples on the spectrophotometer (Perkin Elmer's Lambda 45 UV/VIS Spectrophotometer).

Sampling and Alkalinity Measurement Procedure for Microcosms:

1. Gather 12- 15 mL centrifuge tubes (for 6 microcosms) and label 2 centrifuge tubes for each microcosm. (e.g. 2 tubes labeled MS-1, 2 labeled MS-2, etc.)
2. In this step, the samples need to be diluted 10 times in DI water. In the first set of 6 centrifuge tubes, add 1800 µl of DI water to each tube.
3. In the second set of 6 centrifuge tubes, add 2 mL of alkalinity reagent to each tube.
4. Inside the Coy Instrument Glovebox, use a 5mL Luer-Loc polypropylene Syringe attached with a 23 gauge hypodermic needle to pull out sample from 1 microcosm.
5. Replace the needle attached to the syringe with a syringe filter (Is-Disc Filter, N-25-4 Nylon, 25mm x 0.45 µm, Sapelo, Bellefontaine, PA).
6. Push the sample through the filter into a 10 mL glass beaker.
7. Use the pipette to transfer 200 µl of filtered sample each into: (a) an appropriately labeled centrifuge tube that already contains 1800 µl of DI water, (b). a pre-labeled centrifuge tube that contains 2 mL of alkalinity reagent.
8. Cap the centrifuge tubes and mix their contents up on a vortex mixer.
9. Repeat steps 5-11 with each of the 6 microcosms. Be sure to use a new needle, syringe and pipette tip for each bottle.
10. Bring the samples out of the glovebox and allow them to sit/develop for 30 minutes before the spectrophotometric analysis (Perkin Elmer Lambda 45 UV/VIS Spectrophotometer).

Procedure for Spectrophotometric Analysis of Alkalinity:

1. Begin by turning on the Perkin Elmer Lambda 45 UV/VIS spectrophotometer and allowing it to warm-up (~5 minutes).

2. Once the machine is ready double-click on the LAMBDA 45 icon on computer monitor.

3. Find the appropriate analysis method and double-click on it.

4. Check the information for all of the icons to the left of the sample spreadsheet (data collection, instrument, corrections, Beer's Law Quant, parameters, calibration) to make sure all of the information is correct.

5. In the Accessory tab make sure only the cell changer is checked (not *peltier* or *sipper*).

6. After all of the information has been checked for setting accuracy in the *Sample Info* page, enter the number of samples to be analyzed.

7. Press the *Run* button.

8. Fill cuvette with ~2 mL of sample to be analyzed.

9. Clean the outside of the cuvette gently with Kim Wipes to make sure no liquid or fingerprints are present.

10. Place the cuvette in the cell changer and run the sample.

11. Click *Run Sample* 3 times for each sample, to get triplicate readings.

12. Pour out sample. Rinse and wipe cuvette with DI water and Kim wipes.

13. Repeat steps 8-12 for each sample.

14. Once analysis is finished, click *Save As a Task.*

15. Turn off the spectrophotometer.

Calibration Curve:

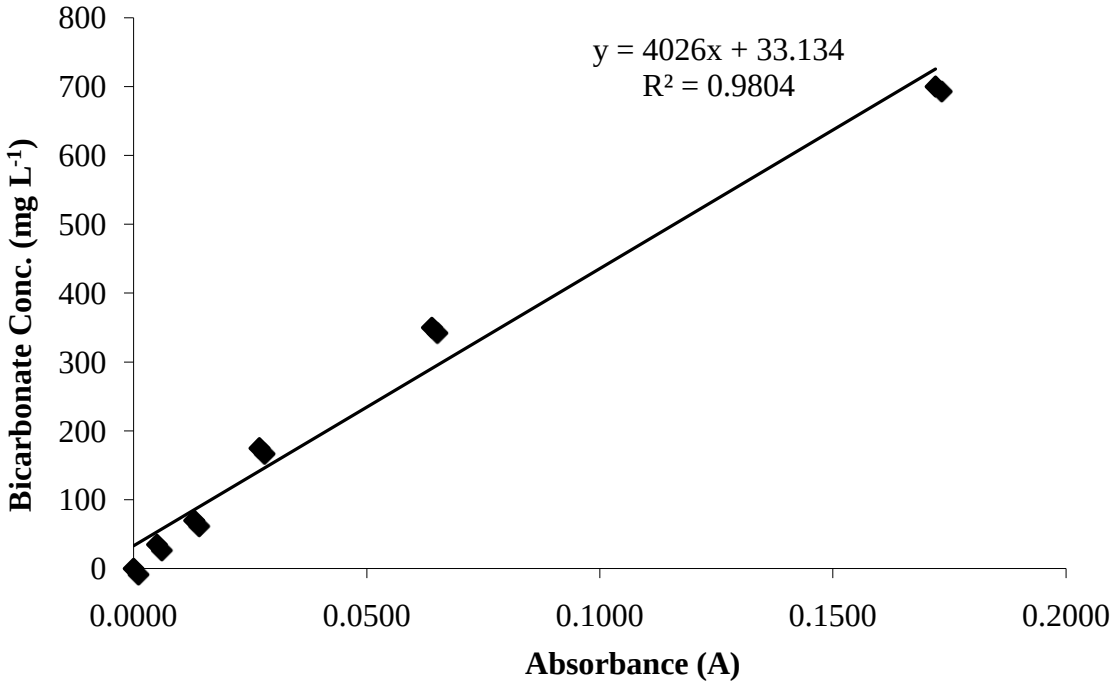

Appendix C

Standard Operating Procedure for Microcosm Fe (II) Determination by Phenanthroline Method (adapted from Fortune and Mellon 1938).

Required Materials:

centrifuge tubes, 5.1 mM 1,10-Phenanthroline, 10% hydroxylamine solution, 1.2M ammonium acetate buffer, 23 gauge needles (B-D; part # 305145), 5 mL plastic syringe (B-D; part # 309603), Iso-Disc Filter, N-25-4 Nylon 25 mm x 0.45 μm filters, pipette

Preparation of Fe (II) Standards:

1. Use a 1000 mg L^{-1} iron stock solution (LabChem Inc.)
2. Dilute the iron stock solution from 1000 mg L^{-2} to 50 mg L^{-1} .
    a. Fill a 50 mL centrifuge tube with filtered DI water using a volumetric flask.
    b. Remove 2.5 mL of water, using a 0-1000 μL Eppendorf pipette, from the centrifuge tube and add 2.5 mL of the iron stock solution
    c. Shake tube well, beneficial to use the Fisher Vortex Genie 2 (Fisher Scientific; Cat. No. 12-812) to make sure the contents are thoroughly mixed).
    d. The final concentration is 50 mg L^{-1}.
3. Label 6 15 mL centrifuge tubes with STD1, STD2, STD3, STD4, STD5, and STD6 and fill each tube, using a 10 mL volumetric flask, with 10 mL of filtered DI water.
4. STD1 functions as a blank so contains 0 mL of iron stock solution. Using a 0-1000μL Eppendorf pipette, the following volumes of DI water were removed from individual tubes, and replaced with freshly prepared 50 mg L^{-1} Fe(II)

solution: 150 μL of water from STD2, 300 μL of water from STD3, 600 μL of water from STD 4, 900 μL from STD5 and 1200 μL from STD6.

5. The contents of the tubes were mixed thoroughly using the vortex mixer (Fisher Vortex Genie 2).
6. Reagent Addition: 6 new 15 mL centrifuge tubes were labeled as before (STD1, STD2, STD3, STD4, STD5, and STD6), and 1 mL of each of the above standard solutions were transferred to the newly labeled tubes. These tubes were prepared for mixing with the reagents, as described below.

   In addition to the 1 mL Fe(II) standards, the following reagents were added to each tube:

   (a). add 1 mL of 5.1 mM 1,10-Phenanthroline, a color reagent, and

   (b). add 0.5 mL of 10% hydroxylamine solution (reductant), and

   (c). 0.5 mL 1.2M ammonium acetate buffer.

   Addition of the above reagents brought the final volume to 3 mL. Any ferrous iron present in the sample will turn orange due to the addition of the coloring agent.
7. The Fe(II) standard solution and the reagents were thoroughly mixed in each tube using the vortex mixer.
8. Due to the addition of the reagents, the standard solutions were diluted. The new, diluted concentrations of the Fe(II) standards in the tubes were as follows:

Standard	Volume (mL)	Conc. of Fe(II) Std (mg L^{-1}) before reagent addition	Conc. of Fe(II) Std (mg L^{-1}) after reagent addition
STD1	Blank	0	0
STD2	0.15	0.75	0.25
STD3	0.3	1.5	0.5
STD4	0.6	3	1
STD5	0.9	4.5	1.5
STD6	1.2	6	2

9. Analyze standards using the Perkin Elmer Lambda 45 UV/VIS spectrophotometer.

Fe (II) Standard Concentration Calculations:

Concentrations for the first dilution are calculated as follows (using STD2 as an example):
$C_1 * V_1 = C_2 * V_2$
Where,
V_1 = 150 µL = 1.5 mL (of 50 mg L^{-1} iron stock solution)
C_1 = 50 mg L^{-1} (iron standard solution)
V_2 = 10 mL (in the centrifuge tube)
C_2 = unknown
$C_2 = (C_1 * V_1)/ V_2 = (50 \text{ mg } L^{-1} * 150 \text{ µL})/10 = 0.75 \text{ mg } L^{-1}$
Concentrations for the addition of the color reagent, reductant, and buffer were calculated as follows (using STD2 as an example):

Where,
V_1 = 1 mL (of 0.75 mg L^{-1} solution)
C_1 = 0.75 mg L^{-1}
V_2 = 3 mL (in the centrifuge tube)
C_2 = unknown
$C_2 = (C_1 * V_1)/ V_2 = (0.75 \text{ mg } L^{-1} * 1.0 \text{ mL})/ 3 \text{ mL} = 0.25 \text{ mg } L^{-1}$

Calibration Curve:

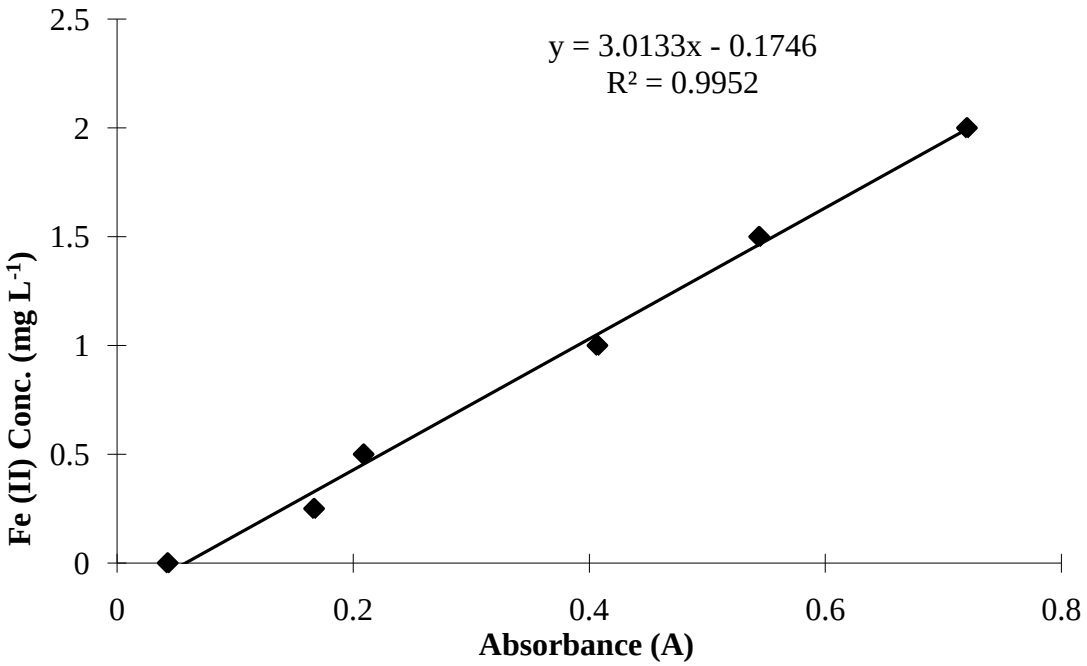

Sampling and Fe (II) Measurement Procedure for Microcosms:

1. Take all 6 microcosm bottles into the anaerobic glovebox (Coy Instrument, Inc, MI).
2. Use a 23 gauge needle and a 5 mL plastic syringe to pull out 2 mL of sample.
3. Remove the needle from the end of the syringe and replace it with a filter.
4. Push the sample through the filter into a small glass beaker.
5. Using a pipette, transfer 1 mL of filtered sample into a 10 mL volumetric flask.
6. Add 9 mL of DI water to the volumetric flask, in order to dilute the sample 10 times.
7. Cap the flask and mix thoroughly.
8. Pour the contents of the flask into a 15 mL centrifuge tube.
9. Acidify each sample by adding, 100 µl of 12 N HCl into the centrifuge tube using a pipette.
10. Sample all 6 microcosms, and prepare the respective samples by repeating steps 2-9 for each. Be sure to use clean needles, syringes, beakers and centrifuge tubes for each sample.
11. Cap all of the centrifuge tubes.
12. Bring them out of the glove box.
13. Transfer 1 mL of each sample into a new centrifuge tube, and then add the following reagents to each sample:

    (a). add 1 mL of 1.2M ammonium acetate buffer, and

    (b). add 1 mL of 5.1 mM 1,10-Phenanthroline.
14. Mix samples well using the Vortex Genie.

Procedure for Spectrophotometer Analysis of Fe (II) in Aqueous Samples:

1. Begin by turning the spectrophotometer on and allowing it to warm-up.
2. When machine is ready double-click on the LAMBDA 45 icon.
3. Find the appropriate analysis method and double-click on it.
4. Check the information for all of the icons to the left of the sample spreadsheet (data collection, instrument, corrections, Beer's Law Quant, parameters, calibration) to make sure all of the information is correct.
5. In the Accessory tab make sure only the cell changer is checked (not *peltier* or *sipper*).
6. After all of the information has been checked for setting accuracy in the *Sample Info* page, enter the number of samples to be analyzed.
7. Press the *Run* button.
8. Fill cuvette with 3 mL of sample to be analyzed.
9. Clean the outside of the cuvette gently with Kim Wipes to make sure no liquid or fingerprints are present.
10. Place the cuvette in the cell changer and run the sample.
11. Click *Run Sample* 3 times for each sample, to get triplicate readings.
12. Pour out sample. Rinse and wipe cuvette with DI water and Kim Wipes.
13. Repeat steps 8-12 above for each sample.
14. This procedure should be repeated 3 times for the same sample.
15. Once analysis is finished, Click *Save As a Task.*
16. Turn off the spectrophotometer.

Appendix D

Standard Operating Procedure for Microcosm Methane Determination by 6890 GC

Preparation of Methane Standards (in 160 mL serum bottles for microcosms):

1. Prepare 7-160 mL serum bottles with 80 mL of DI water.
2. Place a Teflon stopper and metal cap on top of each serum bottle and use a crimper to seal it and remove the flap off on the lid.
3. Prepare a 72 mL serum bottle with a Teflon stopper and metal cap.
4. Bubble methane gas through a 23 gauge needle (B-D, part #305145) into the 72 mL serum bottle and use another needle for a vent.
5. Allow the bottle to be flushed with methane gas for 30 minutes.
6. Take the vent needle out of the 72 mL serum bottle.
7. Withdraw methane from the gas bottle slowly using a gas tight syringe and inject methane into the 160 mL serum bottles.
8. The final concentrations of the standards are:

Standard	Volume (µl)	Mass of Methane (micromoles)
STD1	Blank	0
STD2	100	4.09
STD3	300	12.27
STD4	1000	40.90
STD5	3000	122.71
STD6	10000	409.03
STD7	20000	818.05

Example Calculations for 100 µl Methane Standard:

PV = nRT
P=1 atm
V=1 Liter
n= number of moles
R=Gas Constant=0.082 L*atm* K^{-1} * $mole^{-1}$
T= temperature=298.15 K

$$n = \frac{PV}{RT} = \frac{1atm * 1L}{0.082L * atm/K * mole * 298.15K} = 0.0409 moles * 10^6 micromoles$$

$$= 40902.63 micromoles of\ methane\ in\ 1L\ of\ pure\ gas$$

$$100\,\mu l\ of\ methane = \frac{1\,Liter}{1000\,ml} * \frac{1\,mL}{1000\,\mu L} = 10^{-5}\ L * \frac{40902.63 micromoles}{1\,L}$$

$$= 4.09\,micromoles of\ methane$$

*All bottles were purchased from **Wheaton Science**. Volumes of bottles used in this lab measure 73 and 163 mL bottles (volume measured till the top of bottle).*

DI water used in the lab is obtained from Millipore's Milli-Q Gradient water system

Calibration Curve for microcosms:

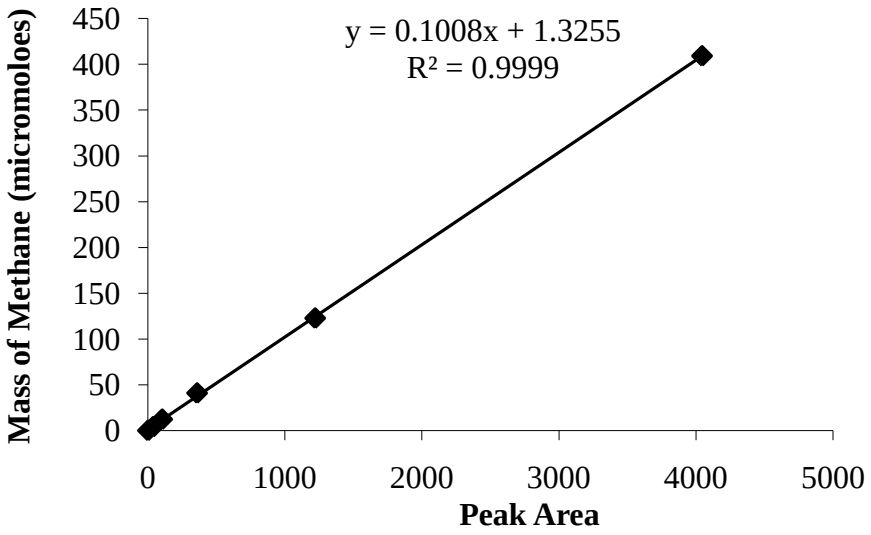

Procedure for Calculation of Methane Mass from *p*CH_4 in bioreactor systems:

Preparation of Methane Calibration Curve for bioreactors:

1. Turn on Methane gas tank, allowing gas to flow freely from the line.
2. Use a gas tight 50 µL syringe to directly pull varying amounts of gas from the CH_4 gas line.

3. Inject the gas sample into the 6890 GC. The run time for CH_4 is approximately two minutes.
4. Each injection volume was done in duplicate.

*Applicable to analyses using a 50 µL gas tight syringe

CH_4 Standard	Injection Volume (µL)	$\%CH_4$	Partial Pressure of CH_4 (atm)
1	1	2	0.02
2	2	4	0.04
3	5	10	0.1
4	10	20	0.2
5	25	50	0.5
6	50	100	1

Calibration Curve for bioreactors:

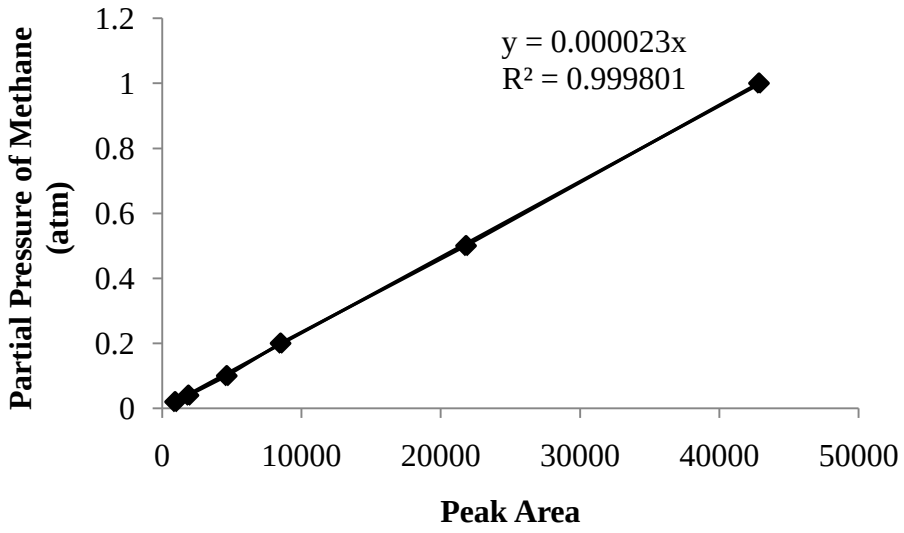

Example Calculation for Total Methane Mass in a Bioreactor:

$$\textbf{\textit{Total Mass of Methane}} = \textit{Mass of Methane in the Headspace} + \textit{Mass of Methane in Aqueous Phase}$$

Step 1: Calculating Methane Mass in the Headspace (in moles) using the Gas Law

$PV = nRT$ or **n= PV/RT**

where P = partial pressure of methane (obtained from calibration curve),
V= headspace volume (see table below)
R= Gas Constant=0.082 L*atm/K*mole
T=Temperature= 298.15 K (273.15 + t, where t = 25 C)
n= moles of methane in headspace (unknown)

Reactor	Head Space Volumes (L)
MR#1	6.2
MR#2	5.1

Step 2: Calculating Methane Mass in the Aqueous Phase (in moles) using Henry's Law

$[CH_4] = K_H * pCH_4$

Where K_H= $1.4*10^{-3}$ moles L^{-1}*atm for methane at STP, and pCH_4 is measured
$[CH_4]$ = Methane concentration (moles L^{-1})

Aqueous Phase Mass of Methane (moles) = Methane Concentration $[CH_4]$ (moles L^{-1}) * Volume of Aqueous Phase (L)

*See table below for aqueous phase volumes

Reactor	Aqueous Phase Volumes (L)
MR#1	1.0
MR#2	2.1

Sampling and Methane Measurement Procedure for Microcosms on 6890 GC:

1. Check gas tanks (Helium, Hydrogen, Nitrogen and Air) for appropriate pressures. (Appropriate levels are marked on the regulators- Tank pressure should never read below 500 psi and line pressure should NEVER exceed recommended limit marked on the gauge)

2. Unscrew head space injection nut and replace septa every day. Finger tighten the screw back on.
3. Go to GC screen on the computer and select PREP.M from *Method* pull down menu.
4. This automatically turns the GC on.
5. Prep.M run takes 30 min.
6. Once Prep.M is complete, go to *Method* pull down menu and select NEW DUAL.M.
7. Wait for approximately 10 min before the GC shows Ready sign in green.
8. Go to *Run Control* tab and go to *Sample info* tab on the GC screen and enter in user information including file name (under which all results will be saved) with date, operator/user name and sample name.
9. To prep samples for analysis, purge each of the 6 160 mL microcosm bottles to remove any negative pressure that has built up in the bottles.
    a. H_2/N_2 (50%/50%) gas mix was used to do this purge for cycles 1-20 in MS bottles and cycles 1-19 in TMS bottles.
    b. Pure nitrogen gas was used to do this purge in MS bottles for cycle 21 and on, and in TMS bottles for cycle 20 and on.
10. Secure the 160 mL serum bottle in place using a clamp that is attached to a ring stand.
11. Position the bottle in a horizontal orientation so that half of the septa is covered by fluid and the other half is exposed to the headspace in the bottle.

12. Now withdraw 50 µl of gaseous sample from the 160 mL bottle using a 50 µl Hamilton glass gastight syringe.
13. Inject the sample through the head space injection nut and immediately hit the *Start* button on the GC. Keep your finger on the syringe plunger and do not remove the syringe until the time screen shows 0.22 minutes
14. Run time can be seen by pressing the *Time* button on the GC.
15. The sample run time from the time it is injected into the GC is 2 minutes because methane should come out at 1.53.
16. Once the run is complete, the GC shows Not Ready sign in red. Wait for the GC to show the ready sign in green before injecting the next sample.
17. Go to *Method and Run Control* pull down menu and go to data analysis.
18. FID gives the peak for methane.
19. The report can be printed from the *Data Analysis* screen.
20. Return to the *Method* screen and go to *Run Control-Sample Info* to change the name of the sample.
21. Each sample was run in duplicate.
22. Once the green ready light comes on, the next sample can be processed.
23. Once all of the samples have been analyzed go to the *Method* pull down menu and select Shut_OGC.M and press NO when software prompts to save the method.
24. Convert peak area given from the GC to micromoles of methane using the calibration curve generated from running the standards.

Appendix E

Standard Operating Procedure for Microcosm Organic and Inorganic Carbon by TOCN Analyzer

Required Materials:

5mL Luer-Loc Tip Syringes (B-D, part # 309603), 23 gauge needles (B-D, part # 305145), filters (Iso-Disc, N-25-4 Nylon, 25 mm x 0.45µm, part # 54123-U), 40 mL vials (Kimble Glass, Inc. Vials, Screw Thread, Opticlear Amber 203, Art. No 60960A 912, size/cap 28 x 95 mm), caps and septa (22 mm TFE/SIL 0.125, Lot# 7H0105)

Preparation of Organic Carbon Standards:

1. Use Tekmar-Dohrmann Aqueous Carbon Potassium Avid Phthalate (1000 mg L^{-1}) as a stock solution.
2. The varying concentrations of the standards are:

C_1 (mg L^{-1})	C_2 (mg L^{-1})	V_2 (mL of DI water)	V_1 (mL of stock)
1000	1	50	0.05
1000	2	50	0.1
1000	5	50	0.25
1000	10	50	0.5
1000	20	50	1

3. The standards were labeled and placed in brown opaque 40 mL vials and sealed off with a cap and septa.
4. The standards were run on the TOCN Analyzer (see TOCN handbook in Appendix L for further detail).

Calibration Curve:

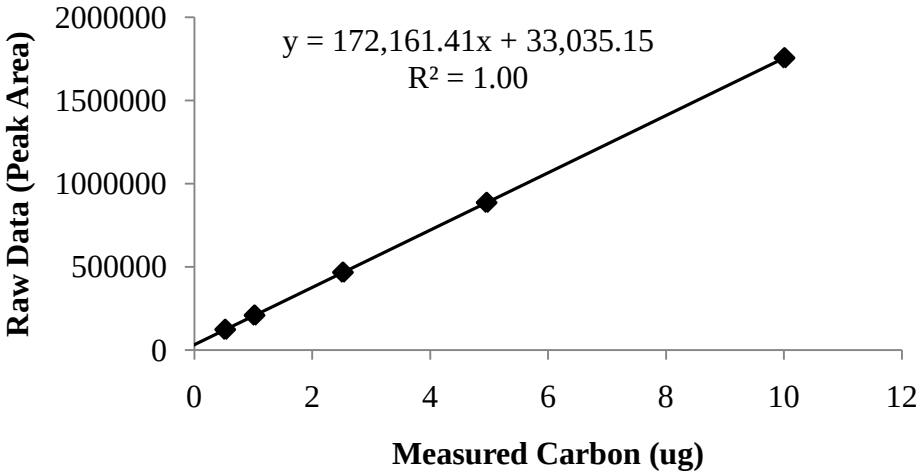

Preparation of Inorganic Carbon Standards:

1. Create a 1.6 g L^{-1} (1600 mg L^{-1}) stock solution of sodium bicarbonate.
    a. Weigh out 400 mg of sodium bicarbonate
    b. Dissolve it in 250 mL of DI water
2. The varying concentrations of the standards are:

C_1 (mg L^{-1})	C_2 (mg L^{-1})	V_2 (L of DI water)	V_1 (L of stock)	V_1 (mL of stock)
1600	400	0.1	0.025	25
1600	200	0.1	0.0125	12.5
1600	100	0.1	0.00625	6.25
1600	50	0.1	0.003125	3.125
1600	0	0.1	0	0

3. The standards were labeled and placed in brown opaque 40 mL vials and sealed off with a cap and septa.
4. TOCN analyzer input needs to be in terms of concentration of carbon for each standard:

$$400\ \text{mg L}^{-1}\text{NaHCO}_3 \rightarrow 400\text{mg L}^{-1}\text{NaHCO}_3 * \frac{12\ \text{g mol}^{-1}\text{of Carbon}}{84\text{g mol}^{-1}\text{of NaHCO}_3}$$

$$= 57.143\ \text{mg L}^{-1}\text{Carbon}$$

$$200\ \text{mg L}^{-1}\text{NaHCO}_3 \rightarrow 200\ \text{mg L}^{-1}\text{NaHCO}_3 * \frac{12\ \text{g mol}^{-1}\text{of Carbon}}{84\ \text{g mol}^{-1}\text{of NaHCO}_3}$$

$$= 28.571\text{mg L}^{-1}\text{Carbon}$$

$$100\ \text{mg L}^{-1}\text{NaHCO}_3 \rightarrow 100\ \text{mg L}^{-1}\text{NaHCO}_3 * \frac{12\ \text{g mol}^{-1}\text{of Carbon}}{84\ \text{g mol}^{-1}\text{of NaHCO}_3}$$

$$= 14.286\ \text{mg L}^{-1}\text{Carbon}$$

$$50\ \text{mg L}^{-1}\text{NaHCO}_3 \rightarrow 50\ \text{mg L}^{-1}\text{NaHCO}_3 * \frac{12\ \text{g mol}^{-1}\text{of Carbon}}{84\ \text{g mol}^{-1}\text{of NaHCO}_3}$$

$$= 7.143\ \text{mg L}^{-1}\text{Carbon}$$

$$0\ \text{mg L}^{-1}\text{NaHCO}_3 \rightarrow 0\ \text{mg L}^{-1}\text{NaHCO}_3 * \frac{12\text{g mol}^{-1}\text{of Carbon}}{84\ \text{g mol}^{-1}\text{of NaHCO}_3}$$

$$= 0\ \text{mg L}^{-1}\text{Carbon}$$

5. The standards were run on the TOCN Analyzer (see TOCN handbook in appendix for further detail).

Calibration Curve:

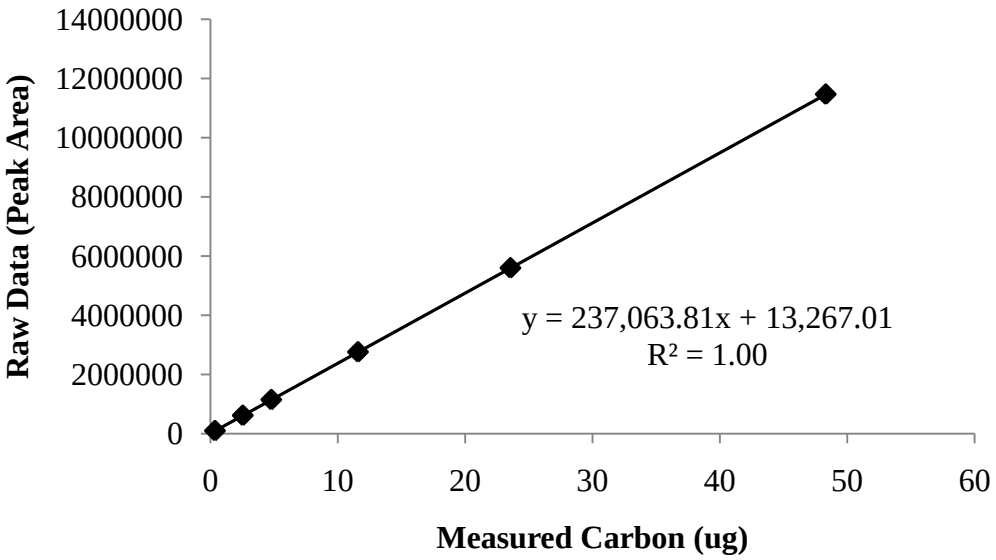

Sampling and Organic and Inorganic Carbon Measurement Procedure for Microcosms:

1. Take the 6 -160 mL microcosm bottles into the anaerobic glovebox (Coy Laboratory Products, Inc.) along with 6- 5 mL polypropylene syringes, 6- 23 gauge needles, 6 filters, 6- 40 mL vials and a beaker full of DI water.
2. Use the syringe to pull out about 1 mL of sample, replace the needle on the end of syringe with a 25 mm x 0.45 um Iso-Disc Filter
3. Push the sample through the filter into a 40 mL brown vial. The filter removes the particulate organic matter, leaving only dissolved organic carbon to be measured.
4. Add 19 mL of water with a Socorex Acura 835 1-10 mL pipette to the brown vial. This makes the total volume in the vial 20 mL.
5. Secure a cap and septa on the vial.
6. Repeat steps 2-5 for each microcosm.
7. Bring the 6 vials out of the glovebox and store them in the refrigerator overnight.

8. Run the samples and blank that only contains DI water on the TOCN Analyzer (see TOCN handbook in Appendix L for further detail on how to run the machine).
9. Print the results from the TOCN analyzer.
10. Subtract the value of the blank from the value of the DOC sample to correct for any DOC that may have been a result of the water itself. Subtract the value of the blank from the value of the DIC sample to correct for any DIC that may have been a result of the water itself.
11. Multiple the corrected DOC value by 20 to account of the dilution factor. Multiple the corrected DIC value by 20 to account of the dilution factor.
12. The samples were tested for inorganic and organic carbon during the same run time on the TOCN Analyzer.

Appendix F

Standard Operating Procedure for Microcosm pH Determination

Required Materials:

10 ml Pyrex beakers, 23 gauge needles (B-D; part # 305145), 5 ml syringes (B-D; part # 309603)

Sampling and pH Measurement Procedure for Microcosms:

1. Calibrate a Denver Instrument AP10 pH/mv meter with 4, 7, and 10 buffers.
    a. Hit the On/Off button to turn on the pH meter
    a. Place the electrode into the 4.0 buffer
    b. Wait for the reading to stabilize ("S" appears on screen)
    c. Hit the standardize button
    d. Rinse the probe with DI water and wipe dry with Kim Wipe
    e. Repeat these steps for the 7.0 and 10.0 buffer
    f. The generated slope shown should be above 95% and the screen will display a message saying that it is a good electrode
2. Take the pH probe, 6- 10 mL Pyrex beakers, 6- 23 gauge needles, 6- 5mL syringes and the 6 microcosms into the glovebox.
3. Inside the anaerobic glovebox (Coy Instrument, Inc, MI). Use a 5mL Luer-Loc Tip Syringe with a 23 gauge needle to pull out a ~3mL of sample from 1 microcosm.
4. Replace the needle on the end of the syringe with a 25mm x 0.45 um Iso-Disc Filter.
5. Push the sample through the filter into a 10 mL Pyrex beaker.

6. Immediately, put the pH electrode into the sample and wait until "*S*" appears on the screen which notes that the reading is stable.
7. Record the pH value.
8. Rinse the pH probe with DI water and wipe dry with Kim Wipe.
9. Repeat steps 3-8 for all 6 microcosms.

*DI water used in the lab is obtained from an **Elix Millipore System** that leads into **Milli-Q Gradient** water system.*

Appendix G

Standard Operating Procedure for Microcosm Carbon Dioxide and Hydrogen Determination by 5890 GC

Sampling, Carbon Dioxide Measurement and Hydrogen Measurement Procedure for Microcosms and Bioreactors:

1. Check gas tanks (Helium, Hydrogen, Nitrogen, and Air) for appropriate pressures and then open the regulators.
2. Unscrew the back head space injection nut and replace septa every day before use. Tighten the screw as much as possible.
3. Open all 4 gas shutoff valves at the rear of the 5890. Turn on (fully open) the TCD REF gas valve on upper left front of 5890.
4. Turn on the power toggle switch which is located on the bottom of the right side of 5890.
5. Go to GC screen on computer and load the PGASCOND.M method.
6. Wait about 5 minutes for system to be purged with gases.
7. Hit *Start* button on 5890 and wait about 30 minutes.
8. Load the appropriate method for analysis (PGAS_5890.M for carbon dioxide or HYD5890.M for hydrogen).
9. Wait about 30 minutes for Signal 2 and the temperature (30^{o}C) to stabilize.
10. Go to the *Run Control-Sample Info* dialog box to enter sample information.
11. Using a Hamilton 50 μL gas tight syringe, inject sample into the back head space injection port of the 5890 GC.
12. Press the *Start* button

13. Keep your finger on the syringe plunger and do not remove the syringe until the time screen shows 0.1 minutes.
14. The sample run time from the time it is injected into the GC is 6.5 minute for carbon dioxide and about 1 minute for hydrogen.
15. Once the run time is finished, go to *Data Analysis* and print report.
16. Return to the *Method* screen and go to *Run Contol-Sample Info* dialog to change the sample info for next injection.
17. All samples were run in duplicate.
18. Once all of the samples have been analyzed go to the *Method* pull down menu and select SHUT5890.M method.
19. Wait for the oven temperature to cool below 30^{o}C
20. Turn off (fully close) the TCD REF gas valve.
21. Close all 4 gas shutoff valves at the rear of the 5890 (Helium, Hydrogen, Nitrogen, and Air).
22. Turn off power switch on back right side of 5890.

Appendix H

Standard Operating Procedure for Microcosm Inorganic Carbon Determination by Gas Law and Henry's Law

Preparation of Carbon Dioxide Standards:

1. Turn the from 50/50% H_2/CO_2 gas tank to open, allowing gas to flow freely from the line.
2. Use a gas tight syringe to directly pull varying amounts of gas from the H_2/CO_2 gas line.
3. Inject the gas sample into the 5890 GC. The run time for CO_2 is approximately 6 minutes.
4. Each injection volume was done in duplicate.

CO_2 Standard	Injection Volume (μL)	$\%CO_2$	Partial Pressure of CO_2 (atm)
1	10	10	0.1
2	20	20	0.2
3	50	50	0.5

Calibration Curve:

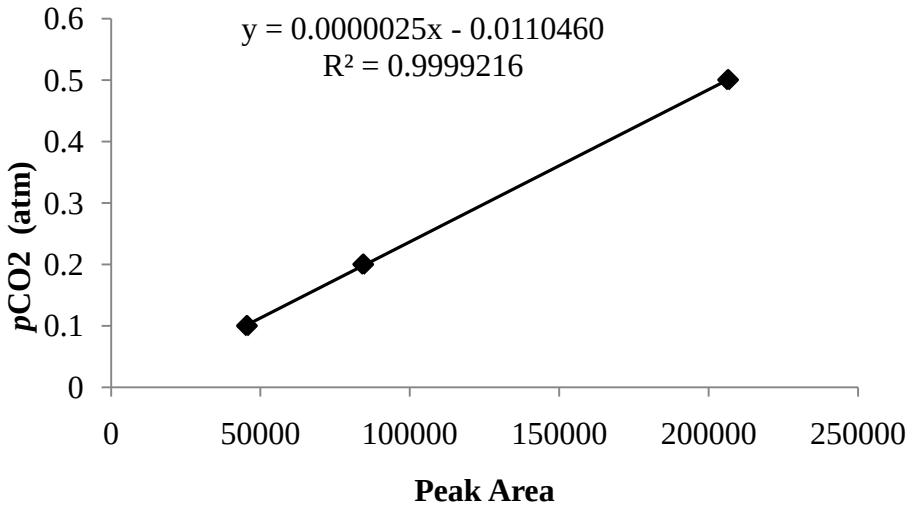

Sampling Procedure:

1. The bottles and reactors were reset and purged with 50/50 H_2/CO_2 gas mix for 1 hour each.
2. After purging, each was analyzed for CO_2. A sample volume of 50 µL was extracted from each with a gas tight syringe and injected into the 5890 GC.
3. Each run was done in duplicate.

Examples of Inorganic Carbon Calculations (for MR#1, MS-1, and TMS-1):

$$\boldsymbol{Total\ Inorganic\ Carbon} = Inorganic\ Carbon\ in\ the\ Headspace + Inorganic\ Carbon\ in\ Aqueous\ Phase$$

Step 1: Calculate Inorganic Carbon in the Headspace (in moles) using the Gas Law

$$PV = nRT$$

where P= partial pressure of Carbon Dioxide from calibration curve,
V= headspace volume. For MR#1, V=6.2 L, MR#2=5.1 L, MS and TMS Bottles =0.08 L
R= Gas Constant=0.082 L*atm/K*mole
T=Temperature= 298.15 K
n= moles of carbon dioxide in headspace (unknown)

Step 2: Calculate Inorganic Carbon in the Aqueous Phase (in moles L^{-1}) using Henry's Law

$$Dissolved\ Inorganic\ Carbon = [H_2CO_3^*] + [HCO_3^-] + [CO_3^{2-}]$$

$$[H_2CO_3^*] = K_H * pCO_2$$

Where $K_H = 10^{-1.47}$ and pCO$_2$ is measured

$$[HCO_3^-] = \frac{K_1 * K_H * pCO_2}{[H^+]}$$

Where $K_1=10^{-6.35}$, $K_H= 10^{-1.47}$, pCO_2 and $[H^+]$ are measured

$[CO_3^{2-}]$ is negligible because of the neutral pH

Example Calculations for MR#1:

Step 1:

$$n = \frac{PV}{RT}$$

$$n = \frac{(0.3171\ atm) * (6.2\ L)}{0.082\ \frac{L * atm}{K * mol} * 298.15K}$$

$$n = \mathbf{0.0804\ moles\ of\ carbon\ dioxide\ in\ headspace}$$

Step 2:

$$[H_2CO_3^*] = K_H * pCO_2$$
$$[H_2CO_3^*] = 10^{-1.47} * 0.3171$$
$$[H_2CO_3^*] = 0.0107\ moles\ L^{-1}$$

$$[HCO_3^-] = \frac{K_1 * K_H * pCO_2}{[H^+]}$$

$$[HCO_3^-] = \frac{10^{-6.35} * 10^{-1.47} * 0.3171}{10^{-6.39}}$$

$$[HCO_3^-] = 0.0118\ moles\ L^{-1}$$

$$Dissolved\ Inorganic\ Carbon = [H_2CO_3^*] + [HCO_3^-] + [CO_3^{2-}]$$
$$Dissolved\ Inorganic\ Carbon = 0.0107\ moles\ L^{-1} + 0.0118\ moles\ L^{-1} + 0$$
$$Dissolved\ Inorganic\ Carbon = 0.0225\ moles\ L^{-1}$$
$$0.0225 moles\ L^{-1} * 1\ L\ of\ aqueous\ phase\ in\ MR\#1$$
$$= \mathbf{0.0225\ moles\ of\ dissolved\ inorganic\ carbon}$$

$$\mathbf{Total\ Inorganic\ Carbon}$$
$$= Inorganic\ Carbon\ in\ the\ Headspace$$
$$+ Inorganic\ Carbon\ in\ Aqueous\ Phase$$

$$Total\ Inorganic\ Carbon = 0.0804\ moles + 0.0225\ moles$$
$$\mathbf{Total\ Inorganic\ Carbon = 0.103\ moles}$$

Example Calculations for MS-1:

Step 1:

$$n = \frac{PV}{RT}$$

$$n = \frac{(0.3265\ atm) * (0.08\ L)}{0.082\ \frac{L * atm}{K * mol} * 298.15K}$$

$$n = \mathbf{0.0011\ moles\ of\ carbon\ dioxide\ in\ headspace}$$

Step 2:

$$[H_2CO_3^*] = K_H * pCO_2$$
$$[H_2CO_3^*] = 10^{-1.47} * 0.3265$$
$$[H_2CO_3^*] = 0.0111\ moles\ L^{-1}$$

$$[HCO_3^-] = \frac{K_1 * K_H * pCO_2}{[H^+]}$$

$$[HCO_3^-] = \frac{10^{-6.35} * 10^{-1.47} * 0.3265}{10^{-6.60}}$$

$$[HCO_3^-] = 0.0197\ moles\ L^{-1}$$

$$Dissolved\ Inorganic\ Carbon = [H_2CO_3^*] + [HCO_3^-] + [CO_3^{2-}]$$
$$Dissolved\ Inorganic\ Carbon = 0.0111\ moles\ L^{-1} + 0.0197\ moles\ L^{-1} + 0$$
$$Dissolved\ Inorganic\ Carbon = 0.0308\ moles\ L^{-1}$$
$$0.0308 \frac{moles}{L} * 0.08\ L\ of\ aqueous\ phase\ in\ MS\ 1$$
$$= \mathbf{0.0025\ moles\ of\ dissolved\ inorganic\ carbon}$$

$$Total\ Inorganic\ Carbon = Inorganic\ Carbon\ in\ the\ Headspace + Inorganic\ Carbon\ in\ Aqueous\ Phase$$

$$Total\ Inorganic\ Carbon = 0.0111\ moles + 0.0025\ moles$$
$$\mathbf{Total\ Inorganic\ Carbon = 0.0035\ moles}$$

Example Calculations for TMS-1:

Step 1:

$$n = \frac{PV}{RT}$$

$$n = \frac{(0.3161\ atm) * (0.08\ L)}{0.082\ \frac{L * atm}{K * mol} * 298.15K}$$

$n = \mathbf{0.0010\ moles\ of\ carbon\ dioxide\ in\ headspace}$

Step 2:

$[H_2CO_3^*] = K_H * pCO_2$

$[H_2CO_3^*] = 10^{-1.47} * 0.3161$

$[H_2CO_3^*] = 0.0107\ moles\ L^{-1}$

$$[HCO_3^-] = \frac{K_1 * K_H * pCO_2}{[H^+]}$$

$$[HCO_3^-] = \frac{10^{-6.35} * 10^{-1.47} * 0.3265}{10^{-6.56}}$$

$[HCO_3^-] = 0.0174\ moles\ L^{-1}$

$Dissolved\ Inorganic\ Carbon = [H_2CO_3^*] + [HCO_3^-] + [CO_3^{2-}]$

$Dissolved\ Inorganic\ Carbon = 0.0107\ moles\ L^{-1} + 0.0107\ moles\ L^{-1} + 0$

$Dissolved\ Inorganic\ Carbon = 0.028\ moles\ L^{-1}$

$0.028\ moles\ L^{-1} * 0.08\ L\ of\ aqueous\ phase\ in\ TMS1$

$= \mathbf{0.0022\ moles\ of\ dissolved\ inorganic\ carbon}$

$Total\ Inorganic\ Carbon$

$= Inorganic\ Carbon\ in\ the\ Headspace$

$+ Inorganic\ Carbon\ in\ Aqueous\ Phase$

$Total\ Inorganic\ Carbon = 0.0010\ moles + 0.0022\ moles$

$\boldsymbol{Total\ Inorganic\ Carbon = 0.003\ moles}$

Appendix I

Standard Operating Procedure for Microcosm Total Hydrogen Determination by Gas Law and Henry's Law

Preparation of Hydrogen Standards:

1. Turn the from 50/50% H_2/CO_2 gas tank to open, allowing gas to flow freely from the line.
2. Use a gas tight syringe to directly pull varying amounts of gas from the H_2/CO_2 gas line.
3. Inject the gas sample into the 5890 GC. The run time for H_2 is approximately 1 minute.
4. Each injection volume was done in duplicate.

H_2 Standard	Injection Volume (μL)	$\%H_2$	Partial Pressure of H_2 (atm)
1	10	10	0.1
2	20	20	0.2
3	30	30	0.3
4	50	50	0.5

Calibration Curve:

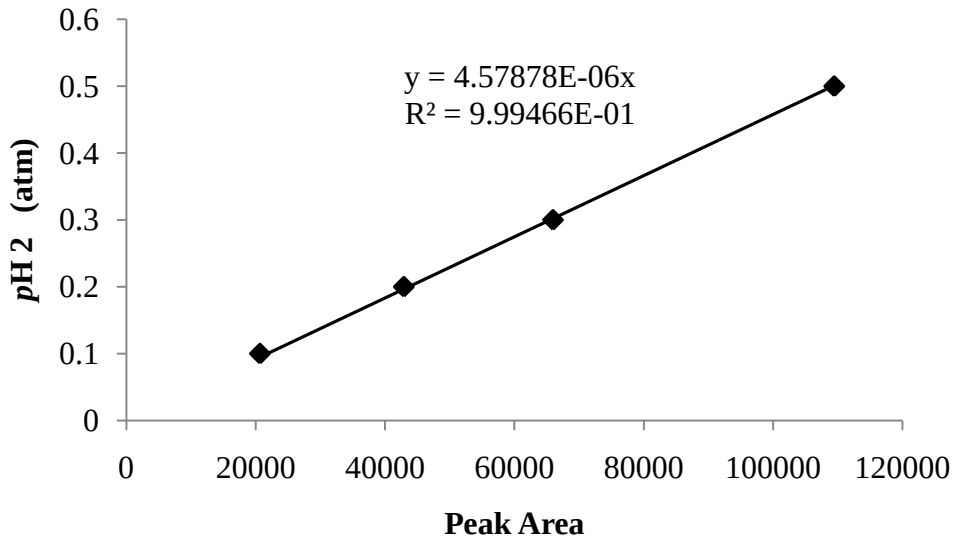

Sampling Procedure:

1. The bottles and reactors were reset and purged with 50/50 H_2/CO_2 gas mix for 1 hour each.
2. After purging, each was analyzed for H_2. A sample volume of 50 µL was extracted from each with a gas tight syringe and injected into the 5890 GC.
3. Each run was done in duplicate.

Examples of Hydrogen Calculations (for MR#1, MS-1, and TMS-1):

$$\boldsymbol{Total\ Hydrogen} = \textit{Hydrogen in the Headspace} + \textit{Hydrogen in Aqueous Phase}$$

Step 1: Calculating Hydrogen in the Headspace (in moles) using the Gas Law

$$PV = nRT$$

where P= partial pressure of hydrogen from calibration curve,
V= headspace volume. For MR#1, V=6.2 L, MR#2=5.1 L, MS and TMS Bottles =0.08 L
R= Gas Constant=0.082 L*atm/K*mole

T=Temperature= 298.15 K
n= moles of hydrogen in headspace (unknown)

Step 2: Calculating Hydrogen in the Aqueous Phase (moles L^{-1}) using Henry's Law

$[H_2] = K_H * pH_2$
Where K_H= $7.8*10^{-4}$ moles/L*atm and pH_2 is measured

Example Calculations for MR#1:

$$n = \frac{PV}{RT}$$

$$n = \frac{(0.4078\ atm) * (6.2\ L)}{0.082\ \frac{L * atm}{K * mol} * 298.15K}$$

$$n = \mathbf{0.1034\ moles\ of\ hydrogen\ in\ headspace}$$

$[H_2] = K_H * pH_2$
$[H_2] = (7.8 * 10^{-4}) * 0.4078$
$[H_2] = 0.0003\ moles\ L^{-1}$

$0.0003 moles\ L^{-1} * 1\ L\ of\ aqueous\ phase\ in\ MR\#1$
$= \mathbf{0.0003\ moles\ of\ dissolved\ hydrogen}$

$Total\ Hydrogen = \ Hydrogen\ in\ the\ Headspace + Hydrogen\ in\ Aqueous\ Phase$
$Total\ Hydrogen = \ 0.1034\ moles + 0.0003\ moles$
$\boldsymbol{Total\ Hydrogen = \ 0.1037\ moles}$

Example Calculations for MS-1:

$$n = \frac{PV}{RT}$$

$$n = \frac{(0.3899\ atm) * (0.08\ L)}{0.082\ \frac{L * atm}{K * mol} * 298.15K}$$

$$n = \mathbf{0.0013\ moles\ of\ hydrogen\ in\ headspace}$$

$[H_2] = K_H * pH_2$
$[H_2] = (7.8 * 10^{-4}) * 0.3899$
$[H_2] = 0.0003\ moles\ L^{-1}$

$$0.0003\ moles\ L^{-1} * 0.08\ L\ of\ aqueous\ phase\ in\ MS\ 1$$
$$= \mathbf{0.00002\ moles\ of\ dissolved\ hydrogen}$$

$$Total\ Hydrogen = \ Hydrogen\ in\ the\ Headspace + Hydrogen\ in\ Aqueous\ Phase$$
$$Total\ Hydrogen = \ 0.0013\ moles + 0.00002\ moles$$
$$\boldsymbol{Total\ Hydrogen = \ 0.0013\ moles}$$

Example Calculations for TMS-1:

$$n = \frac{PV}{RT}$$

$$n = \frac{(0.3684\ atm) * (0.08\ L)}{0.082\ \frac{L * atm}{K * mol} * 298.15K}$$

$$n = \mathbf{0.0012\ moles\ of\ hydrogen\ in\ headspace}$$

$$[H_2] = \ K_H * pH_2$$
$$[H_2] = (7.8 * 10^{-4}) * 0.3684$$
$$[H_2] = 0.00028\ moles\ L^{-1}$$

$$0.00028\ moles\ L^{-1} * 0.08\ L\ of\ aqueous\ phase\ in\ TMS\ 1$$
$$= \mathbf{0.00002\ moles\ of\ dissolved\ hydrogen}$$

$$Total\ Hydrogen$$
$$= \ Hydrogen\ in\ the\ Headspace + Hydrogen\ in\ Aqueous\ Phase$$
$$Total\ Hydrogen = \ 0.0012\ moles + 0.00002\ moles$$
$$\boldsymbol{Total\ Hydrogen = \ 0.00123\ moles}$$

Table 3.1: Sampling Details and Set-up Conditions for Microcosms

Cycle	Cycle Duration	Condition of Set-up	Parameters Measured	Other
MS Cycle #1	7/17/08-7/21/08	Added 20 mL of wetland soil plus 60 mL of basal medium Purged with 80% H2 20% CO2 for 60 min each	Methane, TOC, IC, Fe (II)	H2/CO2 every other day 250 μL GC Injection
MS Cycle #2	7/22/08-7/31/08	Took out 40 mL of Basal Medium from each bottle to create TMS series at the end of MS C1. Adding 40 mL of new anaerobic basal medium to start MS C2 Purged with 80% H2 20% CO2 for 60 min each	Methane, Alk, TOC, IC, TN, Fe (II), pH	H2/CO2 injected every day 250 μL GC Injection Alk sample not diluted
MS Cycle #3	8/1/08-8/8/08	Added a few mL of basal medium to keep 80 hs/80 fluid ratio Purged with 80% H2 20% CO2 for 60 min each	Methane, Alk, TOC, TN, Fe (II), pH	H2/CO2 injected every day First 3 methane samples were 250 μL and the last one 50 μL Alk sample diluted 5x
MS Cycle #4	8/12/08-8/18/08	Replenish 20 mL of basal medium Purged with 80% H2 20% CO2 for 60 min each	Methane, Alk, TOC, TN, Fe (II), pH	H2/N2 injected every day 50 μL GC injection Alk sample diluted 5x

MS Cycle #5	8/19/08-8/22/08	Added a few mL of basal medium to keep 80 hs/80 fluid ratio Purged with 80% H2 20% CO2 for 60 min each	Methane, Alk, TOC, TN, pH	H2/N2 injected every day 50 µL GC injection Alk sample diluted 5x
MS Cycle #6	8/25/08-9/2/08	Replenish 20 mL of basal medium Purged with 80% H2 20% CO2 for 60 min each	Methane, Alk, TOC, TN, pH	H2/N2 injected every day 50 uL GC injection Alk sample diluted 5x 2nd Alk Sample diluted 10x
MS Cycle #7	9/3/08-9/11/08	Added 6 mL of anaerobic basal medium to each bottle at start Purged with 80% H2 20% CO2 for 60 min each	Methane, Alk, TOC, TN, pH	H2/N2 injected every day 50 uL GC injection Alk Sample diluted 10x
MS Cycle #8	9/12/08-9/23/08	Replenish 20 mL of basal medium Purged 3 Bottles at a time with 80% H2 20% CO2 gas mix	Methane, Alk, TOC, TN, pH	H2/N2 injected every day 50 uL GC injection Alk Sample diluted 10x
MS Cycle #9	9/24/08-10/6/08	Replenish 20 mL of basal medium Purged with 50% H2 50% CO2 for 60 min each	Methane, Alk, TOC, TN, pH	H2/N2 injected every day 50 uL GC injection Alk Sample diluted 10x

MS Cycle #10	10/13/08-10/17/08	Added a few mL of basal medium to keep 80 hs/80 fluid ratio Purged with 50% H2 50% CO2 for 60 min each	Methane, pH	H2/N2 injected every day 50 μL GC injection H2/N2 injected every day
MS Cycle #11	10/20/08-10/24/08	Replenish 20 mL of basal medium Purged with 50% H2 50% CO2 for 60 min each	Methane, pH	50 μL GC injection H2/N2 injected every day
MS Cycle #12	10/27/08-10/31/08	20 mL of basal medium transferred to TMS bottles because TOC analysis diluted them too quickly Purged with 50% H2 50% CO2 for 60 min each	Methane	50 μL GC injection
MS Cycle #13	11/3/08-11/7/08	No basal medium added Purged with 50% H2 50% CO2 for 60 min each	Methane, pH	H2/N2 injected every day 50 μL GC injection
MS Cycle #14	11/10/08-11/14/08	Replenished 20 mL of basal medium Purged with 50% H2 50% CO2 for 60 min each	Methane	H2/N2 injected every day 50 μL GC injection

MS Cycle #15	11/17/08-11/24/08	No Basal Medium added Purged with 50% H2 50% CO2 for 60 min each	Methane, pH	H2/N2 injected every day 50 μL GC injection
MS Cycle #16	12/2/08-12/5/08	Replenished 20 mL of basal medium Purged with 50% H2 50% CO2 for 60 min each	Methane, pH	H2/N2 injected every day 50 μL GC injection
MS Cycle #17	12/8/08-12/12/08	Added a few mL of basal medium to keep 80 hs/80 fluid ratio Purged with 50% H2 50% CO2 for 60 min each	Methane, pH	H2/N2 injected every day 50 μL GC injection
MS Cycle #18	12/15/08-12/19/08	Added a few mL of basal medium to keep 80 hs/80 fluid ratio Purged with 50% H2 50% CO2 for 60 min each	Methane, pH	H2/N2 injected every day 50 μL GC injection
MS Cycle #19	2/23/09-2/26/09	Replenished 20 mL of basal medium Purged with 50% H2 50% CO2 for 60 min each	Methane	H2/N2 injected every day 50 μL GC injection

MS Cycle #20	3/2/09-3/4/09	Replenished 20 mL of basal medium Purged with 50% H2 50% CO2 for 60 min each	Methane	H2/N2 injected every day 50 μL GC injection
MS Cycle #21	3/8/09-3/11/09	No basal medium added Purged with 50% H2 50% CO2 for 60 min each	Methane, Carbon Dioxide, hydrogen, pH	N2 injected every day 50 μL GC injection 5890 and 6890
MS Cycle #22	4/13/09-4/21/09	Replenished 6 mL of basal medium to MS-1 and TMS-1 (DNA sequencing) Did not add basal medium to other bottles Purged with 50% H2 50% CO2 for 60 min each	Methane, Carbon Dioxide, hydrogen, pH	N2 injected every day 50 μL GC injection 5890 and 6890
MS Cycle #23	4/22/2009-4/23/09	Added a few mL of basal medium to keep 80 hs/80 fluid ratio Purged with 50% H2 50% CO2 for 60 min each	Methane, Carbon Dioxide, hydrogen, pH	N2 injected every day 50 μL GC injection 5890 and 6890

MS Cycle #24	4/25/2009-4/28/09	No basal medium added Purged with 50% H2 50% CO2 for 60 min each	Methane, Carbon Dioxide, hydrogen, pH	N2 injected every day 50 μL GC injection 5890 and 6890

Cycle	Cycle Duration	Condition of Set-up	Parameters Measured	Other
TMS Cycle #1	7/22/08-7/31/08	40 mL of MS Cycle #1 basal medium, plus 40 mL of anaerobic basal medium Purged with 80% H2 20% CO2 for 60 min each	Methane, Alk, TOC, IC, TN, Fe (II), pH	H2/CO2 injected every day 250 μL GC Injection Alk sample not diluted
TMS Cycle #2	8/1/08-8/8/08	Added a few mL of basal medium to keep 80 hs/80 fluid ratio Purged with 80% H2 20% CO2 for 60 min each	Methane, Alk, TOC, TN, Fe (II), pH	H2/CO2 injected every day First 3 methane samples were 250 μL and the last one 50 μL Alk sample diluted 5x
TMS Cycle #3	8/12/08-8/18/08	Replenish 20 mL of basal medium Purged with 80% H2 20% CO2 for 60 min each	Methane, Alk, TOC, TN, Fe (II), pH	H2/N2 injected every day 50 μL GC injection Alk sample diluted 5x

TMS Cycle #4	8/19/08-8/22/08	Added a few mL of basal medium to keep 80 hs/80 fluid ratio Purged with 80% H2 20% CO2 for 60 min each	Methane, Alk, TOC, TN, pH	H2/N2 injected every day, except TMS 2 50 µL GC injection Alk sample diluted 5x
TMS Cycle #5	8/25/08-9/2/08	Replenish 20 mL of basal medium Purged with 80% H2 20% CO2 for 60 min each	Methane, Alk, TOC, TN, pH	H2/N2 injected every day, except TMS 2 50 µL GC injection Alk sample diluted 5x 2nd Alk Sample diluted 10x
TMS Cycle #6	9/3/08-9/11/08	Added 6 mL of anaerobic basal medium to each bottle at start Purged with 80% H2 20% CO2 for 60 min each	Methane, Alk, TOC, TN, pH	H2/N2 injected every day, except TMS 2 50 µL GC injection Alk Sample diluted 10x
TMS Cycle #7	9/12/08-9/23/08	Replenish 20 mL of basal medium Purged with 80% H2 20% CO2 for 60 min each	Methane, Alk, TOC, TN, pH	H2/N2 injected every day, except TMS 2 50 µL GC injection Alk Sample diluted 10x Purged 3 Bottles at a time

TMS Cycle #8	9/24/08-10/6/08	Replenish 20 mL of basal medium Purged 2 Bottles at a time with 50/50 H2/CO2	Methane, Alk, TOC, TN, pH	H2/N2 injected every day, except TMS 2 50 µL GC injection Alk Sample diluted 10x
TMS Cycle #9	10/13/08-10/17/08	Added a few mL of basal medium to keep 80 hs/80 fluid ratio Purged with 50% H2 50% CO2 for 60 min each	Methane, Alk, TOC, DIC, pH	H2/N2 injected every day, except TMS 2
TMS Cycle #10	10/20/08-10/24/08	Replenish 45 mL of basal medium Purged with 50% H2 50% CO2 for 60 min each	Methane, Alk, TOC, DIC, pH	H2/N2 injected every day, except TMS 2
TMS Cycle #11	10/27/08-10/31/08	20 mL of basal medium transferred to TMS bottles from MS because TOC analysis diluted them too quickly Purged with 50% H2 50% CO2 for 60 min each	Methane, Alk	H2/N2 injected every day, except TMS 2 Purged with 50% H2 50% CO2 for 60 min each
TMS Cycle #12	11/3/08-11/7/08	No basal medium added Purged with 50% H2 50% CO2 for 60 min each	Methane, Alk, pH	H2/N2 injected every day, except TMS 2

TMS Cycle #13	11/10/08-11/14/08	Replenished 20 mL of basal medium Purged with 50% H2 50% CO2 for 60 min each	Methane, Alk	H2/N2 injected every day, except TMS 2
TMS Cycle #14	11/17/08-11/24/08	no basal medium added Purged with 50% H2 50% CO2 for 60 min each	Methane, Alk, pH	H2/N2 injected every day, except TMS 2
TMS Cycle #15	12/2/08-12/5/08	Replenished 20 mL of basal medium Purged with 50% H2 50% CO2 for 60 min each	Methane, Alk, pH	H2/N2 injected every day, except TMS 2
TMS Cycle #16	12/8/08-12/12/08	Added a few mL of basal medium to keep 80 hs/80 fluid ratio Purged with 50% H2 50% CO2 for 60 min each	Methane, Alk, pH	H2/N2 injected every day
TMS Cycle #17	12/15/08-12/19/08	Added a few mL of basal medium to keep 80 hs/80 fluid ratio Purged with 50% H2 50% CO2 for 60 min each	Methane, Alk, pH	H2/N2 injected every day

TMS Cycle #18	2/23/09-2/26/09	Replenished 20 mL of basal medium Purged with 50% H2 50% CO2 for 60 min each	Methane	H2/N2 injected every day
TMS Cycle #19	3/2/09-3/4/09	Replenished 20 mL of basal medium Purged with 50% H2 50% CO2 for 60 min each	Methane	H2/N2 injected every day
TMS Cycle #20	3/8/09-3/11/09	No basal medium added Purged with 50% H2 50% CO2 for 60 min each	Methane, Carbon Dioxide, hydrogen, pH	N2 injected every day
TMS Cycle #21	4/13/09-4/21/09	Replenished 6 mL of basal medium to MS-1 and TMS-1 (DNA sequencing) Did not add basal medium to other bottles Purged with 50% H2 50% CO2 for 60 min each	Methane, Carbon Dioxide, hydrogen, pH	N2 injected every day
TMS Cycle #22	4/22/09-	Added a few mL of basal medium to keep 80 hs/80 fluid ratio Purged with 50% H2 50% CO2 for 60 min each	Methane, Carbon Dioxide, hydrogen, pH	N2 injected every day

TMS Cycle #23	4/25/2009-4/28/09	No basal medium added Purged with 50% H2 50% CO2 for 60 min each	Methane, Carbon Dioxide, hydrogen, pH	N2 injected every day 50 μL GC injection 5890 and 6890

Tables of Raw Data

Table 1: Methane and pH raw data for MS and TMS.

Microcosm ID	Cycle ID #	Initial pH	Final pH	Average Mass of Methane Produced (micromoles)	Average Methane Production Rate (micromoles/hour)	Normalized Rate (micromoles/ Liter/hour)
MS-1	1	N/A	N/A	0.0	0.1	1.7
	2	6.9	7.6	16.6	0.3	3.5
	3	7.4	7.4	850.7	5.9	73.2
	4	7.2	7.7	215.0	9.2	114.5
	5	7.4	8.1	178.9	2.1	26.0
	6	7.5	7.9	244.1	2.6	32.8
	7	7.8	7.1	414.5	3.9	49.0
	8	8.1	7.3	712.3	-0.5	-6.4
	9	6.8	7.1	266.2	0.2	2.8
	10	6.7	6.8	201.4	2.4	29.7
	11	6.9	6.6	206.0	3.2	39.9
	12	N/A	N/A	182.1	2.7	33.3
	13	6.7	6.7	284.6	4.5	55.8
	14	N/A	N/A	379.9	-0.5	-6.3
	15	6.8	6.9	191.0	2.5	31.8
	16	6.6	6.6	184.9	3.2	39.4
	17	6.7	6.7	346.9	4.2	52.9
	18	6.8	6.6	311.8	3.6	45.2
	19	N/A	N/A	304.6	7.8	97.2
	20	N/A	N/A	161.3	2.8	34.7
	21	6.6	6.6	209.3	6.5	81.4
	22	6.7	6.7	221.1	3.8	47.8
	23	6.8	6.8	76.1	5.5	68.3
	24	6.7	6.6	246.7	5.7	71.3
MS-2	1	N/A	N/A	0.0	0.1	1.7
	2	7.1	7.5	33.6	0.5	5.7
	3	7.1	7.2	1014.6	9.6	119.7
	4	6.9	7.3	200.8	8.8	109.8
	5	7.2	7.4	281.7	3.4	42.4
	6	7.2	7.7	244.1	2.6	32.8
	7	7.5	7.3	600.3	8.4	105.1
	8	7.5	7.6	985.7	7.0	87.7
	9	6.7	7.6	731.7	3.0	36.9
	10	6.7	7.0	466.8	8.0	100.0

	11	6.7	6.7	434.1	7.5	94.3
	12	N/A	N/A	395.4	8.7	108.2
	13	6.8	6.8	523.4	7.6	95.2
	14	N/A	N/A	550.1	4.5	55.7
	15	6.7	6.8	301.0	3.8	48.1
	16	6.6	6.6	160.2	1.8	22.3
	17	6.7	6.8	301.0	4.6	57.8
	18	6.7	6.7	338.5	3.7	45.9
	19	N/A	N/A	317.7	8.5	106.5
	20	N/A	N/A	171.3	1.2	15.5
	21	6.8	6.8	69.4	5.3	66.9
	22	6.8	6.6	228.4	4.0	50.1
	23	6.6	6.6	15.1	5.4	67.9
	24	6.6	6.7	231.9	5.9	73.6
MS-3	1	N/A	N/A	12.1	0.1	0.9
	2	7.2	7.3	18.2	0.3	3.4
	3	7.1	7.3	1088.5	10.0	124.7
	4	6.9	7.3	306.3	13.4	168.1
	5	7.2	7.4	295.1	3.6	44.6
	6	7.0	7.7	568.2	0.4	4.5
	7	7.5	7.3	584.2	6.1	76.3
	8	7.3	7.6	875.8	4.8	59.5
	9	6.7	7.2	619.1	3.4	42.7
	10	6.6	6.7	571.1	9.4	117.5
	11	7.0	6.8	498.1	8.0	100.1
	12	N/A	N/A	285.1	7.0	87.6
	13	6.7	6.8	474.2	7.7	96.1
	14	N/A	N/A	507.2	6.1	76.1
	15	6.8	6.9	359.5	5.0	62.4
	16	6.6	6.6	245.8	3.9	48.3
	17	6.6	6.7	283.0	4.2	52.9
	18	6.7	6.7	378.3	3.6	45.4
	19	N/A	N/A	304.4	8.0	100.4
	20	N/A	N/A	183.9	1.3	16.8
	21	6.6	6.6	79.6	6.1	76.3
	22	6.7	6.6	177.4	3.4	42.3
	23	6.6	6.6	58.2	4.0	50.0
	24	6.7	6.7	236.6	5.1	64.1
TMS-1	1	7.0	6.9	10.7	0.2	2.7
	2	7.0	7.0	831.1	8.4	104.5
	3	6.7	7.0	184.2	7.9	99.2
	4	7.1	7.3	267.9	3.2	40.2
	5	7.0	7.5	397.3	5.7	71.2
	6	7.3	7.2	605.3	7.4	93.0

	7	7.3	7.6	767.9	4.4	54.5
	8	6.6	6.7	580.4	2.8	35.1
	9	6.4	6.6	256.9	4.5	56.1
	10	6.5	6.4	121.4	1.8	22.2
	11	N/A	N/A	113.9	1.7	21.8
	12	6.2	6.4	168.1	2.4	30.6
	13	N/A	N/A	286.0	6.1	75.6
	14	6.4	6.4	214.0	2.6	32.8
	15	6.4	6.5	53.3	1.7	20.7
	16	6.4	6.7	138.2	1.7	21.2
	17	6.5	6.6	310.7	4.6	57.4
	18	N/A	N/A	172.2	3.8	47.6
	19	N/A	N/A	162.4	1.1	13.4
	20	6.6	6.6	115.6	3.8	47.0
	21	6.4	6.6	47.3	4.0	50.1
	22	6.5	6.5	48.9	4.0	49.4
	23	6.6	6.7	167.9	3.7	46.1
TMS-2	1	7.3	6.8	12.5	0.2	3.1
	2	6.9	7.0	552.3	2.4	30.3
	3	6.7	6.9	208.1	9.2	114.6
	4	7.0	7.2	314.3	3.7	46.8
	5	7.0	7.4	330.7	4.7	58.5
	6	7.3	7.3	457.8	5.3	66.0
	7	7.2	7.1	493.9	1.6	19.8
	8	6.5	6.6	396.0	1.0	12.4
	9	6.5	6.6	194.5	3.7	45.8
	10	6.4	6.5	121.4	1.8	22.2
	11	N/A	N/A	275.0	5.3	66.1
	12	6.4	6.6	168.2	2.0	25.3
	13	N/A	N/A	186.7	2.4	29.9
	14	6.4	6.5	120.1	1.0	12.4
	15	6.5	6.6	61.8	1.7	21.6
	16	6.4	6.5	176.6	2.7	33.6
	17	6.5	6.6	265.5	3.2	40.3
	18	N/A	N/A	93.8	2.1	26.4
	19	N/A	N/A	124.1	1.6	20.3
	20	6.5	6.5	85.7	2.5	31.4
	21	6.4	6.5	15.7	1.2	15.5
	22	6.5	6.5	35.3	2.7	34.0
	23	6.6	6.6	155.8	4.2	52.0
TMS-3	1	7.0	6.8	5.1	0.1	1.3
	2	6.6	6.5	472.1	2.6	31.9
	3	6.6	6.7	135.5	6.0	74.4
	4	6.6	6.9	201.3	2.5	30.9

	5	6.7	7.2	406.0	5.3	66.3
	6	7.0	7.1	457.9	6.1	76.4
	7	7.1	7.1	692.8	4.0	49.7
	8	6.3	6.6	604.5	3.8	48.1
	9	6.5	6.6	135.9	2.7	33.9
	10	6.4	6.4	101.2	1.8	23.0
	11	N/A	N/A	173.6	3.4	42.4
	12	6.3	6.5	177.3	3.2	40.4
	13	N/A	N/A	248.3	3.5	43.2
	14	6.5	6.5	239.0	3.3	41.5
	15	6.6	6.6	50.2	1.6	20.3
	16	6.4	6.5	85.6	1.2	14.7
	17	6.5	6.6	209.2	3.0	37.1
	18	N/A	N/A	80.3	2.2	27.7
	19	N/A	N/A	150.7	4.1	51.1
	20	6.7	6.7	177.5	3.8	47.6
	21	6.5	6.5	32.6	2.7	33.6
	22	6.5	6.5	34.5	2.6	32.9
	23	6.6	6.6	127.7	3.4	42.0

Table 2: Methane and pH raw data for TMS-4 and TMS-5

Sample Id	Cycle #	Initial pH	Final pH	Average Mass of Methane Produced (micromoles)	Average Methane Production Rate (micromoles/ hour)	Normalized Rate (micromoles/ Liter/hour)
TMS-4 Kaolinite	1	6.5	6.6	91.2	0.9	11.3
	2	6.4	6.5	69.1	1.9	23.8
	3	6.4	6.6	220.9	2.8	35.0
	4	6.5	6.6	270.9	3.1	38.8
	TOTAL AVERAGE			163.17	2.2	
TMS-5 Calcite	1	6.5	6.6	122.8	1.4	17.5
	2	6.4	6.5	84.5	2.2	27.5
	3	6.4	6.6	253.3	3.7	46.3
	4	6.5	6.6	277.9	2.5	31.3
	TOTAL AVERAGE			184.6	2.5	

Table 3: Methane and pH raw data for MR#1 and MR#2

Sample Id	Cycle #	Initial pH	Final pH	Average Mass of Methane Produced (micromoles)	Average Methane Production Rate (micromole/ hour)	Normalized Rate (micromole/ Liter/hour)
MR#1	1	N/A	N/A	395.7	7.6	7.6
	2	N/A	N/A	790.2	1.8	1.8
	3	N/A	N/A	4422.6	28.3	28.3
	4	6.4	6.4	1069.6	35.2	35.2
	5	6.2	6.6	4306.9	30.6	30.6
	6	6.2	6.4	9613.0	56.2	56.2
	7	6.4	6.3	5096.4	48.7	48.7
	8	6.2	6.2	4301.1	41.3	41.3
	9	6.3	6.3	1647.9	36.8	36.8
	TOTAL AVERAGE			3515.9	31.8	
MR#2	1	N/A	N/A	0.0	0.0	0.0
	2	7.0	7.0	37.3	1.0	0.5
	3	6.4	6.8	4514.0	14.0	6.7
	4	6.5	6.5	3522.0	44.8	21.3
	5	6.6	6.7	4026.1	93.4	44.5
	TOTAL AVERAGE			2419.9	30.6	

Table 4: Total inorganic carbon (TIC) and total hydrogen for MS and TMS

This estimation is based on headspace carbon dioxide and hydrogen measurements from the microcosms (see calculation approach in Appendix H and I).

Sample ID#	Cycle #	Total Inorganic Carbon Mass (micromoles)	Total Hydrogen (micromoles)
MS-1	21	4402.4	1300.1
	21	4213.1	768.3
	21	2951.3	75.1
	22	5707.5	879.1

	22	4770.5	639.5
	22	3715.4	334.7
	22	3291.7	122.3
	22	3214.2	31.1
	22	n/a	20.0
	22	4176.7	20.0
	23	6115.2	20.0
	23	4126.9	755.7
	24	6194.0	1644.2
	24	5049.3	581.2
	24	4582.2	0.0
	24	3323.5	0.0
MS-2	21	4622.9	1552.1
	21	4042.3	648.1
	21	3694.9	130.5
	22	6769.6	962.1
	22	5355.6	673.8
	22	5308.2	338.0
	22	4960.9	165.2
	22	5276.2	40.7
	22	n/a	20.0
	22	3685.0	20.0
	23	5209.8	981.6
	23	3095.9	385.9
	24	5618.3	1552.1
	24	4601.9	648.1
	24	3928.3	130.5
	24	3367.4	133.1
MS-3	21	4264.9	1284.0
	21	4391.8	794.3
	21	4247.0	109.6
	22	5592.6	933.0
	22	4325.2	789.9
	22	4695.0	426.5
	22	4095.6	249.4
	22	4391.2	136.8
	22	n/a	106.9
	22	3837.9	20.0
	23	4897.7	1229.5
	23	2274.5	514.9
	24	5760.7	1550.3
	24	4813.6	618.5
	24	4086.4	132.2
	24	4247.4	111.4
TMS-1	20	4096.3	1268.6

	20	3664.4	969.4
	20	3609.3	479.7
	21	3703.6	926.9
	21	2985.3	732.6
	21	3459.3	473.5
	21	3342.4	380.7
	21	3628.9	276.6
	21	n/a	119.3
	21	3999.7	23.3
	22	4425.6	1288.7
	22	2160.0	520.2
	23	5533.3	1532.6
	23	4890.9	848.6
	23	4081.2	451.1
	23	4107.4	254.6
TMS-2	20	3775.6	1219.8
	20	3519.8	909.3
	20	3575.9	507.3
	21	3485.4	936.6
	21	2926.5	815.2
	21	3512.8	633.3
	21	3427.6	571.2
	21	3484.6	561.7
	21	n/a	334.6
	21	4017.8	298.1
	22	4543.0	1231.8
	22	3229.6	613.5
	23	5675.5	1582.0
	23	4646.6	1026.5
	23	3838.2	682.2
	23	3953.1	479.2
TMS-3	20	2324.7	1222.0
	20	4569.4	747.8
	20	4265.5	316.1
	21	4799.1	966.7
	21	3540.9	775.1
	21	3741.5	443.8
	21	3575.0	453.8
	21	3758.8	465.6
	21	n/a	271.7
	21	3834.1	203.1
	22	4989.1	1246.3
	22	3530.1	459.0
	23	5377.2	1486.0
	23	4397.0	992.9

	23	3970.8	690.4
	23	4053.0	477.1

Table 5: Total inorganic carbon (TIC) and total hydrogen for MR#1 and MR#2

This estimation is based on headspace carbon dioxide and hydrogen measurements from the microcosms (see calculation approach in Appendix H and I).

Sample ID#	Cycle #	Total Inorganic Carbon Mass (micromoles)	Total Hydrogen (micromoles)
MR#1	4	128517.8	102206.8
	4	133479.6	93792.3
	4	112676.0	92832.6
	5	132092.1	73857.0
	5	147318.2	46663.4
	5	140949.6	60078.1
	5	121193.4	73286.6
	5	157592.1	91585.0
	5	132135.3	85044.5
	5	132511.6	75693.1
	5	164770.1	62250.0
	5	174096.0	54098.2
	5	147051.2	1180.1
	5	158221.2	0.0
	6	148782.2	116114.6
	6	162205.4	119697.1
	6	148434.8	46341.8
	6	148500.7	50210.0
	6	156340.9	44849.8
	7	159519.9	140841.8
	7	160384.0	114152.5
	7	166849.4	89813.6
	7	165351.9	68755.1
	7	153925.6	40501.6
	8	165252.2	140849.5
	8	153756.9	138929.6
	8	174150.4	129503.2
	8	150750.4	107476.7
	8	154871.7	56333.9

	9	31765.6	116521.9
	9	30879.9	133483.4
	9	32802.7	93647.6
MR#2	2	194970.7	69237.7
	2	245516.7	69163.3
	2	264793.9	70537.9
	3	176564.4	59116.3
	3	155922.7	86510.8
	3	148836.2	67444.9
	3	182356.0	66587.0
	3	161749.3	79489.4
	3	252174.5	85660.7
	3	169303.1	65077.9
	3	213470.3	94239.4
	3	181271.4	98479.7
	3	177313.1	69910.4
	3	186900.9	61788.7
	3	183374.7	49126.6
	3	185236.4	32077.5
	3	186501.9	19304.4
	3	229531.8	1232.3
	4	198187.4	121624.7
	4	181048.5	102827.0
	4	208436.1	94972.4
	4	217850.1	105338.0
	4	202250.8	57199.2
	5	200053.4	105041.0
	5	203046.3	86875.3
	5	210404.6	39297.9

Table 6: Fe(II) raw data for MS and TMS

The data below is by UV-VIS spectrophotometeric technique (see SOP in Appendix C)

Sample Id	Cycle #	Date of Collection	Initial Fe(II) mM	Final Fe(II) mM	Remarks
MS-1	1	7/11/2008	0.346		
	2	7/24/2008	0.097		
	2	7/31/2008		1.030	Increase
	3	8/4/2008	0.597		
	3	8/11/2008		0.473	Decrease
	4	8/12/2008	0.529		
MS-2	1	7/11/2008	0.397		
	2	7/24/2008	0.363		
	2	7/31/2008		0.788	Increase
	3	8/4/2008	0.584		
	3	8/11/2008		0.560	Decrease
	4	8/12/2008	0.455		
MS-3	1	7/11/2008	0.399		
	2	7/24/2008	0.335		
	2	7/31/2008		1.428	Increase
	3	8/4/2008	0.685		
	3	8/11/2008		0.524	Decrease
	4	8/12/2008	0.517		
TMS-1	1	7/24/2008	0.097		
	1	7/31/2008		0.270	Increase
	2	8/4/2008	0.111		

	2	8/11/2008		0.112	Increase
	3	8/12/2008	0.117		
TMS-2	1	7/24/2008	0.039		
	1	7/31/2008		0.153	Increase
	2	8/4/2008	0.070		
	2	8/11/2008		0.060	Decrease
	3	8/12/2008	0.097		
TMS-3	1	7/24/2008	0.038		
	1	7/31/2008		0.090	Increase
	2	8/4/2008	0.058		
	2	8/11/2008		0.065	Increase
	3	8/12/2008	0.100		

Table 7: Spectrophotometer alkalinity raw data for MS and TMS:

This estimation is based on absorbency readings obtained from UV-VIS spectrophotometer analysis (see approach described in Appendix B).

Sample Id	Cycle #	Initial Alkalinity (mg L^{-1})	Final Alkalinity (mg L^{-1})	Remarks
MS-1	2	2232.70		
	3	2461.79		
	3		6179.84	Increase
	4	5935.76		
	4		5990.00	Increase
	5	5339.12		
	5		7779.92	Increase
	6	7698.56		
	6		6722.24	Decrease
	7	10469.59		
	7		10064.69	Decrease
	8	9983.71		
	8		9327.31	Decrease
	9	9821.75		
	9		9158.26	Decrease
MS-2	2	2087.22		
	3	2434.67		
	3		6044.24	Increase
	4	5854.40		
	4		5962.88	Increase
	5	5284.88		
	5		7969.76	Increase
	6	7807.04		
	6		6803.60	Decrease
	7	10510.08		

	7		10064.69	Decrease
	8	9700.28		
	8		9124.45	Decrease
	9	10037.32		
	9		9530.17	Decrease
MS-3	2	2048.71		
	3	2326.19		
	3		6152.72	Increase
	4	5773.04		
	4		5990.00	Increase
	5	5149.28		
	5		7834.16	Increase
	6	7861.28		
	6		6830.72	Decrease
	7	10388.61		
	7		9902.73	Decrease
	8	9821.75		
	8		9158.26	Decrease
	9	9935.89		
	9		9699.22	Decrease
TMS-1	1	1886.11		
	2	2217.71		
	2		5990.00	Increase
	3	5827.28		
	3		5691.68	Decrease
	4	4932.32		
	4		7562.96	Increase
	5	7562.96		
	5		1317.33	Decrease
	6	10024.20		
	6		9700.28	Decrease
	7	9862.24		
	7		9158.26	Decrease
	8	9699.22		
	8		9293.50	Decrease
	9	8786.35		
	9		8515.87	Decrease
	10	8853.97		
	10		7839.67	Decrease
	11	Recovery		

	11			
	12 12	9148.24	8745.64	Decrease
	13 13	n/a	n/a	
	14 14	8423.56	8705.38	Increase
	15 15	8222.26	8302.78	Increase
	16 16	8383.30	10597.60	Increase
	17 17	8302.78	8504.08	Increase
TMS-2	1	2010.20		
	2 2	1973.63	5800.16	Increase
	3 3	5745.92	5745.92	Equal
	4 4	4959.44	7617.20	Increase
	5 5	7698.56	1328.18	Decrease
	6 6	10226.65	9781.26	Decrease
	7 7	9983.71	9124.45	Decrease
	8 8	9902.08	9225.88	Decrease
	9 9	8786.35	8718.73	Decrease
	10 10	8820.16	7907.29	Decrease
	11 11	Recovery		
	12 12	9067.72	8624.86	Decrease
	13 13	n/a	n/a	
	14 14	8665.12	8423.56	Decrease
	15 15	8423.56	8423.56	Equal
	16	8262.52		

	16		8182.00	Decrease
	17 17	8182.00	7859.92	Decrease
TMS-3	1	1928.90		
	2 2	2179.74	5990.00	Increase
	3 3	5908.64	5800.16	Decrease
	4 4	5013.68	7698.56	Increase
	5 5	7725.68	1371.57	Decrease
	6 6	10591.06	9821.75	Decrease
	7 7	9821.75	9192.07	Decrease
	8 8	9902.08	9225.88	Decrease
	9 9	8380.63	8313.01	Decrease
	10 10	8752.54	7873.48	Decrease
	11 11	Recovery		
	12 12	9027.46	8419.53	Decrease
	13 13	n/a	n/a	
	14 14	8584.60	8624.86	Increase
	15 15	8383.30	8383.30	Equal
	16 16	8302.78	8584.60	Increase
	17 17	8262.52	8141.74	Decrease

Table 8: DOC and DIC Analysis Results for MS and TMS
(Equipment model: Apollo TOCN Analyzer, Teledyne Tekmar, Cincinnati, OH)
Note:
MS Data: 1 mL of sample =19 mL of DI water
All samples were filtered with a 0.45 micron filter to isolate only DOC (i.e., POC removed by filtration)
If change in DOC is negative, there is a net decrease in DOC
(Details of sampling approach is described in Appendix E)

Sample Id	Cycle #	Date of Collection	DOC Value (mg L^{-1} C)	Change in DOC (final-initial)	DIC Value (mg L^{-1} C)	Change in DIC (final-initial)	Remarks	Condition of Set-up
MS-1	1	7/15/2008	193.804		*	*		
MS-1	1	7/22/2008	170.784	-23.02	*	*	Net Decrease in DOC	
MS-1	2	7/25/2008	275.412		*	*		20 mL Basal Medium Replenished at beginning of cycle
MS-1	2	7/31/2008	505.486	230.074	*	*	Net Increase in DOC	

MS-1	3	8/4/2008	221.7		*	*		
MS-1	3	8/12/2008	94.066	-127.634	*	*	Net Decrease in DOC	
MS-1	4	8/14/2008	42.46		*	*		20 mL Basal Medium Replenished at beginning of cycle
MS-1	4	8/15/2008	56.322	13.862	*	*	Net Increase in DOC	
MS-1	5	8/19/2008	62.666		*	*		
MS-1	5	8/25/2008	49.774	-12.892	*	*	Net Decrease in DOC	
MS-1	6	8/26/2008	330.882		*	*		20 mL Basal Medium Replenished at beginning of cycle

MS-1	6	9/3/2008	42.01	-288.872	*	*	Net Decrease in DOC	
MS-1	7	9/3/2008	45.726		*	*		
MS-1	7	9/11/2008	53.128	7.402	*	*	Net Increase in DOC	
MS-1	8	9/12/2008	51.018		*	*		20 mL Basal Medium Replenished at beginning of cycle
MS-1	8	9/24/2008	39.552	-11.466	*	*	Net Decrease in DOC	
MS-1	9	9/24/2008	46.148		*	*		20 mL Basal Medium Replenished at beginning of cycle
MS-1	9	10/7/2008	41.794	-4.354	*	*	Net Decrease in DOC	

MS-2	1	7/15/2008	168.44		*	*		
MS-2	1	7/22/2008	151.2	-17.24	*	*	Net Decrease in DOC	
MS-2	2	7/25/2008	205.778		*	*		20 mL Basal Medium Replenished at beginning of cycle
MS-2	2	7/31/2008	388.414	182.636	*	*	Net Increase in DOC	
MS-2	3	8/4/2008	81.26		*	*		
MS-2	3	8/12/2008	64.94	-16.32	*	*	Net Decrease in DOC	
MS-2	4	8/14/2008	32.394		*	*		20 mL Basal Medium Replenished at beginning of cycle

MS-2	4	8/15/2008	40.518	8.124	*	*	Net Increase in DOC	
MS-2	5	8/19/2008	45.176		*	*		
MS-2	5	8/25/2008	35.718	-9.458	*	*	Net Decrease in DOC	
MS-2	6	8/26/2008	342.898		*	*		20 mL Basal Medium Replenished at beginning of cycle
MS-2	6	9/3/2008	39.28	-303.618	*	*	Net Decrease in DOC	
MS-2	7	9/3/2008	35.978		*	*		
MS-2	7	9/11/2008	45.394	9.416	*	*	Net Increase in DOC	

MS-2	8	9/12/2008	40.698		*	*		20 mL Basal Medium Replenished at beginning of cycle
MS-2	8	9/24/2008	41.962	1.264	*	*	Net Increase in DOC	
MS-2	9	9/24/2008	49.138		*	*		20 mL Basal Medium Replenished at beginning of cycle
MS-2	9	10/7/2008	38.888	-10.25	*	*	Net Decrease in DOC	
MS-3	1	7/15/2008	203.784		*	*		
MS-3	1	7/22/2008	192.332	-11.452	*	*	Net Decrease in DOC	
MS-3	2	7/25/2008	362.756		*	*		20 mL Basal Medium Replenished at beginning of cycle

MS-3	2	7/31/2008	541.726	178.97	*	*	Net Increase in DOC	
MS-3	3	8/4/2008	118.376		*	*		
MS-3	3	8/12/2008	75.384	-42.992	*	*	Net Decrease in DOC	
MS-3	4	8/14/2008	37.55		*	*		20 mL Basal Medium Replenished at beginning of cycle
MS-3	4	8/15/2008	42.914	5.364	*	*	Net Increase in DOC	
MS-3	5	8/19/2008	44.94		*	*		
MS-3	5	8/25/2008	31.154	-13.786	*	*	Net Decrease in DOC	

MS-3	6	8/26/2008	337.854		*	*		20 mL Basal Medium Replenished at beginning of cycle
MS-3	6	9/3/2008	32.502	-305.352	*	*	Net Decrease in DOC	
MS-3	7	9/3/2008	31.882		*	*		
MS-3	7	9/11/2008	43.148	11.266	*	*	Net Increase in DOC	
MS-3	8	9/12/2008	37.986		*	*		20 mL Basal Medium Replenished at beginning of cycle
MS-3	8	9/24/2008	36.814	-1.172	*	*	Net Decrease in DOC	
MS-3	9	9/24/2008	40.468		*	*		20 mL Basal Medium Replenished at beginning of cycle

MS-3	9	10/7/2008	41.834	1.366	*	*	Net Increase in DOC	
TMS-1	1	7/25/2008	114.644		*	*		
TMS-1	1	7/31/2008	460.966	346.322	*	*	Net Increase in DOC	
TMS-1	2	8/4/2008	90.788		*	*		
TMS-1	2	8/12/2008	76.516	-14.272	*	*	Net Decrease in DOC	
TMS-1	3	8/14/2008	29.384		*	*		20 mL Basal Medium Replenished at beginning of cycle
TMS-1	3	8/15/2008	32.734	3.35	*	*	Net Increase in DOC	
TMS-1	4	8/19/2008	41.344		*	*		

TMS-1	4	8/25/2008	24.424	-16.92	*	*	Net Decrease in DOC	
TMS-1	5	8/26/2008	326.184		*	*		20 mL Basal Medium Replenished at beginning of cycle
TMS-1	5	9/3/2008	7.318	-318.866	*	*	Net Decrease in DOC	
TMS-1	6	9/3/2008	5.606		*	*		
TMS-1	6	9/11/2008	18.438	12.832	*	*	Net Increase in DOC	
TMS-1	7	9/12/2008	9.76		*	*		20 mL Basal Medium Replenished at beginning of cycle
TMS-1	7	9/24/2008	5.858	-3.902	*	*	Net Decrease in DOC	

TMS-1	8	9/24/2008	9.714		*	*		20 mL Basal Medium Replenished at beginning of cycle
TMS-1	8	10/7/2008	10.006	0.292	*	*	Net Increase in DOC	
TMS-1	9	10/13/2008	20.8316		313.5036			
TMS-1	9	10/17/2008	59.0926	38.261	250.7282	-62.7754	Net Increase in DOC and DIC	
TMS-1	10	10/20/2008	37.6527		275.8755			20 mL Basal Medium Replenished at beginning of cycle
TMS-1	10	10/24/2008	36.7157	-0.937	266.8796	-8.9959	Net Decrease in DOC and DIC	
TMS-2	1	7/25/2008	84.018					

TMS-2	1	7/31/2008	337.064	253.046	*	*	Net Increase in DOC	
TMS-2	2	8/4/2008	82.972					
TMS-2	2	8/12/2008	64.42	-18.552	*	*	Net Decrease in DOC	
TMS-2	3	8/14/2008	26.282		*	*		20 mL Basal Medium Replenished at beginning of cycle
TMS-2	3	8/15/2008	29.716	3.434	*	*	Net Increase in DOC	
TMS-2	4	8/19/2008	33.066		*	*		
TMS-2	4	8/25/2008	23.352	-9.714	*	*	Net Decrease in DOC	

TMS-2	5	8/26/2008	327.64		*	*		20 mL Basal Medium Replenished at beginning of cycle
TMS-2	5	9/3/2008	2.486	-325.154	*	*	Net Decrease in DOC	
TMS-2	6	9/3/2008	0.706		*	*		
TMS-2	6	9/11/2008	9.538	8.832	*	*	Net Increase in DOC	
TMS-2	7	9/12/2008	6.9		*	*		20 mL Basal Medium Replenished at beginning of cycle
TMS-2	7	9/24/2008	1.596	-5.304	*	*	Net Decrease in DOC	
TMS-2	8	9/24/2008	8.798		*	*		20 mL Basal Medium Replenished at beginning of cycle

TMS-2	8	10/7/2008	5.994	-2.804	*	*	Net Decrease in DOC	
TMS-2	9	10/13/2008	23.6787		297.8869	*		
TMS-2	9	10/17/2008	35.585	11.9063	275.1868	-22.7001	Net Increase in DOC, Decrease in DIC	
TMS-2	10	10/20/2008	27.1116		275.8755	*		20 mL Basal Medium Replenished at beginning of cycle
TMS-2	10	10/24/2008	52.4647	25.3531	266.8796	-8.9959	Net Increase in DOC, Decrease in DIC	
TMS-3	1	7/25/2008	131.958					
TMS-3	1	7/31/2008	451.75	319.792	*	*	Net Increase in DOC	

TMS-3	2	8/4/2008	100.288		*	*		
TMS-3	2	8/12/2008	85.78	-14.508	*	*	Net Decrease in DOC	
TMS-3	3	8/14/2008	37.672		*	*		20 mL Basal Medium Replenished at beginning of cycle
TMS-3	3	8/15/2008	35.348	-2.324	*	*	Net Decrease in DOC	
TMS-3	4	8/19/2008	56.002		*	*		
TMS-3	4	8/25/2008	38.63	-17.372	*	*	Net Decrease in DOC	
TMS-3	5	8/26/2008	381.188		*	*		20 mL Basal Medium Replenished at beginning of cycle

TMS-3	5	9/3/2008	24.122	-357.066	*	*	Net Decrease in DOC	
TMS-3	6	9/3/2008	31.402		*	*		
TMS-3	6	9/11/2008	25.81	-5.592	*	*	Net Decrease in DOC	
TMS-3	7	9/12/2008	26.074		*	*		20 mL Basal Medium Replenished at beginning of cycle
TMS-3	7	9/24/2008	13.156	-12.918	*	*	Net Decrease in DOC	
TMS-3	8	9/24/2008	19.048		*	*		20 mL Basal Medium Replenished at beginning of cycle
TMS-3	8	10/7/2008	8.022	-11.026	*	*	Net Decrease in DOC	

TMS-3	9	10/13/2008	40.0816		267.4219	*		
TMS-3	9	10/17/2008	72.855	32.7734	243.6546	-23.7673	Net Increase in DOC, Decrease in DIC	
TMS-3	10	10/20/2008	79.2584		275.8755	*		20 mL Basal Medium Replenished at beginning of cycle
TMS-3	10	10/24/2008	96.2326	16.9742	266.8796	-8.9959	Net Increase in DOC, Decrease in DIC	